Technical Report Documentation Page

1. Report No. FHWA/TX-09/0-5824-2	2. Government Accession No.	3. Recipient's Catalog No.
4. Title and Subtitle Characterization of Undrained Shear Strength Profiles for Soft Clays at Six Sites in Texas		5. Report Date August 2008; Revised January 2009 6. Performing Organization Code
7. Author(s) David A. Varathungarajan, Scott M. Garfield, Stephen G. Wright		8. Performing Organization Report No. 0-5824-2
9. Performing Organization Name and Address Center for Transportation Research The University of Texas at Austin 3208 Red River, Suite 200 Austin, TX 78705-2650		10. Work Unit No. (TRAIS) 11. Contract or Grant No. 0-5824
12. Sponsoring Agency Name and Address Texas Department of Transportation Research and Technology Implementation Office P.O. Box 5080 Austin, TX 78763-5080		13. Type of Report and Period Covered Technical Report September 1, 2006–August 31, 2008 14. Sponsoring Agency Code
15. Supplementary Notes Project performed in cooperation with the Texas Department of Transportation and the Federal Highway Administration.		

16. Abstract

TxDOT frequently uses Texas Cone Penetrometer (TCP) blow counts to estimate undrained shear strength. However, the current correlations between TCP resistance and undrained shear strength have been developed primarily for significantly stronger soils than are often encountered at shallow depths. Updated existing correlations would allow TxDOT to estimate better the undrained shear strength of soft soils for the design of embankments and retaining structures. Considering the limited data for these soils, the primary objective of this study was to characterize the undrained shear strength profiles for six sites with strengths generally less than 750 psf, such as those commonly found at depths up to approximately 30 feet. The undrained shear strength profiles developed in this study were used in further research by Garfield (2008) to develop and assess the reliability of new correlations between Texas Cone Penetrometer resistance and undrained shear strength of soft clays.

An analysis was performed comparing strengths measured in unconsolidated-undrained, consolidated-undrained, field vane shear, and piezocone penetration tests with respect to strengths from the average strength profiles. The degree of sample disturbance in unconsolidated-undrained tests was assessed based on values of axial strain at 75 percent of the principal stress difference at failure. While there was significant scatter in the data, unconsolidated-undrained tests gave strengths that tended to be significantly lower than strengths from the average profiles. The degree of sample disturbance in consolidated-undrained tests was assessed based on the volumetric strain during consolidation to the in-situ effective overburden stress. Consolidated-undrained tests on disturbed specimens gave strengths that were approximately 50 percent higher than what was believed to be the correct strength. Strengths measured in field vane shear tests were corrected with Bjerrum's (1972) correction factor and found to generally agree well with strengths from the average strength profiles. However, vane tests in sandy clays tended to overestimate undrained strengths. Analyses also indicated that piezocone penetration tests can be used to establish reasonably accurate undrained shear strength profiles without the need for site specific correlations.

17. Key Words	18. Distribution Statement
soil shear strength, soft clay, geotechnical engineering, penetration tests	No restrictions. This document is available to the public through the National Technical Information Service, Springfield, Virginia 22161; www.ntis.gov.

19. Security Classif. (of report)	20. Security Classif. (of this page)	21. No. of pages	22. Price
Unclassified	Unclassified	160	

Form DOT F 1700.7 (8-72) Reproduction of completed page authorized

Characterization of Undrained Shear Strength Profiles for Soft Clays at Six Sites in Texas

David A. Varathungarajan
Scott M. Garfield
Stephen G. Wright

CTR Technical Report:	0-5824-2
Report Date:	August 2008; Revised January 2009
Project:	0-5824
Project Title:	Correlation of Shallow, Low Blow Count Texas Cone Penetrometer Values and Shear Strength for Texas Soils
Sponsoring Agency:	Texas Department of Transportation
Performing Agency:	Center for Transportation Research at The University of Texas at Austin

Project performed in cooperation with the Texas Department of Transportation and the Federal Highway Administration.

Center for Transportation Research
The University of Texas at Austin
3208 Red River
Austin, TX 78705

www.utexas.edu/research/ctr

Disclaimers

Author's Disclaimer: The contents of this report reflect the views of the authors, who are responsible for the facts and the accuracy of the data presented herein. The contents do not necessarily reflect the official view or policies of the Federal Highway Administration or the Texas Department of Transportation (TxDOT). This report does not constitute a standard, specification, or regulation.

Patent Disclaimer: There was no invention or discovery conceived or first actually reduced to practice in the course of or under this contract, including any art, method, process, machine manufacture, design or composition of matter, or any new useful improvement thereof, or any variety of plant, which is or may be patentable under the patent laws of the United States of America or any foreign country.

Engineering Disclaimer

NOT INTENDED FOR CONSTRUCTION, BIDDING, OR PERMIT PURPOSES.

Research Supervisor: Stephen G. Wright

Acknowledgments

The authors wish to thank Dr. Robert B. Gilbert of the University of Texas for his review and suggestions during the course of this work. We also wish to express our gratitude to Tolunay-Wong Engineers, Inc., including Art Stephens and John Hebert for performing the field exploration and testing for this research. Their efforts were instrumental in the success of the project. Mr. Mark McClelland and Ms. Dina Dewane served as Program Coordinator and Project Director, respectively, for TxDOT. Their vision, support, and encouragement throughout the work are sincerely appreciated.

Table of Contents

List of Tables

List of Figures

Chapter 1. Introduction to Research Study

Undrained shear strength is used in the design and analysis of foundations, retaining structures, and embankments, and is measured using a variety of laboratory and in-situ tests. To perform laboratory tests, such as triaxial or unconfined compression tests, relatively undisturbed samples must be recovered using an appropriate form of drilling and sampling. The sampling and subsequent laboratory testing can be a time-consuming and expensive process. Additionally, it is often difficult to recover samples of high enough quality to obtain meaningful laboratory test results. Compared with the traditional technique of drilling, sampling, and laboratory testing, in-situ testing offers the advantage of generally being less expensive and quicker to perform. While in-situ testing is often more convenient and cost effective than laboratory strength testing, appropriate correlations must be developed for each in-situ test in order to successfully apply the results to design.

The Texas Department of Transportation has used the Texas Cone Penetrometer test to estimate drained and undrained strengths for the design of deep foundations. Recently, there has been a desire to update existing Texas cone correlations to better estimate the undrained shear strength of soft soils for the design of embankments and earth retaining structures. Existing correlations between undrained shear strength and Texas Cone Penetrometer resistance have been developed primarily for significantly stronger soils than are often encountered at shallow depths (Garfield, 2008). As a result of limited data for weaker soils, there is considerable uncertainty when predicting the undrained shear strength of soft to medium clays from Texas Cone Penetrometer resistance. Considering the limited data for these soils, the primary objective of this research is to characterize the undrained shear strength profiles of six sites with strengths generally less than 750 psf, such as those commonly found at depths up to approximately 30 feet.

1.1 Scope of Research

In this study, six sites were selected and undrained shear strengths profiles were determined by a variety of laboratory and in-situ tests. The undrained strength profiles were then used in further research by Garfield (2008) to develop a correlation between undrained shear strength and Texas Cone Penetrometer resistance and to assess the reliability of the correlation. In-situ tests included piezocone penetration and field vane shear. Laboratory strength tests included unconsolidated-undrained and consolidated-undrained triaxial compression tests. One-dimensional consolidation tests and Atterberg limit tests were also performed on representative samples. The results of these tests were then analyzed and interpreted to determine a single, appropriate undrained shear strength profile as well as upper and lower bounds representative of the spatial variability and uncertainty for each site.

1.2 Report Overview

The following aspects are addressed in this study to accomplish the objectives of the study:

- review of undrained shear strength and undrained shear strength testing, including triaxial, field vane shear, and piezocone penetration tests,
- description of testing equipment and procedures used in this study,

- analysis of test results, including discussion of undrained shear strength profiles, and
- summary and conclusions.

This report is organized into seven chapters. Following the introduction presented in this chapter, an overview of the field investigation and laboratory testing program for this study is provided in Chapter 2. Field and laboratory testing apparatus and procedures are described in Chapter 2.

A review of undrained shear strength and field and laboratory testing is given in Chapter 3. Issues affecting the measurement of undrained shear strengths are discussed, as well as how they relate to unconsolidated-undrained and consolidated-undrained triaxial compression tests and field vane shear tests.

In Chapter 4, piezocone penetration testing is discussed. This includes a review of several methods available to determine undrained shear strengths from cone penetration test results. The rationale for selecting the method used in this study to determine undrained shear strengths from cone penetration tests results is also discussed in this chapter.

For each site, a representative undrained shear strength profile with upper and lower bounds is presented and discussed in Chapter 5. Field and laboratory test results are presented and discussed.

Chapter 6 presents an evaluation of undrained strengths measured in unconsolidated-undrained, consolidated-undrained, field vane shear, and piezocone penetration with respect to strengths believed to be most representative of the undrained strength profiles. The various tests are then analyzed and discussed.

The findings of this study are summarized in Chapter 7. Conclusions are made regarding the effectiveness of the test methods used in this study to determine undrained shear strengths.

Chapter 2. Field Investigation and Laboratory Testing Program

Both a field and laboratory testing program were conducted for this study. An overview of the sampling and testing in presented in this chapter. Results of the testing are presented later in Chapter 5.

2.1 Field Investigation

All field investigations were performed by Tolunay-Wong Engineers, Inc. of Houston, Texas. The primary purpose was to obtain Texas Cone Penetrometer N-values for the upper 25 to 35 feet of each site while obtaining continuous undisturbed samples for laboratory testing from adjacent borings. Field vane shear testing was also performed in other adjacent borings except when the soil strengths exceeded the range of the vane shear apparatus. Multiple piezocone penetration test soundings were also performed at most sites. The location of the cone soundings in relation to the undisturbed sampling, Texas cone and field vane borings varied from site to site.

2.1.1 Thin-Walled Tube Sampling

Continuous, relatively undisturbed samples were obtained by pushing thin-walled sample tubes into the ground. The tubes used for sampling had an inner-diameter of 2.850 inches and a wall thickness of 0.085 inch. A fixed-piston sampler was used when soft clays were encountered in order to reduce disturbance.

After tubes were removed from the ground, the samples were classified in the field based on a visual inspection of the soil in the ends of the tube. Torvane or Pocket Penetrometer tests were also performed on the ends of the tubes to measure undrained shear strength. The tubes were then sealed with plastic caps and duct tape and transported to Tolunay-Wong's office before being transported to The University of Texas at Austin.

2.1.2 Field Vane Shear Testing

Field vane shear tests were performed to measure peak and remolded undrained shear strengths of clay soils. All field vane shear tests were performed using a GEONOR model H-10 field shear vane borer (Figure 2.1). The apparatus essentially consists of a lower vane borer and shoe, the vane itself, extension tubes and rods, and a gear-driven hand crank device equipped with a torque readout. The apparatus is self-contained, i.e., it is designed to be pushed into place without the use of a borehole.

The apparatus is capable of using two different sized vanes, one with rectangular blades measuring 55 mm x 110 mm and the other with rectangular blades measuring 65 mm x 130 mm. Both vanes consist of four blades set at right-angles. The larger and smaller vanes are capable of measuring undrained shear strength up to 1,300 psf and 2,100 psf, respectively. Tolunay-Wong used both the larger and smaller vanes for the field investigations for this study. Field vane shear tests were not performed in soils with undrained shear strengths greater than approximately 2,000 psf.

To perform a test, the vane was first retracted into the lower vane borer. The apparatus was then be pushed into the ground using a hydraulic drill rig. Once the vane borer reached the desired test zone, the vane was advanced 1 to 1.5 feet from the borer shoe. As the vane was pushed from the shoe, any soil adhering to the vane blades was removed by the shoe. After the

vane was been pushed into position, there was a waiting period of approximately one minute before the test proceeded.

Following the waiting period, a torque was applied to the vane using the gear-driven hand crank. The vane was rotated at a rate of approximately 0.1 degrees per second. This typically resulted in failure occurring in about one minute. During vane rotation, the torque displayed on the readout was observed and the maximum torque was recorded. Once the maximum torque had been determined, the soil was remolded by rapidly rotating the vane through at least five to ten revolutions. Immediately after the soil had been remolded, the vane was again rotated at approximately 0.1 degrees per second and the torque corresponding to the remolded strength was recorded. With the GEONOR device there was no need to correct torque recordings for friction on the rod-soil interface because the rod segments are fully encased in plastic tubes. After recording the remolded strength, the vane was again retracted into the shoe and the borer was advanced to perform the next test. Vane tests were typically performed over intervals of no less than 2 feet.

Peak undrained shear strength, $s_{u\text{-}FV}$, was computed using the conventional test interpretation for a vane with rectangular blades and height-to-diameter ratio of 2:1 (Chandler, 1988; ASTM, 2007a):

$$s_{u-FV} = \frac{6T}{7\pi D^3} \tag{2.1}$$

where T is maximum recorded torque and D is the diameter of the vane. This interpretation assumes the soil shears as a cylinder and that the shear stress is distributed uniformly across the horizontal planes at the top and bottom of the vane, and along the vertical plane circumscribed by the vertical perimeter of the vane. The same equation was used to compute the remolded undrained shear strength, $s_{u\text{-}FV,r}$, using the torque measured after remolding the soil.

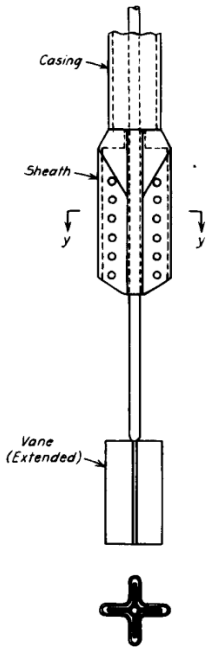

Figure 2.1: Drawing of GEONOR vane device showing vane extended from shoe (from Terzaghi, Peck, and Mesri, 1996)

2.1.3 Texas Cone Penetrometer Testing

Texas Cone Penetrometer testing was performed according to Test Method Tex-132, described in the Texas Department of Transportation Geotechnical Manual (TxDOT, 2006). The cone is made from hardened steel, with a base-diameter of 3 inches and apex angle of 60° (Figure 2.2). The cone is driven by dropping a 170-lb hammer a height of 2 feet.

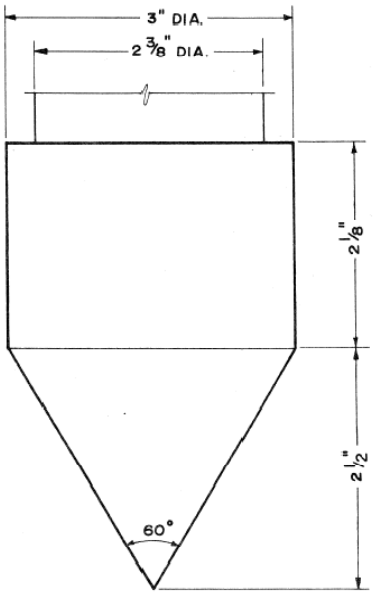

Figure 2.2: Texas Cone Penetrometer point (from Duderstadt et al., 1977)

To perform the test, the cone is first attached to the drill stem and lowered to the bottom of a borehole. The anvil is then placed on top of the drill stem and an automatic 2-foot drop tripping mechanism with the 170-lb hammer is placed on top of the anvil. The penetrometer is then seated 12 blows or 12 inches, whichever comes first. After seating, the penetrometer is driven a final 12 inches in two 6-inch increments and the blowcount for each interval is recorded. The sum of the blowcounts for the two 6-inch increments is recorded as a penetration value, N_{TCP}. The reader is referred to Garfield (2008) for a further discussion of the Texas Cone Penetrometer test and existing correlations with undrained shear strength.

2.1.4 Piezocone Penetration Testing

Piezocone penetration testing was overseen by Tolunay-Wong and subcontracted to either Southern Earth Sciences or Fugro Geosciences, depending on the particular site. Tests were performed using a standard penetrometer tip with an apex angle of 60° and a cone base area of 10 cm^2. A standard test procedure was used where the penetrometer was advanced at a constant rate of approximately 20 mm per second while cone resistance, q_c, friction sleeve resistance, f_s, and pore water pressure, u_2, were recorded every 2 cm. Pore water pressures were measured at the u_2 position, located directly behind the shoulder of the cone point (Figure 2.3). Data from piezocone penetration tests was reduced using the freeware computer program CPTINT 5.2.

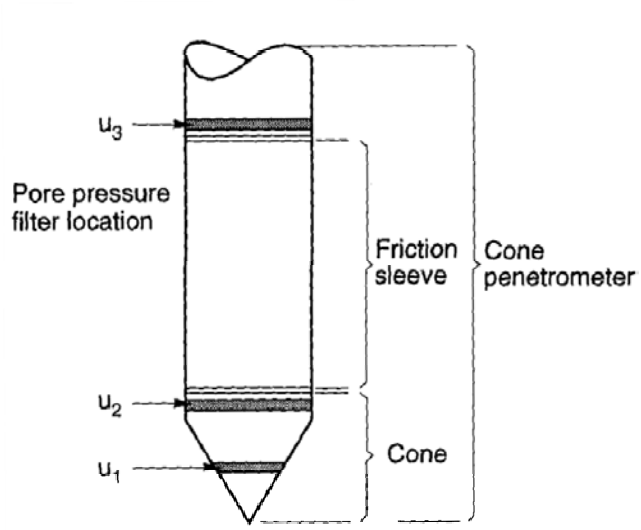

Figure 2.3: Cone penetrometer terminology (from Lunne et al., 1997)

2.2 Laboratory Testing Program

The laboratory testing program was undertaken at The University of Texas at Austin. Both unconsolidated-undrained and consolidated-undrained triaxial compression tests were performed. Representative samples were also classified according to the Unified Soil Classification System. Consolidation tests were performed on selected samples to characterize the stress history of each site. The laboratory tests are described in greater detail below.

2.2.1 Triaxial Test Apparatus

Unconsolidated-undrained (UU) and consolidated-undrained (CU) triaxial compression tests were performed using commercially available equipment. Triaxial cells manufactured by Trautwein Soil Testing Equipment and capable of testing samples up to 3 inches in diameter were used for all tests. The triaxial cells were used with 2-inch or 2.8-inch acrylic endcaps, depending on whether the specimen was trimmed to reduce the effects of disturbance. Endcaps permitting drainage from the top and bottom of the specimen were used for consolidated-undrained tests, while solid endcaps with no drainage provisions were used for unconsolidated-undrained tests.

De-aired water was used as the cell fluid, and cell pressure was applied through a pressure panel using an air-over-water accumulator. The pressure panel was manufactured by Trautwein Soil Testing Equipment and was used both to control specimen backpressure and to record volume change during consolidated-undrained tests.

Load was applied at a constant rate of deformation to the specimen using either a Wykeham Farrance motor-driven loading press or a GeoJac computer-controlled actuator manufactured by Trautwein Soil Testing Equipment. Both devices are capable of appropriate rates of deformation for consolidated-undrained and unconsolidated-undrained tests.

During unconsolidated-undrained and consolidated-undrained tests, axial load was measured with a load cell and axial deformation was measured using a linear variable differential transducer (LVDT). In consolidated-undrained tests, pore water pressures in the specimens were

measured with a pressure transducer. Volume change during consolidation was measured and manually recorded using pipettes on the pressure panel.

For tests performed using the Wykeham Farrance loading press, DC voltage signals from the load cell, LVDT, and pressure transducer were recorded using a National Instruments model USB-6210 data acquisition system connected to a personal computer. For tests performed using the GeoJac actuator, DC voltages were recorded using a personal computer and a GEOTAC data acquisition system manufactured by Trautwein Soil Testing Equipment.

2.2.2 Unconsolidated-Undrained Triaxial Compression Tests

Specimens for unconsolidated-undrained triaxial compression tests were prepared by first cutting a 6 or 8-inch long (depending on whether a 2-inch or 2.8-inch diameter specimen was being tested) portion of a sample tube with a horizontal band saw. The soil within the tube was then extruded vertically using a hand-operated hydraulic jack. After extruding, 2-inch specimens were prepared by first cutting the ends of the specimen square. The specimen was then trimmed on a turntable to a diameter of 2 inches. After trimming, the specimen was cut with a wire saw in a miter box to a nominal length of 4 inches. After extruding, 2.8-inch specimens were prepared by cutting the specimen in a miter box with a wire saw to a nominal length of 6 inches.

The moisture content and total unit weight of the soil cut from the ends of the specimen were measured. The length and diameter of the specimen were then measured with dial calipers and the specimen was mounted in a triaxial cell. After mounting, a 0.012-inch-thick latex rubber membrane was placed around the specimen and sealed at the ends with Neoprene o-rings.

Once the specimen was sealed, the triaxial cell was filled with de-aired water and a confining pressure equal to the in-situ total vertical overburden stress was applied to the specimen. The sample was allowed approximately 10 minutes to equilibrate under the confining pressure. After equilibrating, the specimen was sheared in compression at an axial strain rate of approximately 1 percent per minute. Tests were generally carried out to 15 percent axial strain or stopped after the principal stress difference peaked and dropped about 20 percent below the peak value. After the specimen was sheared, the cell was disassembled and water contents were measured at the top, middle, and bottom of the specimen.

2.2.3 Consolidated-Undrained Triaxial Compression Tests

Specimens were prepared for the consolidated-undrained triaxial compression tests using the same procedure used for unconsolidated-undrained tests and described in the previous section. Once the specimen was trimmed to the appropriate dimensions and measured, it was mounted in the triaxial cell. Filter paper discs were placed at the ends of the specimen and filter paper strips were placed around the perimeter of the specimen to facilitate end and radial drainage. Porous stones were boiled in water for approximately 10 minutes, allowed to cool, and then placed at each end of the specimen between the filter paper disc and the acrylic endcap. A latex rubber membrane was then placed around the specimen, sealed at the ends with Neoprene o-rings, and the cell was filled with de-aired water.

Once the cell was filled with water, the specimen was backpressure saturated until the measured pore pressure coefficient *B* (Skempton, 1954) was at least 0.95. This typically took 10 to 15 hours. After backpressure saturation was complete, the specimen was consolidated isotropically under a pressure equal to the in-situ effective overburden stress. Once the end of primary consolidation was reached, the specimen was allowed to rest overnight before shearing.

After resting overnight, the specimen was sheared undrained in compression at a constant rate of deformation. The deformation rate was selected to ensure equalization of pore water pressures throughout the specimen at failure. For a specimen with end and radial drainage, the time to failure, t_f, corresponding to 95 percent pore water pressure equalization was estimated using the following equation derived from consolidation theory (Blight, 1963):

$$t_f = 2 \bullet t_{100} \quad (2.2)$$

where t_{100} is the time for 100 percent consolidation calculated using either log-time or square root-time fitting methods. Also, ASTM (2004) suggests computing the time to failure with the following equation:

$$t_f = 10 \bullet t_{50} \quad (2.3)$$

where t_{50} is the time for 50 percent consolidation calculated using either log-time or square root-time fitting methods. The time to failure was computed using both Equations 2.2 and 2.3 and data from log-time and square root-time fitting methods. A deformation rate was selected based on whichever equation and fitting method gave the longest time to failure.

During the shearing stage, DC voltage signals from the load cell, LVDT, and pressure transducer were read using the data acquisition system and recorded on the personal computer. Tests were carried out to 15 percent axial strain or terminated earlier if the principal stress difference peaked and dropped about 20 percent below the peak value. At the end of the test, the cell was disassembled and moisture contents were determined at the top, middle, and bottom of the specimen.

2.2.4 One-Dimensional Consolidation Test Apparatus

One-dimensional consolidation tests were performed using both incremental load and constant rate of strain test procedures. The first two consolidation tests performed, which were on specimens from Site 2, were incremental load tests, while the third test for Site 2 and all other consolidation tests were constant rate of strain tests.

Incremental load tests were performed using a standard 0.75-inch-high by 2.5-inch-diameter consolidation ring and a Wykeham Farrance Bishop-type consolidation frame. Settlement was measured using an LVDT. DC voltages from the LVDT were recorded using a GEOTAC data acquisition system and a personal computer.

Constant rate of strain consolidation tests were performed using a 1.0-inch-high by 2.5-inch-diameter consolidation ring and backpressure consolidation cell manufactured by Trautwein Soil Testing Equipment. Backpressure and cell pressure were both applied through a pressure panel using an air-over-water accumulator and manufactured by Trautwein Soil Testing Equipment. Axial load was applied to specimens using a GeoJac computer controlled actuator. Settlement was measured using an LVDT. Pore water pressure and cell pressure were both measured using pressure transducers. Axial load was measured using a load cell. DC voltages from the instruments were recorded using a personal computer and GEOTAC data acquisition system.

2.2.5 One-Dimensional Consolidation Tests

Specimens were prepared for both incremental load and constant rate of strain consolidation tests using essentially the same procedure. Specimens were prepared first by cutting a 3-inch portion of a thin-walled sample tube with a horizontal band saw. The soil was then extruded vertically using a hand-operated hydraulic jack. After extruding, a thin layer of

vacuum grease was applied to the inside of the consolidation ring and the soil was trimmed into the ring. The top and bottom of the specimen were then trimmed with a wire saw and smoothed with a steel blade.

For the incremental load consolidation tests, a “standard” procedure was used to load the specimen once it was trimmed into the consolidation ring. A load increment ratio of one was used for the tests and each load was held for 24 hours. Data from the tests were reduced using both log-time and square root-of-time fitting methods. The e-log(p) curve was plotted using the void ratio at the end of each 24-hour load increment.

For constant rate of strain consolidation tests, the specimen was backpressure saturated once it was trimmed into the consolidation ring. After the specimen was saturated, axial load was applied to produce a constant rate of strain. The strain rate was selected to produce a pore pressure ratio of 3 to 15 percent, where the pore pressure ratio is defined as the ratio of the change in pore water pressure to the change in total vertical stress. This resulted in strain rates generally between 0.1 and 1.5 percent per hour. Data from the tests were reduced using the procedure described by Wissa et al. (1971).

Chapter 3. Measurement of Undrained Shear Strength

Undrained shear strength is often measured in the laboratory using unconsolidated-undrained and consolidated-undrained triaxial tests, and in-situ using the field vane shear test. In this chapter, several of the issues affecting undrained shear strengths are first explained and discussed in general. Interpretation of triaxial test and the field vane shear test results is then discussed, as well as how the various issues affecting undrained strengths relate to these tests.

3.1 Issues Affecting Undrained Shear Strength

Undrained shear strengths are influenced by a number of factors including:

- Sample disturbance
- Anisotropy
- Deformation state
- Strain rate
- Sample size

3.1.1 Sample Disturbance

Regardless of whether undrained shear strengths are measured in the laboratory or in-situ they are probably affected to some extent by sample disturbance. In general, specimen disturbance leads to measured strengths lower than what can actually be mobilized in the field.

Specimens tested in the laboratory will experience disturbance due to stress release and possible disruption of natural soil structure caused by sampling and handling in the field, transport to the laboratory, laboratory storage, and specimen preparation. During long-term storage, disturbance may also result from redistribution of water and chemical changes, as well as possible changes in water content if the samples are not properly sealed.

In-situ tests, such as the field vane test, offer the advantage of testing soil in its natural environment and not being influenced by specimen sampling and handling. However, disturbance still remains an issue that must be considered. Destruction of natural soil fabric, displacement of soil, and changes in the effective stresses may occur during the installation of in-situ testing equipment.

3.1.2 Anisotropy

Undrained shear strength also generally depends on the orientation of the failure plane. The most common shear tests used to measure undrained shear strengths of fine-grained soils in the laboratory are triaxial compression, triaxial extension, and direct simple shear. The relationship between each type of test and the failure plane for a typical slip surface in the field is suggested in Figure 3.1. The triaxial compression test simulates the *active* mode of shear in the field, where the major principal stress acts vertically and is increased or the horizontal stress is decreased until failure is occurs. The triaxial extension test simulates the *passive* mode of shear in the field, where the horizontal stress is increased or the vertical stress decreased until failure occurs and the principal stress acts horizontally at failure. Direct simple shear simulates shearing along horizontal portions of the slip surface, where the major principal stress at failure is inclined

at some angle less than 45° from horizontal. Data showing relationships between the normalized undrained shear strength, s_u/σ'_{vc}, where σ'_{vc} is the vertical effective consolidation pressure, and plasticity index are plotted in Figure 3.2 for triaxial compression, triaxial extension, and direct simple shear tests performed on a variety of normally consolidated fine-grained soils. The data show that most normally consolidated fine-grained soils exhibit a substantial degree of undrained shear strength anisotropy, especially lean soils.

While undrained strengths may vary greatly with the orientation of the failure plane, Ladd and DeGroot (2003) note that the strength measured in direct simple shear is approximately equal to the average of the strengths measured in triaxial compression, triaxial extension and direct simple shear for most normally consolidated and lightly overconsolidated fine-grained soils. Therefore, the strength measured in direct simple shear gives an approximate average strength of normally consolidated and lightly overconsolidated fine-grained soils for stability analyses involving circular failure surfaces, while conventional triaxial compression tests may slightly overestimate strengths .

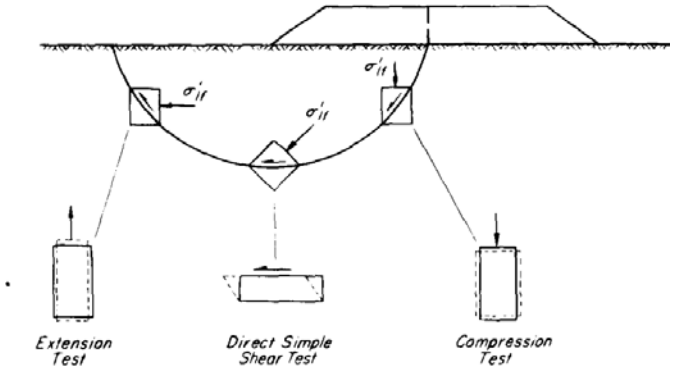

Figure 3.4: Relationship between laboratory tests and shear modes in the field (from Terzaghi, Peck, and Mesri, 1996)

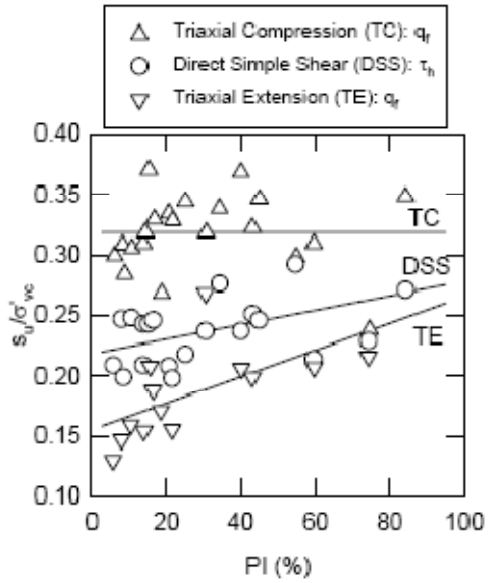

Figure 3.5: Undrained strength anisotropy for normally consolidated silts and clays (from Ladd and DeGroot, 2003)

3.1.3 Deformation State

For many geotechnical structures, such as retaining walls, embankments, and strip footings, the deformation conditions correspond much more closely to plane strain conditions rather than the conditions in triaxial tests. Compared to triaxial deformation conditions, soil particles subject to plane strain deformations will be more constrained and have less freedom to move in any direction. This results in an average increase in undrained strength of approximately 15 percent for plane strain versus triaxial conditions (Ladd and DeGroot, 2003). While this is a significant difference in strength, it is not practical in most cases to perform plane strain tests.

3.1.4 Strain Rate Effects

Undrained shear strengths of fine-grained soils are affected by strain rate or time to failure. This effect has two components, a *viscous* effect and an effect due to partial drainage or consolidation during loading. For short-term failures and failures during construction in the field, loading usually occurs over a period of weeks to months. During this period, some consolidation or expansion may occur, leading to increases or decreases, respectively, in strength. For cases such as embankments or retaining structures on normally or lightly overconsolidated soils, partial drainage will result in consolidation and an increase in undrained shear strength. The opposite is true for cases such as excavations, where partial drainage may lead to swelling and a reduction in undrained shear strength. While partial drainage may occur in the field, the hydraulic conductivity of saturated clays is usually assumed to be low enough that significant drainage will not occur over a typical construction period of several weeks to months.

Even if no drainage occurs, undrained strengths will still depend on the time to failure due to a viscous effect. Data in Figure 3.3 show that the undrained strength of San Francisco Bay mud decreases by about 30 percent as the time to failure increases from 10 minutes to 1 week.

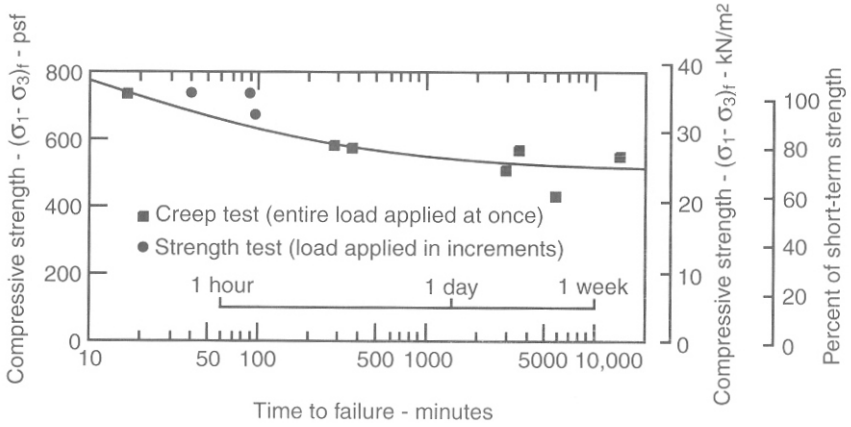

Figure 3.6: Effect of time to failure on undrained strengths of San Francisco Bay mud (from Duncan and Wright, 2005)

3.1.5 Sample Size

Sample size can significantly affect the undrained strength measured in laboratory tests, especially for stiff fissured clays. Data from Peterson et al. (1960) for the Bearpaw Shale, a heavily overconsolidated stiff fissured clay, are shown in Table 3.1. They performed unconfined compression tests on 1.4-inch and 6-inch diameter specimens. Average strengths determined for both sample sizes are reported in the table for a "medium" and "hard" zone of the shale. Depending on the sample size, the strengths varied by as much as a factor of 6.

Table 3.1: Summary of unconfined compressive strength of Bearpaw Shale

Description	Unconfined Compressive Strength, q_u (psi)	
	1.4-inch diameter specimens	6-inch diameter specimens
Medium zone	53 (22*)	20 (16*)
Hard zone	300 (34*)	50 (23*)

* Numbers in parentheses represent the number of specimens tested.

Depending on sample size, tests performed on smaller samples may be measuring the strength of intact clay, while tests performed on larger samples may be influenced by features such as fissures. Although strengths measured in the laboratory can be significantly affected by sample size, this is not a major concern for this research because the focus is on testing intact soft to medium clays.

3.2 Strengths Measured in Triaxial Compression Tests

Undrained strengths measured in the laboratory may not be the same as strengths in the field due to the issues discussed in Section 3.1. The various issues as they relate to triaxial tests are discussed in the following sections.

3.2.1 Sample Disturbance

Sample disturbance can significantly reduce the undrained strength measured in the laboratory. The undrained shear strengths of Chicago clay measured from thin-walled ("Shelby") tube samples and measured on samples trimmed from block samples is shown in Figure 3.4. The undrained shear strengths shown in the figure were measured using unconfined compression tests. The data show that the strength measured on tube samples was approximately 70 percent of the strength measured for specimens trimmed from block samples. While strengths measured in unconfined compression tests are generally more influenced by disturbance than strengths measured in unconsolidated-undrained or consolidated-undrained triaxial tests, the data illustrate the potential magnitude of the effect of disturbance on undrained shear strengths.

In order to overcome the stress relief and strength reduction associated with disturbance, specimens can be tested in consolidated-undrained triaxial tests and consolidated to any desired stress state. The two most commonly used techniques to determine undrained strengths from consolidated-undrained tests are the Recompression method and the SHANSEP method.

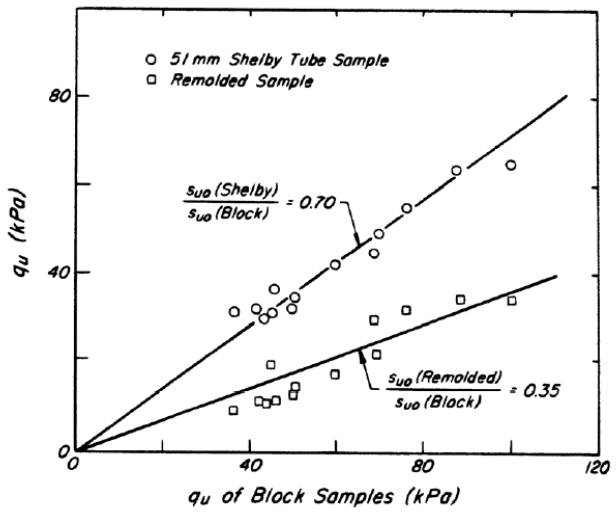

Figure 3.7: Effects of sample disturbance on Chicago Clay (from Terzaghi, Peck, and Mesri, 1996)

In the Recompression method, Bjerrum (1973) proposed reconsolidating specimens to the same vertical and horizontal effective stresses, σ'_{vo} and σ'_{ho}, they carried in-situ. However, this assumes the reduction in water content during consolidation is small enough to produce undrained shear strengths representative of in-situ conditions. Berre and Bjerrum (1973) suggested that for soft clays the volumetric strain during consolidation should be less than 1.5 to 4 percent. If samples are badly disturbed, consolidation can excessively reduce the water content and void ratio, leading to an overestimation of undrained shear strength. This behavior is in contrast to unconsolidated-undrained tests where disturbance reduces the measured strength.

Andersen and Kolstad (1979) suggested that sample quality can be evaluated quantitatively based on the volumetric strain of a specimen in an odometer test subjected to the in-situ vertical effective stress, σ'_{vo}, or a specimen in triaxial test subjected to the vertical and lateral effective stresses the specimen was subjected to in the field. Andersen and Kolstad's

sample quality criteria based on volumetric strain measured in laboratory tests are shown in Table 3.2.

Table 3.2: Sample quality based on volumetric strain measured in laboratory tests (after Andersen and Kolstad, 1979)

		Sample Quality		
		Perfect	Acceptable	Disturbed
Overconsolidation Ratio	Depth (m)	Volumetric Strain (%)	Volumetric Strain (%)	Volumetric Strain (%)
1 – 1.2	0 – 10	< 3.0	3.0 – 5.0	> 5.0
1.2 – 1.5	0 – 10	< 2.0	2.0 – 4.0	> 4.0
1.5 – 2	0 – 10	< 1.5	1.5 – 3.5	> 3.5
2 – 3	0 – 10	< 1.0	1.0 – 3.0	> 3.0
3 – 8	0 – 10	< 0.5	0.5 – 1.0	> 1.0

The SHANSEP method proposed by Ladd and Foott (1974) is based on the observation that the undrained strength of most non-structured clays is governed by the stress history of a given soil deposit. According to the procedure, specimens are consolidated under K_o (at rest) stress conditions to beyond the maximum previous effective stress (*preconsolidation pressure*). For overconsolidated soil, specimens are then unloaded to an appropriate overconsolidation ratio. The relationship between overconsolidation ratio and normalized strength, s_u/σ'_v, is thus established for use in the SHANSEP procedure, which is further discussed in Chapter 4. Once the relationship between the normalized strength and overconsolidation ratio is established, undrained strengths can be computed using appropriate values for the in-situ effective overburden stress, σ'_{vo}, and the maximum previous effective stress.

While it is possible to consolidate specimens to a K_o state of stress, the testing procedure to do so is difficult and time consuming. As a result, it is more common to consolidate specimens isotropically to an effective stress equal to σ'_{vo}. In the standard consolidated-undrained triaxial test, specimens are isotropically consolidated to σ'_{vo} and then sheared in compression while pore water pressures are measured.

3.2.2 Anisotropy

In conventional unconsolidated-undrained and consolidated-undrained triaxial tests, specimens are sheared in compression, simulating the active mode of shear in the field. This leads to undrained strengths being measured on a failure plane inclined at approximately $(45° + \phi'/2)$ from the horizontal plane, or about 60° for most clays. Although much less frequently performed, extension tests, which simulate the passive mode of shear in the field, measure strength on a failure plane oriented at approximately $(45° - \phi'/2)$ from the horizontal plane, or about 30° for most clays.

In the field, the orientation of the failure plane and the mode of shear will usually vary along the slip surface. Strengths measured in triaxial compression tests also tend to be greater than those measured in direct simple shear or triaxial extension for most normally and lightly overconsolidated fine-grained soils. Thus, triaxial compressive strengths may overestimate the average undrained strength mobilized along a particular slip surface.

3.2.3 Deformation State

While triaxial compression tests may tend to overestimate the strength that can be mobilized in the field due to the orientation of the failure plane, they at the same time may underestimate strength due to difference between the triaxial and plane strain deformation states. As was previously discussed, the plane strain conditions that typically exists in the field results in strengths approximately 15 percent greater than for a triaxial deformation state.

3.2.4 Strain Rate Effects

Strain rate effects have two components, one due to partial drainage and one due to a viscous effect. Although partial drainage is usually not a significant source of error in triaxial tests since drainage can be controlled in the laboratory, the viscous effect can lead to significant differences in strengths from triaxial tests and the strength that can be mobilized in the field

In the field, loading occurs over extended periods of time, typically several weeks to months. During unconsolidated-undrained triaxial tests, specimens are sheared quickly, with times to failure of approximately 5 minutes, typically resulting in strengths higher than those which can be mobilized at the strain rates in the field. In conventional consolidated-undrained triaxial tests, specimens are sheared at a much slower rate than in unconsolidated-undrained tests to allow for pore pressure equalization throughout the specimen and accurate measurement of pore water pressures. Times to failure for consolidated-undrained tests are approximately several hours, yielding strengths somewhere between that which can be mobilized in the field and strengths from unconsolidated-undrained tests. The viscous effect is illustrated schematically in Figure 3.5. While the values in the figure are approximate, they illustrate the potential magnitude of the viscous effect for different loading rates. The figure shows that due to the viscous effect, the undrained strength that can be mobilized in the field could be expected to be about 10 percent lower than the strength measured in conventional consolidated-undrained tests. The figure also shows that the strength measured in unconsolidated-undrained tests is about 15 percent greater than the strength measured in consolidated-undrained tests.

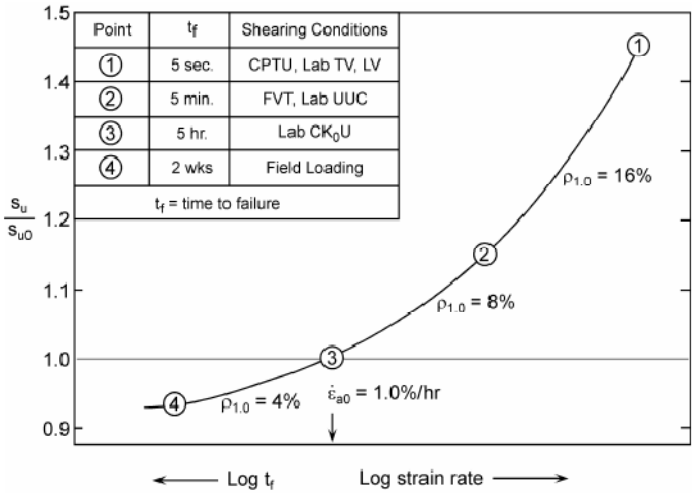

Figure 3.8: Schematic illustration of strain rate effect for normally consolidated clays (from Ladd and DeGroot, 2003)

While specimens in standard consolidated-undrained triaxial tests are sheared at a rate slow enough to allow for accurate pore water pressure measurement and determination of effective stresses, it may be preferable to shear specimens at the same, higher rate used for unconsolidated-undrained triaxial tests if the test is being performed to determine undrained strengths comparable to unconsolidated-undrained test conditions. By shearing specimens in consolidated-undrained and unconsolidated-undrained tests at the same rate, the results from both tests can be compared directly without consideration of strain rate effects. This is especially useful when performing consolidated-undrained tests to assess and reduce the effects of disturbance on undrained strengths measured in the laboratory. However, in practice specimens in consolidated-undrained tests are rarely, if ever, sheared at the same rate used for unconsolidated-undrained tests.

Due to the difference in strain rate, unconsolidated-undrained triaxial tests may yield strengths approximately 10 percent greater than those from consolidated-undrained tests. This difference will likely be offset by various other factors. Given this, the strain rate effect can likely be ignored when comparing strengths from the two tests. Additionally, the effects of relatively fast strain rates during laboratory triaxial testing are probably partially offset by the effects of partial drainage and consolidation during loading in the field

3.2.5 Expression of Undrained Shear Strength

In undrained triaxial tests, the undrained shear strength (s_u) is usually taken as one-half the principal stress difference at failure, i.e.:

$$s_u = \frac{1}{2}(\sigma_1 - \sigma_3)_f \tag{3.1}$$

where $(\sigma_1 - \sigma_3)_f$ is defined as the maximum principal stress difference at an axial strain not to exceed 15 percent (ASTM, 2004; ASTM, 2007b; USACE, 1986). However, the strength of a saturated clay is governed by the effective stress strength parameters ϕ' and c'; and the effective stress on the failure plane at failure. The shear stress on the failure plane at failure, τ_{ff}, is not the same as the maximum shear stress on which Equation 3.1 is based. The shear stress on the failure plane at failure is represented by the point of tangency between the Mohr circle at failure for effective stresses and the effective stress failure envelope, i.e.:

$$\tau_{ff} = \frac{1}{2}(\sigma_1 - \sigma_3)_f \cos\phi' \tag{3.2}$$

For typical values of ϕ', τ_{ff} is 10 to 15 percent lower than s_u defined by Equation 3.1.

3.3 Shear Strengths Measured in Field Vane Shear Tests

Conventional interpretation of field vane shear tests assumes that the soil shears as a cylinder. At failure (peak torque) the undrained shear strength is assumed to be fully mobilized around the vertical perimeter of the vane as well as along the horizontal planes comprising the two ends of the cylinder. For the conventional vane with a height-to-diameter ratio of 2:1 and rectangular blades, this results in the following equation for calculating undrained shear strength from a vane test, $s_{u\text{-}FV}$:

$$s_{u-FV} = \frac{6M}{7\pi D^3} \tag{3.3}$$

where M is the recorded torque and D is the diameter of the vane.

While the field vane shear test is a useful method for measuring the undrained shear strength of soft to medium clays, experience indicates that the undrained strength measured in the test ($s_{u\text{-}FV}$) is not representative of the strength that can be mobilized in the field (s_u) because of factors such as disturbance, anisotropy, stress state, and strain rate effects.

3.3.1 Disturbance

While the vane test has the advantage of testing soil in its natural environment and not being influenced by specimen removal from the ground and handling, disturbance remains an issue that must be considered. In the case of the vane test, disturbance results from soil displacement and alteration of soil fabric caused by insertion of the vane. Insertion of the vane is somewhat analogous to the insertion of a sampling tube. Data presented by Terazaghi, Peck, and Mesri (1996) show a significant decrease in undrained strength measured using the field vane as the thickness of the vane blade increases (Figure 3.6).

Chandler. (1988) found that sensitivity is a controlling factor in the amount of disturbance caused by insertion of the vane. Chandler extrapolated the strength data available for various blade thicknesses to the hypothetical case of zero blade thickness and estimated an "undisturbed" strength 11 percent higher than measured using a standard 1.95-mm-thick blade, such as the blades used in this study.

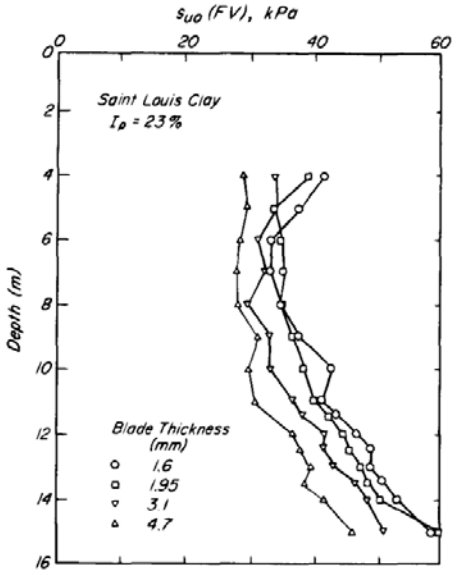

Figure 3.9: Effect of vane blade thickness on measured undrained shear strength (from Terzaghi, Peck, and, Mesri, 1996)

Vane insertion will also generate excess pore water pressures. As the pore pressures dissipate, the soil will consolidate and the undrained strength will increase. Data from Terzaghi, Peck, and Mesri (1996) shows how undrained strength increases with waiting period between vane insertion and rotation (Figure 3.7).

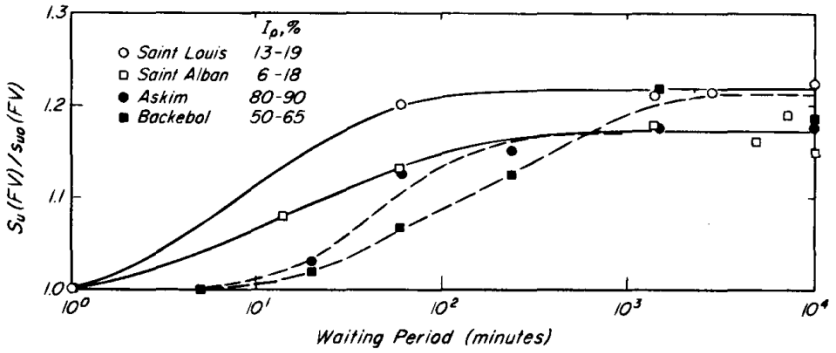

Figure 3.10: Effect of waiting period on undrained shear strength measured using field vane (from Terzaghi, Peck, and Mesri, 1996)

3.3.2 Anisotropy

Because the field vane shear test shears soil on both horizontal and vertical planes, the test reflects some combination of the shear strengths on these two planes. Using the conventional test interpretation for a vane with a height-to-diameter ratio of 2, the torque contributed by the shear resistance on the vertical plane is six times the torque contributed from the shear resistance on the horizontal planes. Thus, shear strength on the vertical plane tends to govern the undrained shear strength measured in the vane test. Chandler (1988) has suggested that deformation conditions on the vertical plane at failure are similar to either direct shear or direct simple shear. While data from direct simple shear tests where specimens are sheared on vertical planes are limited, one study by Karube et al. (1988) found the undrained shear strengths measured using a direct simple shear device were equal along horizontal and vertical planes. Based on this, Chandler suggested the strength measured using the field vane may be analogous to the strength measured in direct simple shear.

3.3.3 Strain Rate Effects

As noted earlier, strain rate has two effects, one related to drainage and the other related to a viscous effect. Both components may affect the undrained strength measured in field vane shear tests.

Partial drainage may occur during the course of the vane test if the vane is not rotated at a rate quick enough to ensure undrained conditions. If the vane is rotated too slowly, excess pore water pressures generated by shear will dissipate leading to consolidation of the soil and an overestimation of the undrained strength. Based on Blight's (1968) approximate theory of consolidation, a time to failure which ensures undrained conditions during the vane test can be estimated. Using Blight's theory, Chandler determined that during the standard test (time to failure of approximately 1 minute) undrained behavior would result in most soils having a coefficient of consolidation of 1,000 square-feet per day or less. Given this, the standard vane test performed in most uniform clays should produce undrained conditions.

In addition to drainage effects during a vane test, rapid shearing during the test may result in a significant viscous effect on the measured undrained strength. A compilation of data from Chandler relating the undrained strength of high plasticity clays to the rate of vane rotation is shown in Figure 3.8. The data indicate that even in the range of undrained loading, as the time to

failure is decreased from 100 minutes to 0.01 minute, the measured undrained strength increases by approximately 45 percent. Over this 4-log-cycle change in strain rate, the undrained strength increases by slightly over 10 percent per log cycle, which is typical for strain rate effects seen in many soft, saturated clays.

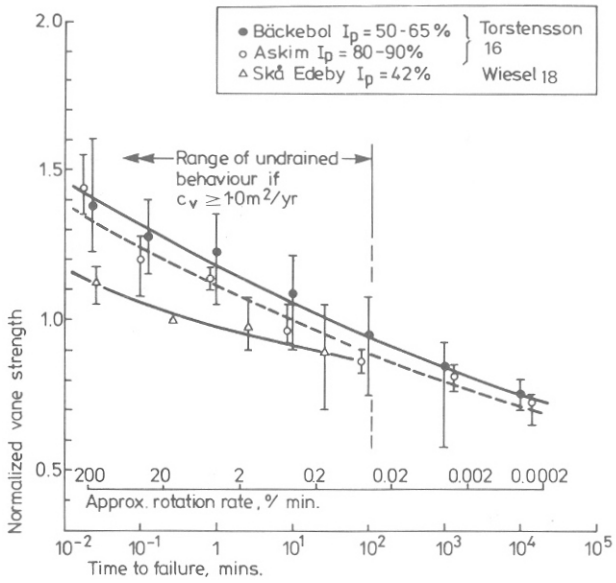

Figure 3.11: Effect of time to failure on strength measured using field vane (from Chandler, 1988)

3.3.4 Field Vane Corrections

Use of the undrained strengths measured in the field vane test for design has resulted in overestimates of the factor of safety leading to unexpected failures. In order to use undrained strengths measured in the vane tests for design, factors such as disturbance, anisotropy, and strain rate effects must be considered and corrected for.

The most widely used correction for field vane shear tests comes from Bjerrum (1972, 1973). Bjerrum computed factors of safety for documented failures of excavations, embankments, and footings using undrained shear strengths measured in field vane shear tests. The computed factors of safety, *FS*, were then plotted against the plasticity indices, I_p, of the soil and a straight line was fit to the data. Based on the plot, Bjerrum suggested using a field vane correction factor $\mu = 1/FS$. Using this relationship, the corrected undrained shear strength, $s_{u\text{-}FVc}$, can be computed as follows:

$$s_{u-FVc} = s_{u-FV}\mu \tag{3.4}$$

Bjerrum's correction and data are shown in Figure 3.9, along with additional data compiled by Terzaghi, Peck, and, Mesri (1996). The additional data show more scatter than the data originally presented by Bjerrum. Terzaghi, Peck, and Mesri suggested this scatter is due to the fact that the data come from different parts of the world and because of variations in the test procedure and equipment used. As shown in the previous sections, variations in blade thickness, duration of waiting period, and rate of rotation can all significantly affect strengths measured with the field vane. Terzaghi, Peck, and Mesri also suggest using an additional reduction factor of 0.85 for organic soils, not including peats.

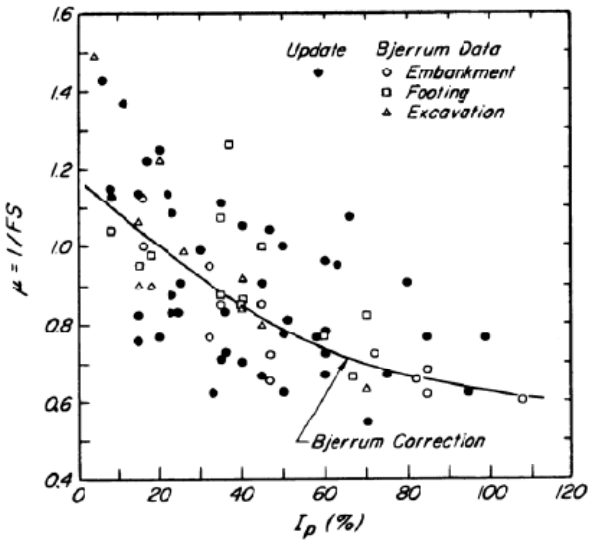

Figure 3.12: Bjerrum's field vane correction factor (from Terzaghi, Peck, and Mesri, 1996)

While the correction factor μ broadly takes into account all the factors that contribute to differences between the undrained shear strength measured using the field vane test and the undrained shear strength that can be mobilized in the field, Bjerrum suggested a more correct procedure where the effects of anisotropy and strain rate could be considered separately, i.e.:

$$\mu = \mu_R \mu_A \tag{3.5}$$

where μ_R is a correction factor for the rate effect which depends on the plasticity index of the clay and μ_A is a correction for the anisotropy of the clay which will depend on the inclination of the failure surface and the plasticity of the clay. Bjerrum's (1973) correction factor is plotted along with his estimates of the correction for rate and anisotropy effects in Figure 3.10. As Figure 3.10 shows, the undrained shear strength measured using the field vane test in low plasticity clays will be slightly higher than the strength that can be mobilized in the field due to the anisotropy of lean clays. For very lean clays, $I_p < 20$, the undrained strength measured using the field vane test may even underestimate mobilized strengths, i.e. $\mu > 1$, due to disturbance associated with vane insertion (Chandler 1988). Figure 3.10 also shows that for high plasticity clays, strain rate effects will lead to mobilized strengths being significantly lower than strengths measured using the field vane test.

Keeping with Bjerrum's idea that it is more accurate to separate the effects of strain rate and anisotropy, Chandler expressed Bjerrum's estimate of the relationship between the correction factor for strain rate effects, μ_R, and plasticity index, I_p, shown in Figure 3.10 with the following equation:

$$\mu_R = 1.05 - b(I_p)^{0.5} \tag{3.6}$$

where the value of b depends on the time to failure, t_f, for which the correction is required. Chandler assumed t_f = 10,000 minutes when fitting this equation to Bjerrum's estimate of μ_R. For t_f = 100 minutes, b = 0.030; for t_f = 10, 000 minutes, b = 0.045. More generally, for 10 minutes < t_f < 10,000 minutes:

$$b = 0.015 - 0.0075 \log t_f \tag{3.7}$$

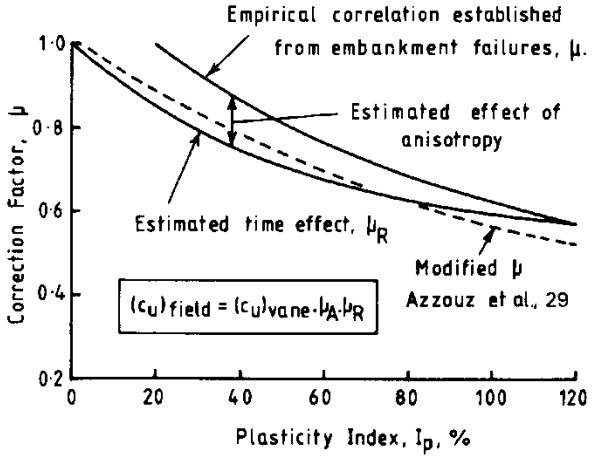

Figure 3.13: Bjerrum's estimate of corrections for rate and anisotropy effects (from Chandler, 1988)

Chandler compared his expression for μ_R to data collected from field vane tests (Figure 3.11) with times to failure of 10,000 minutes and 100 minutes and found an apparent close agreement between the two. While Chandler thought this agreement may be fortuitous, he did believe it confirmed the relative magnitude of the rate effect and its dependence on plasticity. ASTM (2007a) suggests using the correction factor given in Equation 3.6 with $b = 0.045$ (t_f = 10, 000 minutes).

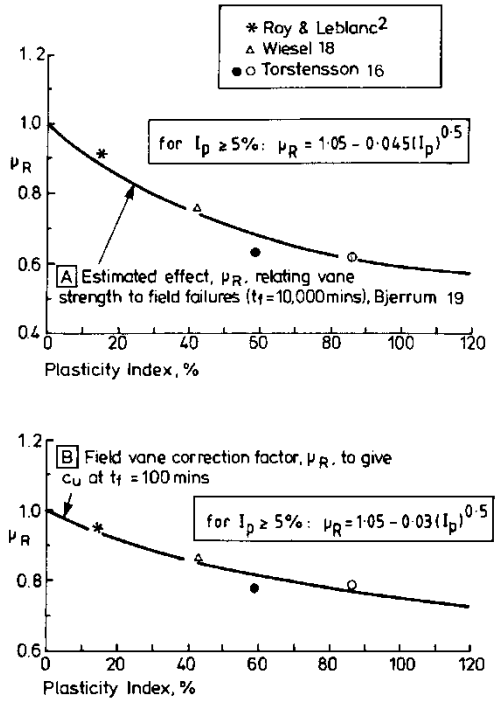

Figure 3.14: Comparison of μ_R determined from field vane tests with t_f = 10,000 minutes and t_f = 100 minutes with estimate of μ_R (from Chandler, 1988)

Although Chandler and Bjerrum each attempted to separate the correction factors for anisotropy (μ_A) and strain rate effects (μ_R), doing so seems to be unnecessary and impractical. Bjerrum was only able to estimate the factor μ_R. Also, the correction factor μ_A will depend on the orientation of a given failure surface, i.e., it will likely vary along the length of a slip surface in the field. Additionally, Chandler was only able to verify the relative magnitude of Bjerrum's estimate of μ_R. Given that Bjerrum's correction factor μ is based on strengths back-calculated from actual failures in the field, this correction seems to be more practical and reliable. The correction factor μ also has the advantage of not only accounting for anisotropy and strain rate effects, but it also probably accounts for other sources of error, such as disturbance associated with vane insertion and progressive failure during full-scale loading in the field.

3.4 Summary of Undrained Shear Strength Testing

Both field and laboratory measurements of undrained shear strengths are subject to errors. In both triaxial and field vane shear tests, some of these errors tend to be offsetting. For example, the effects of disturbance may reduce undrained strengths from unconsolidated-undrained tests by approximately 20 to 30 percent, but the relatively fast shearing rate in the test may result in an overestimate of the undrained strength by a similar amount.

In laboratory triaxial tests, corrections are not consistently applied for the effects of issues such as disturbance, anisotropy, deformation state, strain rate, and sample size. Depending on sample quality, unconsolidated-undrained tests probably tend to underestimate undrained strengths, but to an unknown degree. However, procedures like SHANSEP and Bjerrum's recompression technique can be used with consolidated-undrained tests to reduce effects of disturbance observed in unconsolidated-undrained tests. If consolidated-undrained compression tests are used to reduce effects of disturbance, consideration may also need to be given simultaneously to anisotropy and strain rate effects which may lead to an overestimation of undrained strengths. Although the sources of error in triaxial testing, such as sample disturbance, anisotropy, deformation state, strain rate, and sample size, can be considered individually and strengths adjusted accordingly, the typical interpretations of unconsolidated-undrained and consolidated-undrained triaxial tests have been and continue to be successfully applied in practice without usually resulting in failures. For cases where an unusually low factor of safety is used, more rigorous testing and analysis is likely required. In these cases, the various sources of error discussed in this chapter may need to be considered and accounted for.

When using strengths measured with the field vane for design, experience indicates these strengths should be corrected because field vane tests tend to overestimate the strength in the field. It is common practice to correct field vane strengths with Bjerrum's correction factor μ based on the plasticity index of the soil. This correction probably accounts for strain rate and anisotropy effects, as well as possibly other factors, such as disturbance and progressive failure. However, it should be noted that there is significant scatter in the data used to develop Bjerrum's correction factor. In the end, judgment is required to establish appropriate design undrained shear strengths based on all the available data.

Chapter 4. Piezocone Penetration Testing

Multiple piezocone penetration test soundings were performed at most of the sites to supplement other field and laboratory undrained strength tests and to define better the lateral variability in the subsurface stratigraphy. Compared to traditional drilling, sampling, and testing, the piezocone penetration test has the advantage of providing nearly continuous data. Multiple piezocone soundings can also be performed at a site without significant cost or time requirements. For this research, emphasis was placed on the ability of the piezocone to define the undrained shear strength profile for each site.

4.1 Correction of Piezocone Penetration Resistance

During piezocone soundings, measurements of cone resistance, q_c, friction sleeve resistance, f_s, and pore water pressure at the shoulder of the cone, u_2, were recorded at 2-cm intervals. Because of the geometry of the cone penetrometer, pore water pressures act on the recessed area behind the cone. Therefore, the total force due to pore water pressures acting on the tip of the cone includes forces due to water pressures on the face of the cone and on the smaller area behind the back edge of the cone. This is referred to as the "unequal area effect" and is illustrated in Figure 4.1.

Correcting cone resistance for the effect of pore water pressures and unequal areas is important, especially in soft, fine-grained, saturated soils, where pore water pressures can be large in relation to the cone resistance (Lunne et al., 1997). The corrected total cone resistance, q_t, can be calculated using the following equation:

$$q_t = q_c + u_2(1-a) \tag{4.1}$$

where a is the area ratio, which is approximately equal to the cross-sectional area of the load cell or shaft, A_n, divided by the projected area of the cone, A_c, as shown in Figure 4.1. Ideally, the area ratio should be as close to 1.0 as possible. Southern Earth Sciences performed testing at Sites 1, 2, and 3 with a cone having an area ratio (*a)* of 0.8. Fugro Geosciences performed testing at Site 4 with a cone having an area ratio of 0.59.

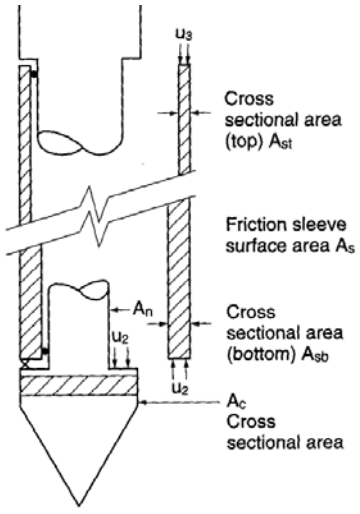

Figure 4.15: Illustration of unequal area effect resulting from geometry of cone (from Lunne et al., 1997)

4.2 Soil Stratigraphy and Classification

Data from piezocone penetration tests can be used to estimate soil stratigraphy and layering. Traditionally, soil classification from piezocone penetration data has been performed using the corrected total cone resistance (q_t) and the friction ratio, f_r, defined as:

$$f_r = \frac{f_s}{q_t} \tag{4.2}$$

where f_s is the sleeve friction. Since friction sleeve resistance measurements are generally less reliable than cone resistance measurements, Robertson et al. (1986) suggested classification could be performed using the friction ratio as well as a pore water pressure ratio, B_q, defined as:

$$B_q = \frac{u_2 - u_o}{q_t - \sigma_{vo}} \tag{4.3}$$

Robertson et al. established a database of piezocone penetration test results in various soil types and developed 12 *zones* based on soil behavior type. Based on the data, they then developed two soil classification charts, one relating cone resistance and friction ratio to soil type, and another relating cone resistance and the pore water pressure ratio to soil type. These charts are shown in Figure 4.2. Classification performed with each chart may sometimes disagree with one another. In these cases, Robertson et al. suggest selecting a soil zone based on judgment. Lunne et al. (1997) also suggested that total unit weights can be approximated using the soil classification charts shown in Figure 4.3 and the total unit weights for each zone given based on Table 4.1.

The classification charts developed by Robertson et al. were used in this study to judge lateral variations in the subsurface profile and stratigraphy at each site where piezocone penetration tests were performed. All soil classification was performed using the friction ratio since any additional accuracy gained from performing classification with the pore pressure ratio was deemed unnecessary. The approximate unit weights given in Table 4.1 were also used to compute the in-situ overburden pressure when reducing data from piezocone penetration tests.

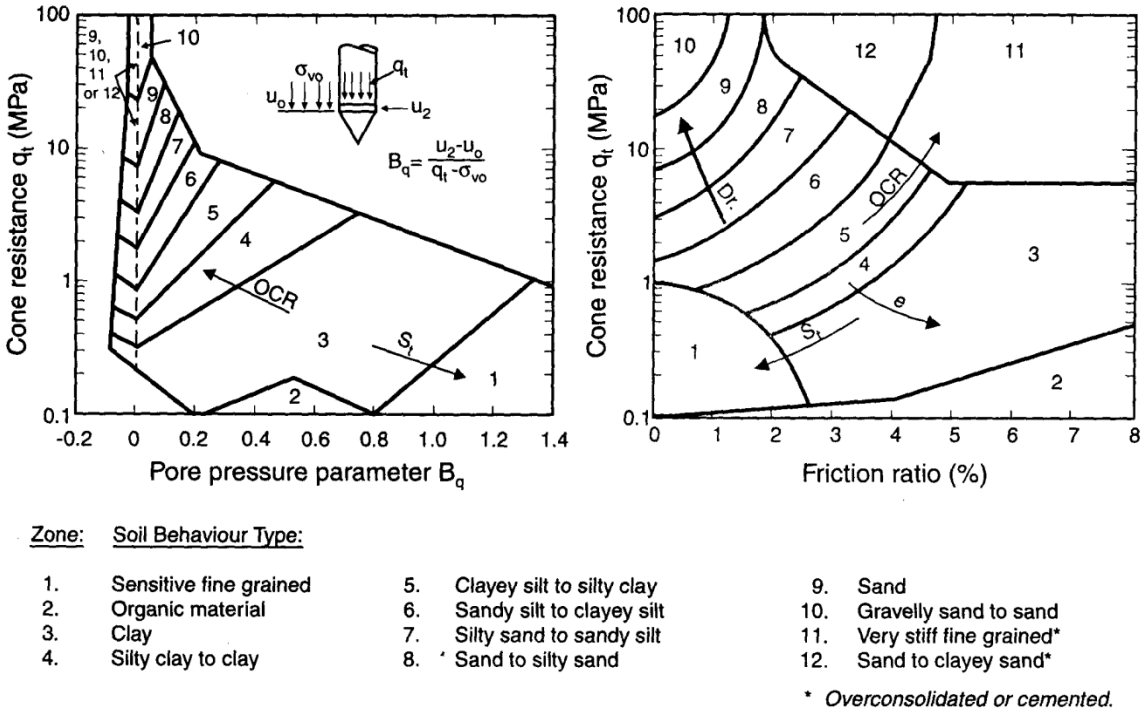

Figure 4.16: Robertson et al. (1986) classification charts (from Lunne et al., 1997)

Table 4.3: Estimate of unit weights based on soil zone from Figure 4.2

Zone	Approximate unit weight (pcf)
1	111
2	80
3	111
4	114
5	114
6	114
7	118
8	121
9	124
10	127
11	130
12	121

4.3 Determination of Undrained Shear Strength

The piezocone has the advantage that, unlike traditional sampling and laboratory testing, results are not influenced by sampling disturbance. Additionally, an undrained shear strength profile can be defined by the piezocone with significantly less time and effort than required for traditional sampling and laboratory tests. Furthermore, the undrained strength profile is

continuous rather than based on strengths at only a relatively few points where samples have been taken and tested

A variety of methods have been described in the literature for calculating the undrained shear strength, s_u, from piezocone penetration tests. These methods can be divided into theoretical solutions and empirical relationships. Given that cone penetration is a complex phenomenon and theoretical methods are limited in their ability to accurately model soil behavior, empirical relationships are preferred, more widely used, and the only methods considered for this research. These empirical relationships involve either direct or indirect correlations between cone penetration resistance and undrained shear strength. Direct and indirect discussed separately below.

4.3.1 Direct Empirical Correlations for Undrained Shear Strength

Several empirical relationships exist for relating undrained shear strength to cone penetration resistance. These empirical relationships can be divided into three main categories, those based on:

1) *net* cone resistance,

2) *effective* cone resistance, or

3) *excess* pore water pressure.

Net Cone Resistance

It is common practice to relate s_u to a *net* cone resistance, where net cone resistance is defined as (q_t - σ_{vo}) and σ_{vo} is the in-situ total overburden stress. Undrained shear strength is related to the net cone resistance by the equation:

$$s_u = \frac{q_t - \sigma_{vo}}{N_{kt}} \qquad (4.4)$$

where N_{kt} is an assumed constant. A relatively large number of studies have been performed to determine appropriate values of N_{kt}. Sampling and testing methods used in such studies vary, making comparison slightly difficult. The bulk of studies show N_{kt} increasing with the plasticity index of the soil and ranging from about 10 to 20 in intact clays (Lunne et al., 1997). The large range in values of N_{kt} is certainly affected by testing and sampling methods, reinforcing the need to use a consistent test method and to minimize effects of sampling.

Some of the highest-quality data available come from Karlsrud et al. (2005). They analyzed a database of sixteen Norwegian sites and one United Kingdom site. High-quality samples were taken with the Sherbrooke block sampler (Lefebvre and Poulin, 1979) and undrained shear strength was determined using K_o consolidated-undrained triaxial compression tests. Their results showed N_{kt} depended on overconsolidation ratio, sensitivity, and plasticity. The data from their study along with their proposed relationship for N_{kt} is shown in Figure 4.3. For the clays tested, N_{kt} ranged from about 5 to 16. This is slightly lower than the range of 10 to 20 previously reported in literature. Karlsrud et al. likely found lower values of N_{kt} since they tested high-quality samples which would give higher strengths. Despite the quality of the testing and sampling, there is still significant scatter in their data. The undrained strength calculated using their correlations was typically ± 15 percent of the strength measured in triaxial tests for

high sensitivity clays and ± 30 percent the strength measured in triaxial tests for low sensitivity clays.

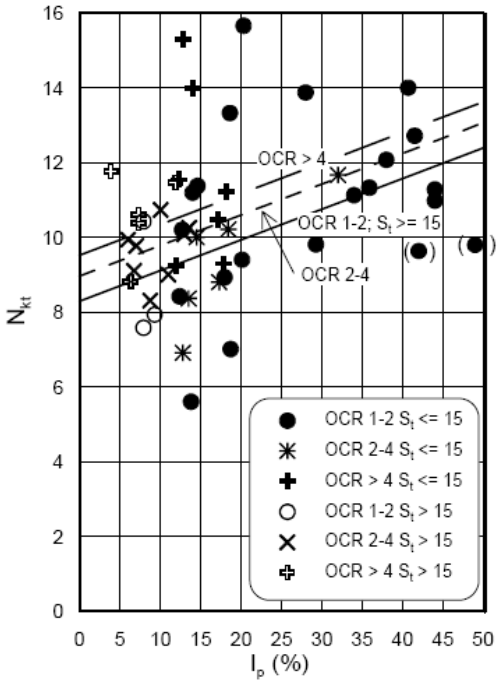

Figure 4.17: Relationship between plasticity index and N_{kt} (from Karlsrud et al., 2005)

Effective Cone Resistance

Attempts have also been made to correlate s_u with an *effective* cone resistance, defined as ($q_t - u_2$), although this is much less common than relating s_u to net cone resistance. The relationship between the undrained shear strength and effective cone resistance is expressed by the following equation:

$$s_u = \frac{q_t - u_2}{N_{ke}} \tag{4.5}$$

where N_{ke} is an assumed constant. Although studies have shown N_{ke} to be independent of stress history and plasticity, Lunne et al. (1997) advised against using the effective cone resistance to estimate undrained shear strength in soft normally consolidated clays on the basis that the pore water pressure generated behind the cone may be 90 percent or more of the measured cone resistance. This leads to the effective cone resistance being a very small quantity, sensitive to small errors in measured cone resistance and pore water pressure.

Excess Pore Water Pressure

The third direct empirical method to estimate the undrained shear strength relates s_u to the *excess* pore water pressure, defined as ($u_2 - u_o$), where u_o is the in-situ equilibrium pore water pressure. Undrained shear strength is related to excess pore water pressure by the equation:

$$s_u = \frac{u_2 - u_o}{N_{\Delta u}} \tag{4.6}$$

where $N_{\Delta u}$ is an assumed constant. Several theoretical and semi-theoretical studies based on cavity expansion theory have shown that $N_{\Delta u}$ ranges from approximately 2 to 20 (Lunne et al., 1997). Using K_o consolidated-undrained triaxial compression tests as a reference for undrained shear strengths, Lunne et al. (1985) found $N_{\Delta u}$ correlated well with the pore water pressure ratio, B_q (Equation 4.3). Values of $N_{\Delta u}$ varied between 4 and 10 for North Sea clays. Using uncorrected field vane strength as a reference for the undrained shear strength of three Canadian clays, La Rochelle et al. (1988a) found $N_{\Delta u}$ varied between 7 and 9, while the overconsolidation ratio ranged from 1.2 to 50. Karlsrud et al. (1996) used anisotropically consolidated-undrained triaxial compression tests on block samples for reference strengths and found $N_{\Delta u}$ varying from 6 to 8 with no clear relationship between $N_{\Delta u}$ and B_q for normally to lightly overconsolidated clays.

4.3.2 Indirect Empirical Correlations for Undrained Shear Strength

While the net cone resistance along with the constant N_{kt} is widely used in practice to determine undrained shear strengths from piezocone soundings, the parameter N_{kt} itself can vary significantly from site to site. Despite substantial research focused on determining appropriate values of N_{kt}, no clear consensus has been reached. This is in large part because the undrained shear strength is not a unique value and will depend on the testing methods used to determine reference strengths as discussed earlier in Chapter 3. Mayne (2007) suggests an alternative and rational approach in which piezocone penetration tests are used to determine the maximum previous effective stress, σ'_p, and these values are then used in conjunction with a normalized undrained shear strength relationship. Several normalized undrained shear strength relationships exist and may be used for this purpose.

Normalized Strength Relationships

The undrained shear strength (s_u) is frequently expressed in normalized form as s_u/σ'_{vo}, where σ'_{vo} is the in-situ effective overburden stress. These normalized values are also widely referred to as "*c/p*" ratios. For normally consolidated clays, Skempton (1957) suggested the *c/p* ratio could be related to the plasticity index as shown in Figure 4.4.

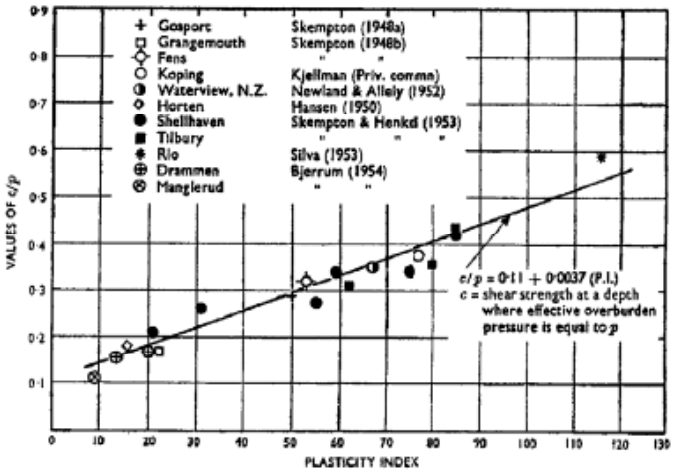

Figure 4.18: Relationship between c/p ratio and plasticity index suggested by Skempton (1957)

Undrained strengths can also be normalized to the maximum previous effective stress (σ'_p). In Figure 4.5, data are presented showing the relationship between values of undrained strengths normalized to the maximum previous effective stress, s_u/σ'_p, and plasticity index for normally to lightly overconsolidated fine-grained soils. In this case, the undrained shear strengths were determined from field vane tests, although other measures could be used. Figure 4.5 includes the relationship between s_u/σ'_p based on field vane tests and plasticity index suggested by Bjerrum (1973).

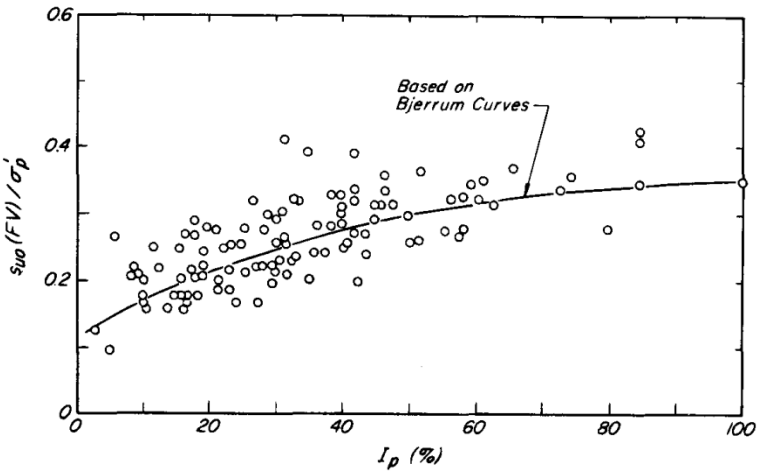

Figure 4.19: Relationship between s_u/σ'_p and plasticity index (from Terzaghi, Peck, and Mesri, 1996)

Normalized strengths can also be applied to overconsolidated soils. Data from Ladd and Foot (1974) showing the variation of s_u/σ'_v with overconsolidation ratio, *OCR*, are shown in Figure 4.6 for five clays with a range of index properties. Overconsolidation ratio is defined as the ratio of the maximum previous effective stress, σ'_p, to the present vertical effective stress, σ'_v, i.e.:

$$OCR = \frac{\sigma'_p}{\sigma'_v} \qquad (4.7)$$

Figure 4.6 is based on undrained strengths measured using consolidated-undrained direct simple shear tests. The data for the various soils all show a similar trend of increasing values of s_u/σ'_v with overconsolidation ratio. The same trend is seen when the undrained shear strength is measured using other types of tests, however the values of s_u/σ'_v are different due to the effects of anisotropy, deformation state, and probably other factors as well.

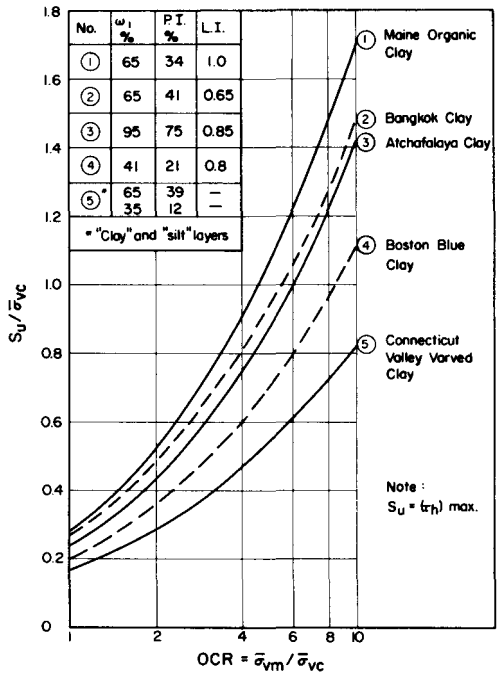

Figure 4.20: Variation of s_u/σ'_v with overconsolidation ratio for 5 clays (from Ladd and Foott, 1974)

Ladd and Foott found that the relationship between s_u/σ'_v and *OCR* could be expressed by an empirical equation of the form:

$$\frac{s_u}{\sigma'_v} = S \times OCR^m \tag{4.8}$$

where *S* is the value of s_u/σ'_v for a normally consolidated soil and *m* is an exponent. Equation 4.8 can also be written in the form:

$$s_u = S \times OCR^m \sigma'_v \tag{4.9}$$

Ladd and DeGroot (2003) indicate that for most soils, *m* is nearly constant and approximately 0.8. They also recommend using a value of 0.22 for *S* for most homogeneous inorganic clays. For organic soils, not including peats, they recommend a value of 0.25.

Mesri (1975, 1989) found that the undrained shear strength of normally consolidated and lightly overconsolidated clays (overconsolidation ratio less than 2) could be expressed practically independent of plasticity by combining Bjerrum's (1973) proposed relationship (see Figure 4.6) between $s_{u\text{-}FV}/\sigma'_p$ and plasticity with Bjerrum's correction factor μ (see Figure 3.9). This relationship led to the following equation:

$$s_u = s_{u-FV}\,\mu = 0.22\sigma'_p \tag{4.10}$$

For organic soils, Teraghi, Peck, and Mesri note that Equation 4.10 will tend to under-predict s_u due to the reinforcing effect of organic matter. For these soils, they suggest the constant 0.22 in Equation 4.10 should be replaced by 0.26.

Maximum Previous Effective Stress (Preconsolidation Pressure)

Equations 4.9 and 4.10 both require that the maximum previous effective stress (σ'_p) be known to compute undrained shear strength. Several methods are available to determine the maximum previous effective stress from piezocone penetration tests. The available methods can be divided into the following three general categories:

1) methods based on *net* cone resistance,
2) methods based *effective* cone resistance, and
3) methods based on *excess* pore water pressure.

Net Cone Resistance

The most widely used and preferred method to determine σ'_p relates maximum previous effective stress to net cone resistance by an equation of the form:

$$\sigma'_p = \frac{(q_t - \sigma_{vo})}{N_{\sigma t}} \tag{4.11}$$

where $N_{\sigma t}$ is an assumed constant. Using this relationship, Powell et al. (1988) found an average value of 3.33 for $N_{\sigma t}$ with a range of 2 to 5. Chen and Mayne (1996) suggested a value of 3.28 for $N_{\sigma t}$ for data that showed significant scatter. A later compilation of data by Mayne (2007) showed an average value of approximately 3 for $N_{\sigma t}$ in intact clays (Figure 4.7).

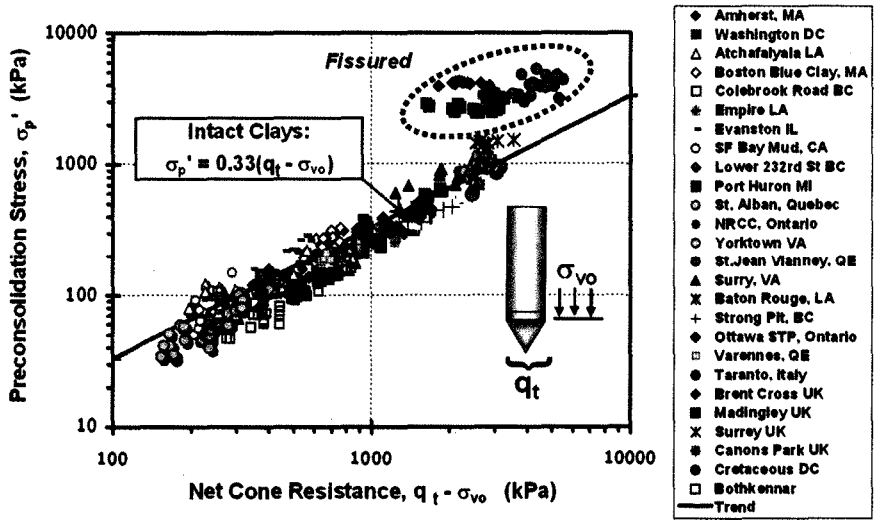

Figure 4.21: Compilation of data relating σ'_p to net cone resistance (from Mayne, 2007).

Effective Cone Resistance

The maximum previous effective stress, σ'_p, has also been related to the effective cone resistance by the following equation:

$$\sigma'_p = \frac{q_t - u_2}{N_{\sigma e}} \tag{4.12}$$

where $N_{\sigma e}$ is an assumed constant. Chen and Mayne (1996) reported a value of 0.5 for $N_{\sigma e}$ for a compilation of 84 worldwide sites. Larsson and Mulabdic (1991) reported a value of 1.0 for $N_{\sigma e}$ in Scandinavian clays. They also found that $N_{\sigma e}$ ranged from 0.5 to 1.0 when additional data from heavily overconsolidated soils from the United Kingdom were included. Interestingly, Larsson and Mulabdic observed significant scatter in values for $N_{\sigma e}$ when σ'_p was less than 3,100 psf. A similar trend was observed by Demmers and Leroueil (2002). For eastern Canadian clays, they found significant scatter in the relationship between $(q_t - u_2)$ and σ'_p measured in the laboratory for values of σ'_p less than 4,200 psf. This scatter may be due to the fact that the effective cone resistance in soft, normally consolidated clays will be a small quantity and sensitive to small errors in the measured cone resistance and pore water pressure. Considering that σ'_p for the shallow, soft clays that are the focus of this study will typically be less than 4,200 psf, any correlations between $(q_t - u_2)$ and σ'_p do not appear to be reliable for use in this research.

Excess Pore Water Pressure

Several methods have also been proposed to determine the maximum previous effective stress based on excess pore water pressures. Most relationships described in the literature relate σ'_p to the excess pore water pressure by the relationship:

$$\sigma'_p = \frac{(u_2 - u_o)}{N_{\sigma u}} \tag{4.13}$$

where $N_{\sigma u}$ is an assumed constant. The correlations based on excess pore water pressures are generally less reliable than correlations based on either net or effective cone resistance and the data show more scatter (Demers and Leroueil, 2002). The lack of reliability can be seen extensive collections of data reported by Mayne and Holtz (1988), Kulhawy and Mayne (1990), and Chen and Mayne (1996). The fact that σ'_p cannot be related to measured excess pore water pressures is also supported by Campanella and Robertson (1988), who found no unique relationship between overconsolidation ratio and measured pore water pressures. They suggested the poor correlation was "…because the pore pressures measured at any location are also influenced by clay sensitivity, preconsolidation mechanism, soil type and local heterogeneity."

4.3.3 Recommendations for Determination of Undrained Shear Strength

While several methods exist for determining undrained shear strength directly from piezocone penetration test results, the methods all rely on highly variable parameters. For example, the constant N_{kt} has been shown to range from 5 to 20, depending on various soil properties. However, the maximum previous effective stress can be determined fairly accurately based on the effective cone resistance in intact clays without the use of site specific correlations. Mayne's (2007) compilation of data suggests a value of 3 for the constant $N_{\sigma t}$ for a broad variety of soils.

Once the maximum previous effective stress has been determined, undrained shear strength can be determined using normalized strength relationships. The relationships given in Equations 4.9 and 4.10 are well-established and based on extensive laboratory testing and back-analyses of failures that are strongly representative of the undrained shear strength that can be mobilized in the field. Based on the review of the available correlations, undrained strengths were determined in this study from piezocone penetration test results by determining the

maximum previous effective stress and vertical effective overburden stress from the piezocone penetration test and using these values in the empirical undrained strength relationship shown in Equations 4.9. Although Equation 4.9 was used throughout the course of this study, Equation 4.10 may be preferred in normally to lightly overconsolidated clays for the sake of simplicity.

Chapter 5. Undrained Shear Strength Profiles

Undrained shear strength profiles, including upper and lower bounds, were developed for each site based on the results of the laboratory and field tests. Representative undrained shear strength profiles were selected based on judgment and the evaluation and interpretation of results of field and laboratory tests. These profiles are referred to as the *average* undrained shear strength profiles. These average profiles, and upper and lower bounds are presented along with an overview of site conditions in this chapter. A more detailed description of site geology and subsurface conditions is given by Garfield (2008).

5.1 Interpretation of Strength Test Data

For each site, a subsurface profile was developed based on observations of specimens recovered from tube samples. Undrained shear strengths were determined from:

- Piezocone penetration tests
- Field vane shear tests, and
- Unconsolidated-undrained and consolidated-undrained
- triaxial compression tests.

5.1.1 Piezocone Penetration Test

Undrained strengths were determined from piezocone penetration tests using the following equation, previously discussed in Chapter 4:

$$s_u = S \times OCR^m \sigma'_{vo} \tag{5.1}$$

where S is a constant, OCR is the overconsolidation ratio, m is an exponent, and σ'_{vo} is the in-situ effective overburden stress. Based on the recommendation of Ladd and DeGroot (2003), a value of 0.22 was used for S when inorganic clays were encountered. For organic clays, a value of 0.25 was used. A value of 0.8 was used for the exponent m at all sites.

To determine the overconsolidation ratio used in Equation 5.1, the maximum previous effective stress (σ'_p) was first determined from the net cone resistance and the following equation:

$$\sigma'_p = \frac{(q_t - \sigma_{vo})}{N_{\sigma t}} \tag{5.2}$$

where q_t is the corrected cone resistance and σ_{vo} is the in-situ overburden stress. A value of 3 was used for the parameter $N_{\sigma t}$. The in-situ effective overburden stress (σ'_{vo}) was computed based on the soil classification zones and total unit weights described by Robertson et al. (1986). Pore water pressures were determined from observation of ground water levels at the sites. The overconsolidation ratio was then computed as σ'_p/σ'_{vo}.

5.1.2 Field Vane Shear Test

When field vane shear tests were performed, the corrected undrained shear strength ($s_{u\text{-}FVc}$) was computed using the undrained shear strength measured in the vane test ($s_{u\text{-}FV}$) and Bjerrum's correction factor (μ.) For vane tests performed in organic clay, such as those at Site 4,

an additional reduction factor of 0.85 was used, as recommended by Terzaghi, Peck, and Mesri (1996) since the fiber content of organic soils may act as localized reinforcement or drainage veins and lead to vane strengths that are too high. Sensitivities, S_t, were computed by taking the ratio of the undisturbed undrained shear strength to the remolded undrained shear strength ($s_{u\text{-}FV,\ r}$) measured in the vane test. From this point forward, unless otherwise noted, all strengths indicated as measured using the field vane test refer to the strength corrected using Bjerrum's (1972) correction factor μ.

5.1.3 Undrained Triaxial Compression Tests

In unconsolidated-undrained and consolidated-undrained triaxial compression tests, the undrained shear strength was taken as one-half the principal stress difference at failure, i.e.:

$$s_u = \frac{1}{2}(\sigma_1 - \sigma_3)_f \tag{5.3}$$

where $(\sigma_1 - \sigma_3)_f$ is defined as the maximum principal stress difference at an axial strain not to exceed 15 percent (ASTM 2004; ASTM, 2007b; USACE, 1986).

5.2 Site 1

The first site where an undrained shear strength profile was developed is located within the West Crane Bayou, just west of Lake Sabine, in Port Arthur, Texas. Beginning at the ground surface, the subsurface profile consists of a 6-foot-thick layer of sandy clay fill, a 4-foot-thick layer of rock fill, a 3-foot-thick layer of fat clay, a 3-foot-thick layer of lean clay with sand and silt seams, a 4-foot-thick layer of medium dense sand with calcareous nodules and clay pockets, and a layer of fat clay with silt pockets extending to the sampling depth of 26 feet. The ground surface at the site ranges from approximately El. +8 to +17 feet. The ground surface at the location of the boring where tube samples were taken is approximately El. +10 feet. At the time field work was performed, the groundwater table was observed to be at the ground surface of the boring where tube samples were taken. No one-dimensional consolidation tests were performed on specimens from Site 1.

5.2.1 Piezocone Penetration Testing

Five piezocone penetration test soundings, labeled FB1 through FB5, were performed at Site 1. Overconsolidation ratios determined from the piezocone soundings are plotted versus elevation for soundings FB1 through FB5 in Figure 5.1. Depths where soils were encountered for which undrained strengths were not considered applicable are indicated by gray shading. The overconsolidation ratio profiles shown in Figure 5.1 indicate an approximately 10-foot-thick crust of heavily overconsolidated clay. Below the crust, all five piezocone soundings indicate an overconsolidation ratio of about 1.5 from El. 0 to -6 feet (10 to 16 foot depth) and approximately 8 from El. -10 to -16 feet (20 to 26 foot depth). It would not be typically expected for the overconsolidation ratio to increase with depth. This increase is likely due to a larger portion of sand and the resulting increase in cone penetration resistance at greater depths. Undrained shear strengths were determined from the piezocone soundings using Equation 5.1 and are shown in Figure 5.2. Horizontal gray bands in this figure indicate depths where undrained shear strengths are not considered applicable.

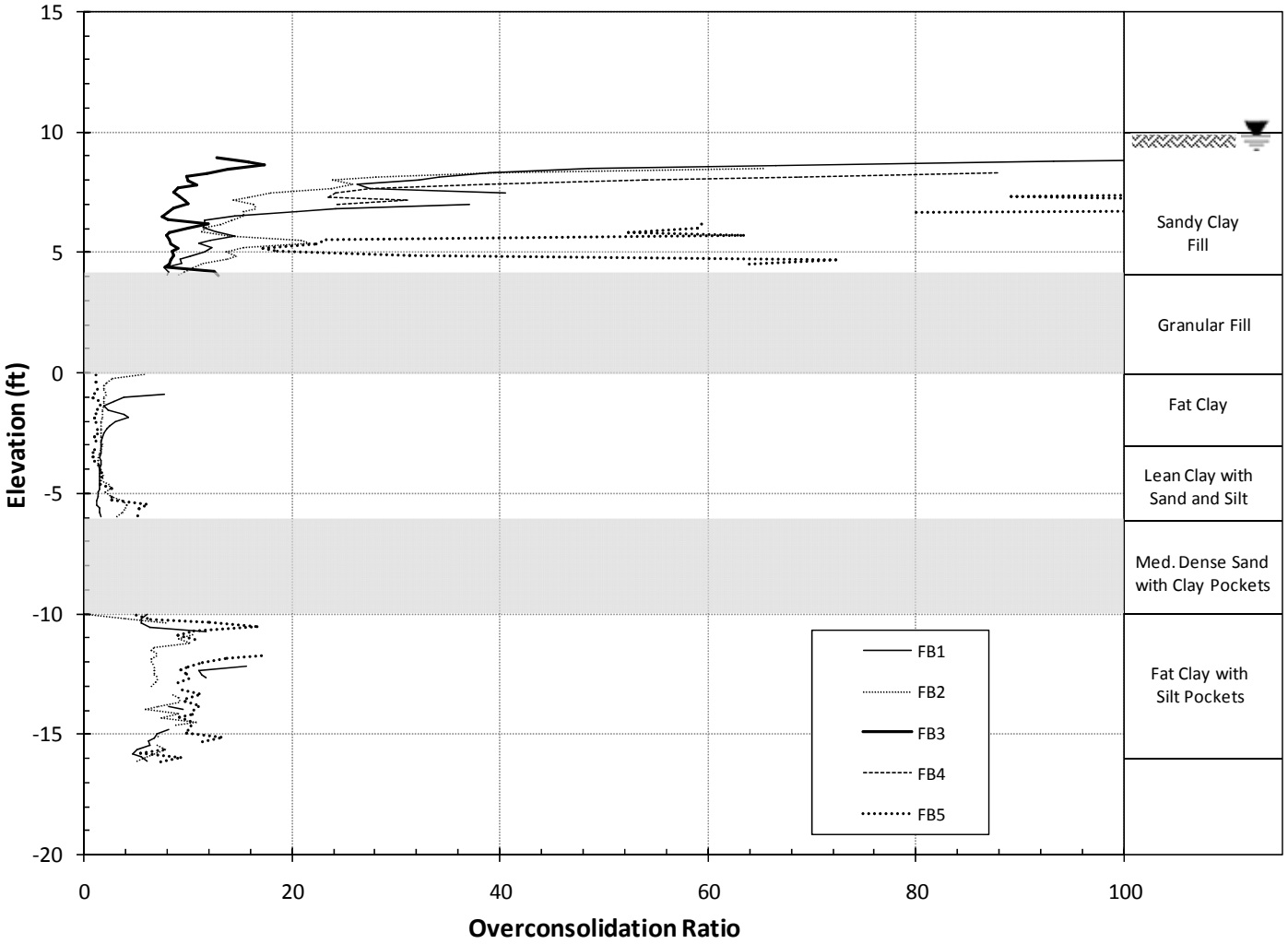

Figure 5.22: Overconsolidation ratio profiles determined from piezocone soundings at Site 1

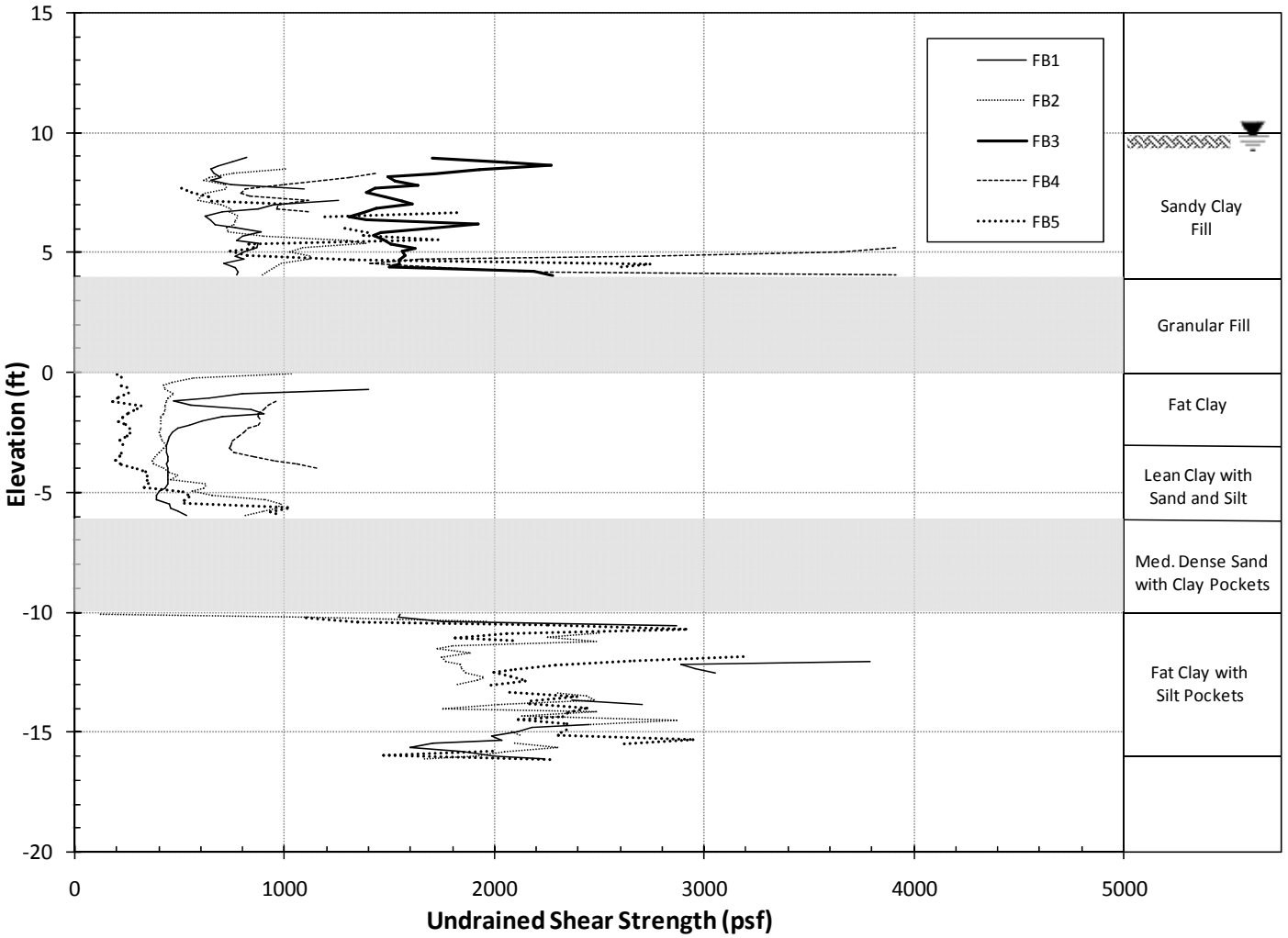

Figure 5.23: Undrained shear strength profiles determined from piezocone soundings at Site 1

The piezocone soundings were spaced at approximately 100-foot intervals horizontally along a nearly straight line. While the soundings were spaced relatively far apart, the overconsolidation ratios and undrained strengths determined from the piezocone were similar below the upper 10 feet of fill. Thus, the data from all 5 soundings are considered together. Piezocone data are not shown for soil that was classified as something other than clay according to the classification charts developed by Robertson et al. In the layer of fat clay with silt pockets (El. -10 to -16 feet), the soil classification from the piezocone soundings suggests the presence of seams and pockets of granular material mixed with varying amounts of fine-grained material.

5.2.2 Field Vane Shear Testing

Field vane (FV) shear tests were performed in a boring approximately 5 feet from piezocone sounding FB4. Although three vane tests were attempted, the capacity of the vane shear device was reached in two of the tests (El. +6 feet and -7 feet) before a peak strength could be reached. However, even though peak strengths could not be recorded in these two tests, the results can be used to estimate a lower bound on strength at these depths. Test results are summarized in Table 5.1.

Table 5.4: Summary of field vane shear test results at Site 1

Elevation (ft)	Measured Peak $s_{u\text{-}FV}$ (psf)	Measured Remolded $s_{u\text{-}FV,\,r}$ (psf)	S_t	Plasticity Index (%)	μ	Corrected $s_{u\text{-}FVc}$ (psf)
6	>1,441	-	-	26	0.9	>1,297
-1	439	167	2.6	69	0.7	307
-7	>1,441	-	-	26	0.9	>1,297

5.2.3 Triaxial Testing

Thin-walled tube samples were taken in a boring approximately 5 feet from the vane boring and piezocone sounding FB4. Eleven unconsolidated-undrained (UU) triaxial compression tests and one consolidated-undrained (CU) triaxial compression test were performed on specimens from the tube samples.

In order to judge possible disturbance and assess the quality of UU test results based on observed stress-strain behavior, the principal stress difference was normalized with respect to peak principal stress difference and plotted versus axial strain for each test. These normalized stress-strain curves could then be compared to each other. In Figure 5.3, normalized stress-strain curves from all eleven UU tests are shown. Of the eleven UU tests performed, the results of four tests were considered questionable due to the relatively large strains in these tests. The stress-strain curves for the questionable tests showed the principal stress difference continuing to increase to axial strains as high as 15 percent. In contrast, the principal stress difference tended to reach a peak value at lower axial strains for tests that were accepted. The large strains in the tests that were questionable are believed to be due in part to the presence of sand and silt pockets in the specimens.

Values of strains may be used to assess sample disturbance. For normally to lightly overconsolidated clays, axial strains tend to increase with increasing amounts of sample disturbance. While strains at failure may best reflect disturbance, strains at failure tend to show a

large amount of scatter due to the flatness of the stress-strain curve. Thus, the axial strain at 75 percent of the principal stress difference at failure was chosen as a measure of strains and disturbance.

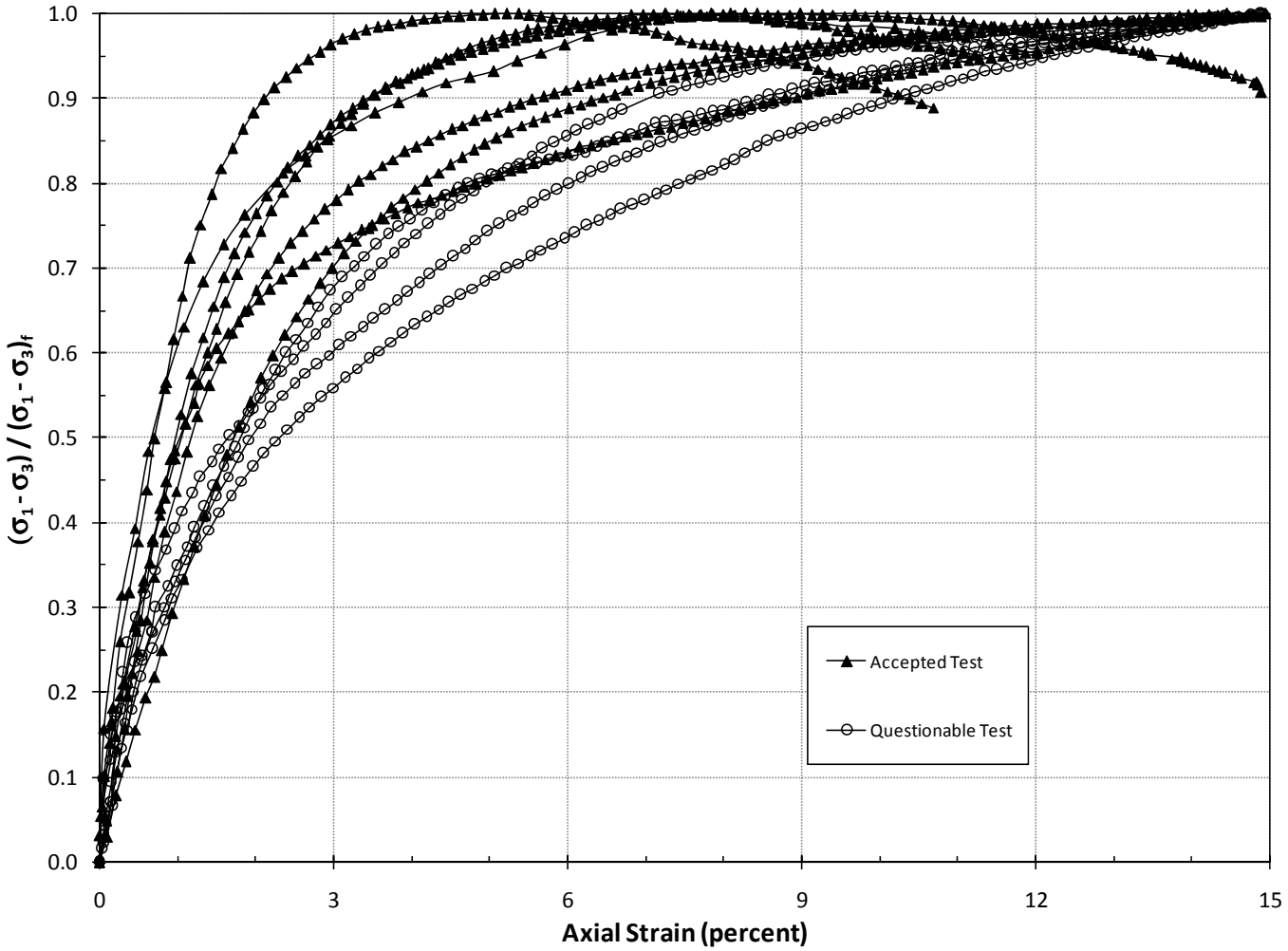

Figure 5.24: Normalized stress-strain curves from accepted and questionable UU tests at Site 1

In Table 5.2, the axial strain at 75 percent of the principal stress difference at failure, $\varepsilon_{75\%}$, is shown for each UU test. The $\varepsilon_{75\%}$ values from the questionable tests ranged from approximately 3.8 to 6.1 percent, while the $\varepsilon_{75\%}$ values for the tests that were accepted ranged from 1.2 to 3.5 percent. Stress-strain curves for two of the accepted tests (El. +6 and -3 feet) exhibited behavior similar to that of tests that were considered questionable. However, these two tests were accepted on the basis that their strengths agreed with strengths from field vane shear and piezocone penetration tests. These tests had $\varepsilon_{75\%}$ values slightly higher than the rest of the accepted tests, the values being 3.5 and 3.4 percent, respectively, but the values were still less than the values for the questionable tests.

Table 5.5: Values of axial strain at 75 percent of principal stress difference at failure for UU tests at Site 1.

Elevation (ft)	Test Result	$\varepsilon_{75\%}$ (%)
+8	Accepted	1.9
+7	Accepted	2.6
+6	Accepted	3.5
+5	Accepted	1.2
-1	Accepted	1.6
-2	Accepted	2.1
-3	Accepted	3.4
-5	Questionable	6.1
-11	Questionable	4.1
-13	Questionable	5.0
-14	Questionable	3.8

A single CU test was performed on a specimen from El. -2 feet (12 foot depth). Volumetric strain during consolidation to the effective overburden stress, $\varepsilon_{v\text{-}c}$, and sample quality based on Andersen and Kolstad's (1979) criterion is shown in Table 5.3. The volumetric strain during consolidation to the effective overburden stress was approximately 1.9 percent. Andersen and Kolstad stipulate for clay with an overconsolidation ratio of 1.5 or less, like the sample tested, that sample quality is "acceptable" with a volumetric strain during consolidation of less than 4 percent. Based Andersen and Kolstad's criterion, the CU test specimen from El. -2 feet is acceptable.

Table 5.6: Values of volumetric strain during consolidation to effective overburden stress for CU tests at Site 1.

Elevation (ft)	Sample Quality	$\varepsilon_{v\text{-}c}$ (%)
-2	Acceptable	1.9

5.2.4 Undrained Shear Strength Profile

Undrained strengths determined from undrained triaxial and field vane shear tests are plotted versus elevation in Figure 5.4. Data in this figure are shown combined with piezocone penetration data in Figure 5.5. The data was then analyzed and interpreted to determine a representative average undrained shear strength profile and upper and lower undrained shear strength bounds, which are also shown in Figure 5.5. In the following sections, the average, upper- and lower-bound undrained strength profiles, and test results are discussed further for various ranges of elevation.

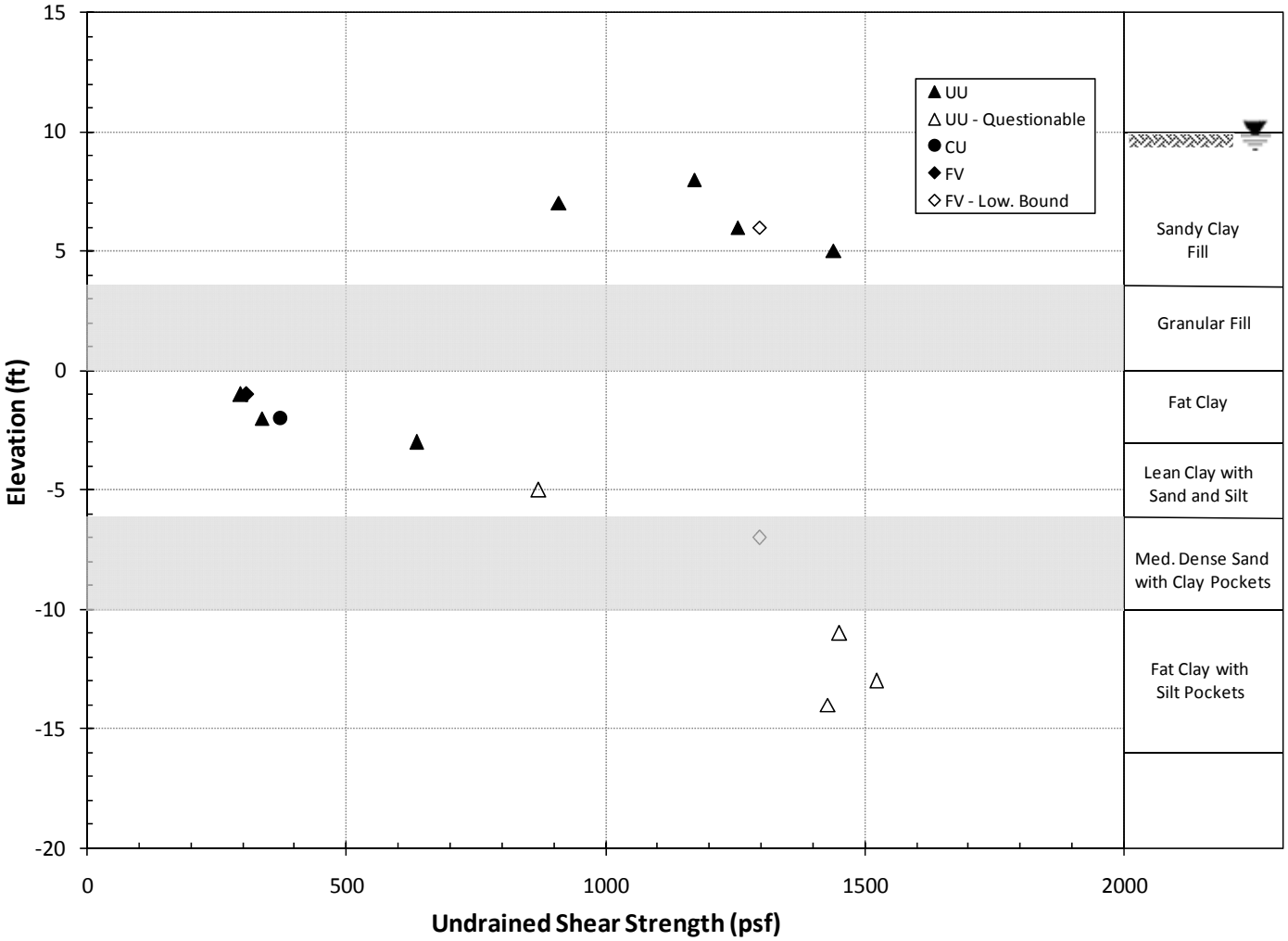

Figure 5.25: Undrained shear strengths from triaxial and field vane tests at Site 1

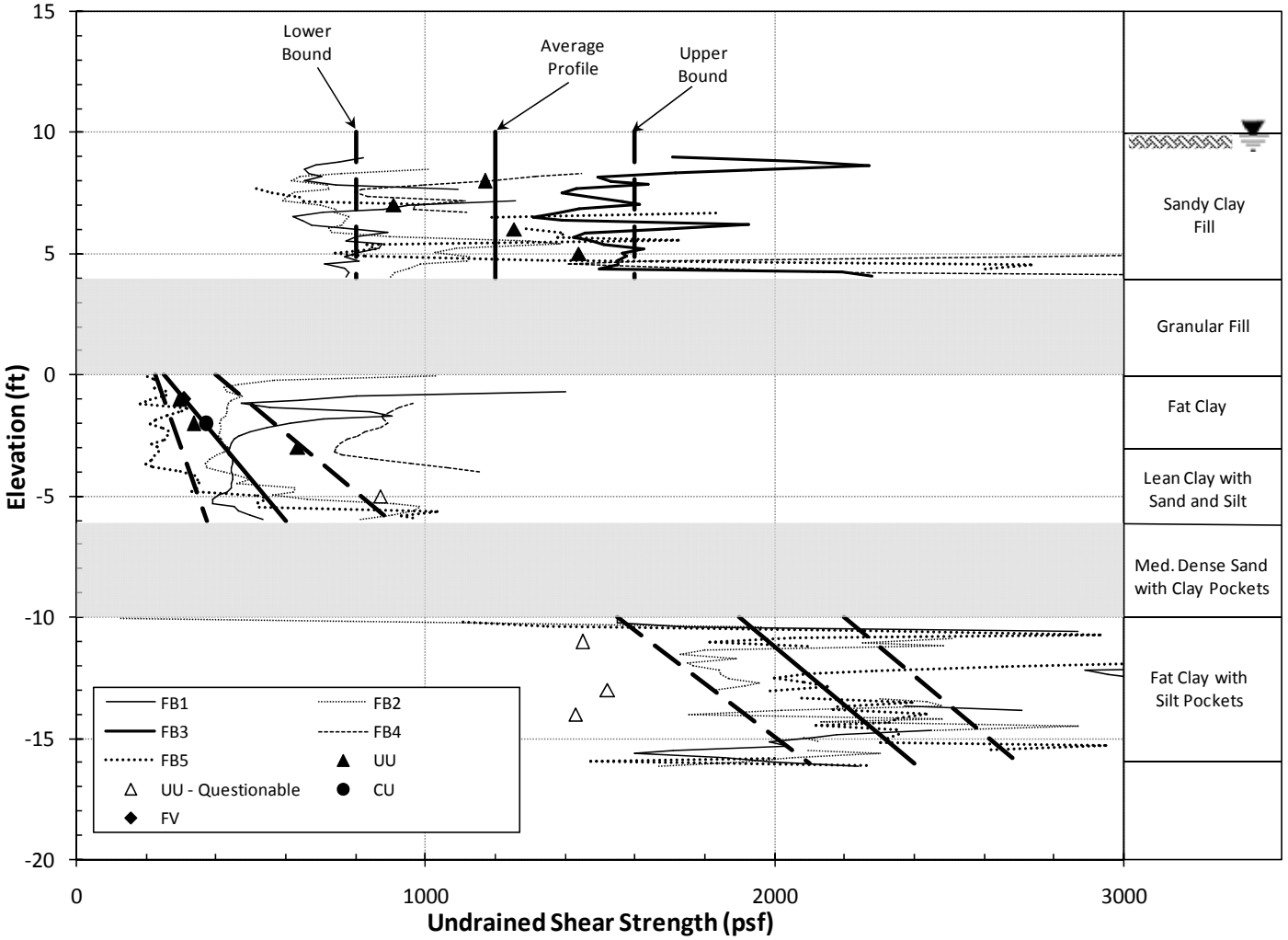

Figure 5.26: Undrained shear strength profile and bounds with piezocone, vane, and triaxial test strengths for Site 1

El. +10 to +4 feet (Zero to 6 Foot Depth)

In the upper 6 feet of sandy clay fill material, strengths measured using the piezocone ranged from 800 to 2,000 psf. Unconsolidated-undrained tests performed on specimens from this layer indicated the strength varied from 900 to 1,400 psf. During the single vane test performed in the fill, the capacity of the vane device was reached, and thus the test suggested a minimum corrected strength of approximately 1,300 psf at El. +6 feet (4 foot depth). A constant strength of 1,200 psf was selected as the representative average undrained shear strength in this elevation range since piezocone soundings indicated strength decreasing slightly with depth and three of the four unconsolidated-undrained tests showed strength increasing slightly from approximately 1,170 psf to 1,400 psf. Upper and lower bounds for undrained shear strength in this elevation range were selected based on piezocone soundings that showed the minimum and maximum strengths. These strengths were also in reasonably close agreement with the minimum and maximum strengths from unconsolidated-undrained tests.

El. +4 to 0 feet (6 to 10 foot depth)

At these depths, the soil is non-clay and undrained strengths are not applicable.

El. 0 to -6 feet (10 to 16 foot depth)

From El. 0 to -6 feet, two unconsolidated-undrained tests, one consolidated-undrained test, and one field vane shear test were performed. The strengths measured in unconsolidated-undrained tests and field vane shear at El. -1 feet (11 foot depth) were almost identical, 296 psf and 307 psf, respectively. Similarly, the strengths measured using unconsolidated-undrained and consolidated-undrained tests at El. -2 feet (12 foot depth) agreed very well, the values being 336 psf and 373 psf, respectively. These tests all agree well with the representative average profile line determined for the data and shown in Figure 5.5.

The piezocone data in this elevation range also generally agreed well with the average profile, although piezocone soundings FB1 and FB4 indicate the presence of some slightly stronger material. An unconsolidated-undrained test at a depth of 13 feet (El. -3 feet) also showed a slightly stronger soil than the average strength profile represents. This strength was used in conjunction with the piezocone soundings to establish the upper bound on the undrained shear strength profile. In this layer, the basis for the representative profile was the strengths from unconsolidated-undrained, consolidated-undrained, and field vane shear tests. Strengths from piezocone sounding FB5 were used to establish the lower bound on the undrained shear strength profile. The upper bound strength profile was selected on the basis of two unconsolidated-undrained tests (El. -3 and -5 feet) that showed strengths notably higher than those from the representative average profile.

El. -6 to -10 feet (16 to 20 foot depth)

Soil from these depths is sandy and undrained strengths are not applicable.

El. -10 to -16 feet (20 to 26 foot depth)

At these depths, the presence of pockets of sandy material in the laboratory specimens resulted in poor quality tests with strengths which were likely substantially lower than the strength that could be mobilized in the field. As a result, in this range of elevations the

representative average undrained shear strength profile and bounds were selected based on strengths from piezocone soundings.

5.3 Site 2

Site 2 is located near the border of Jefferson and Orange Counties in Port Arthur, Texas and is approximately 4 miles northeast of Site 1. The subsurface profile consists of a 5-foot-thick layer of gray clayey and silty sand underlain by a 25-foot-thick layer of soft gray fat clay with some sand. The subsurface exploration terminated in a layer of gray sandy clay. The ground surface at the site ranges from approximately El. +3 to +11 feet. The ground surface at the location of the boring where tube samples were taken is approximately El. +3 feet. At the time of the field investigation, the water table at the site was located approximately 4 feet below the ground surface of the boring where tube samples were taken.

5.3.1 Piezocone Penetration Testing

Four piezocone soundings, labeled BH108, BH109. BH109A, and BH112, were performed at Site 2. The overconsolidation ratios determined from the piezocone soundings are plotted versus depth in Figure 5.6. The data in the figure suggest the presence of an approximately 8-foot-thick heavily overconsolidated crust. Below the crust, the piezocone data indicate the soil is lightly overconsolidated, with an overconsolidation ratio ranging from approximately 1.2 to 2.5.

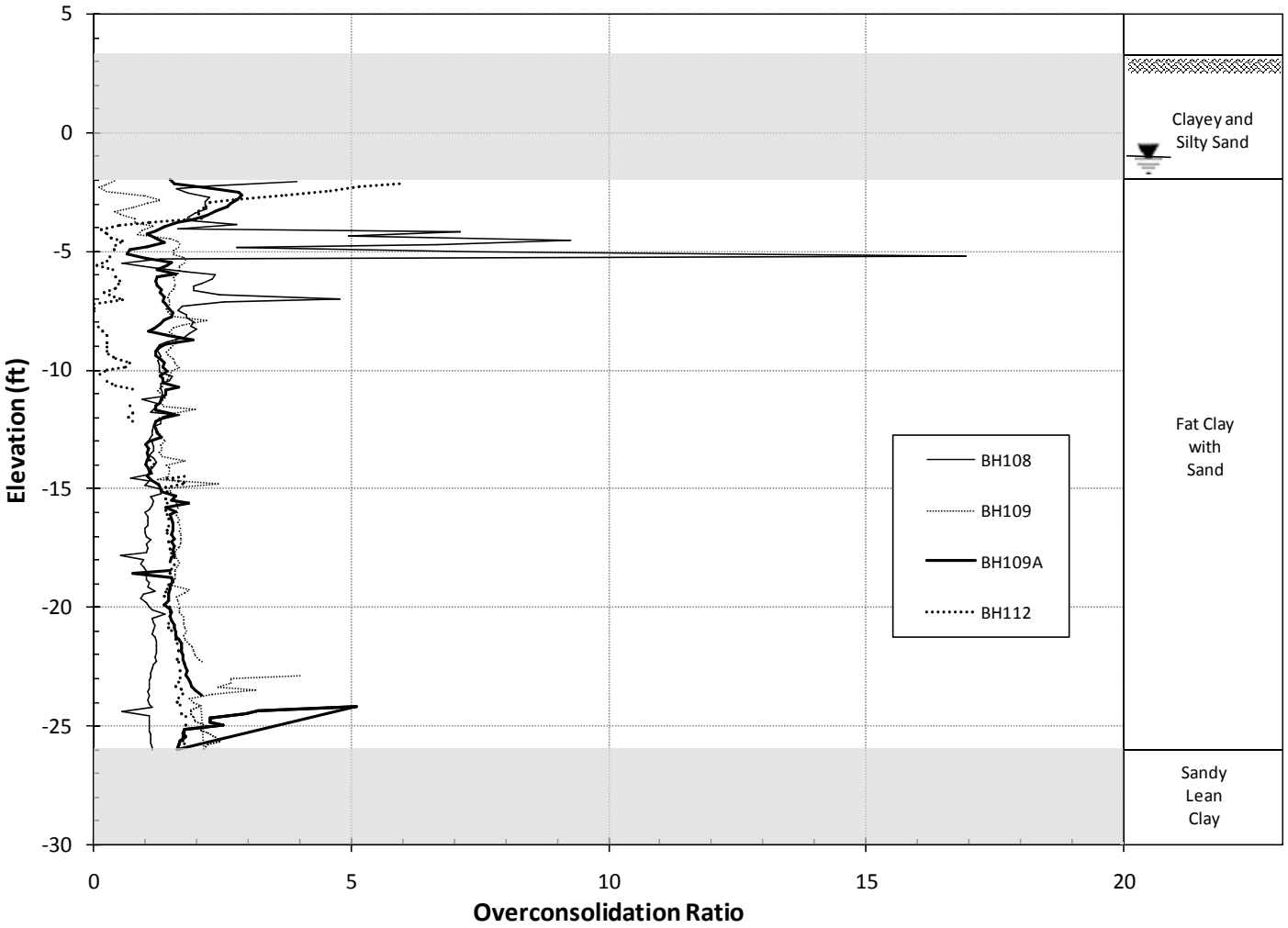

Figure 5.27: Overconsolidation ratio profiles determined from piezocone soundings at Site 2

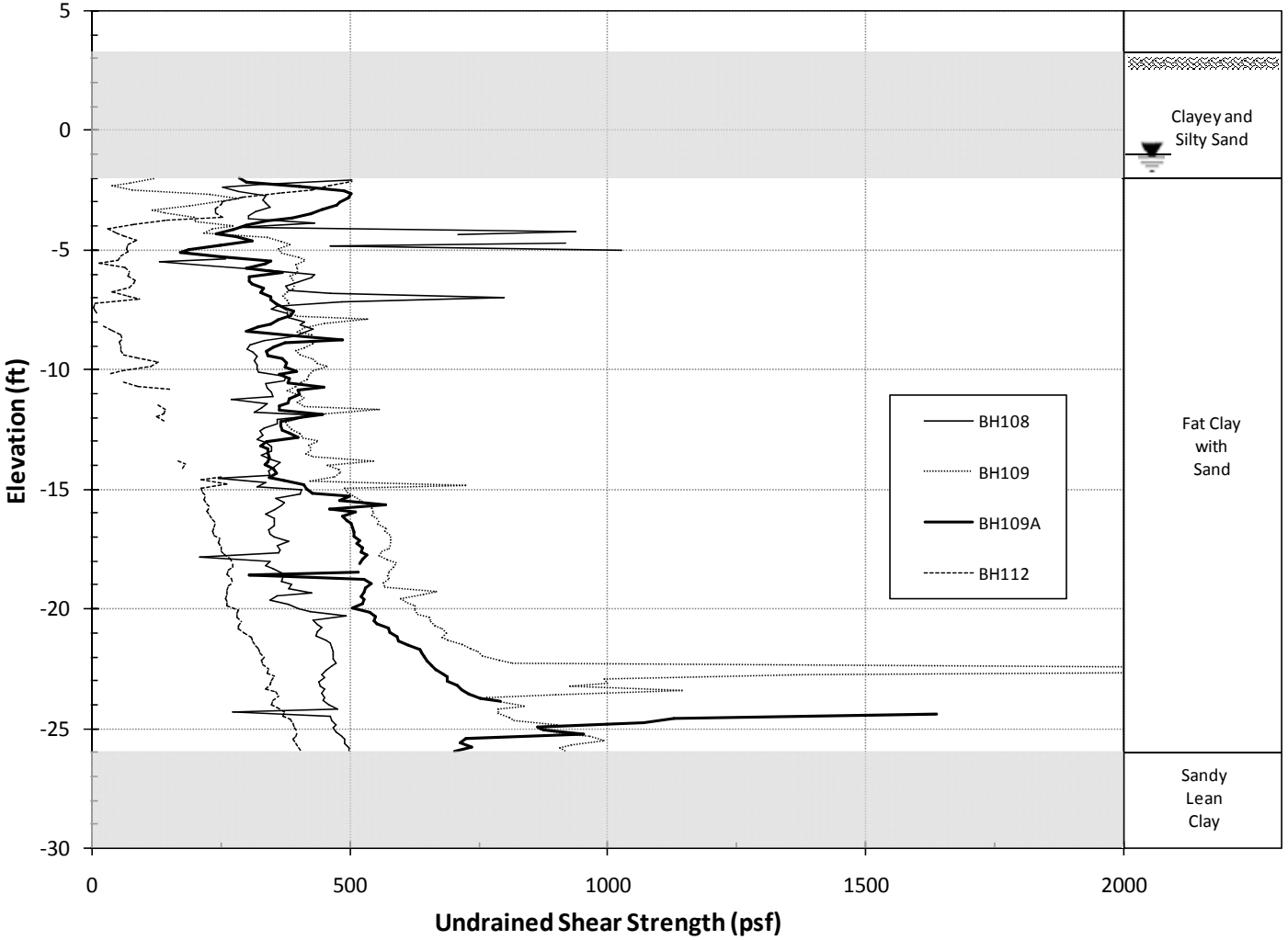

Figure 5.28: Undrained shear strength profiles determined from piezocone soundings at Site 2

Data from piezocone sounding BH112 indicate the presence of soil with an overconsolidation ratio of less than one from El. -4 to -10 feet (7 to 13 foot depth). Additional fill may have been placed in the vicinity of sounding BH112, causing soil near the surface to begin actively consolidating. However, with the available data, it is uncertain whether this is the case. It is also a possibility that sounding BH112 indicated overconsolidation ratios of less than one due to errors associated with the piezocone penetration test and the method used to determine the maximum previous effective stress. At greater depths, data from sounding BH112 is in agreement with data from the other soundings.

Undrained shear strengths were computed for each sounding using Equation 5.1 and are shown in Figure 5.7. The relatively low strengths indicated by sounding BH112 at depths from approximately El. -4 to -10 feet (7 to 13 foot depth) may be due to excess pore water pressures induced by the recent placement of fill or errors in the piezocone penetration test and determination of the maximum previous effective stress.

5.3.2 Field Vane Shear Testing

Field vane shear tests were performed in a boring approximately 200 feet from piezocone soundings BH109, BH109A, and BH112, and 400 hundred feet from sounding B108. Eight vane tests were performed, the results of which are presented in Table 5.4. The results of the field tests show that the clay is relatively sensitive, with sensitivities ranging from 5 to 10 in this layer.

Table 5.7: Summary of field vane shear test results at Site 2.

Elevation (ft)	Measured Peak $s_{u\text{-}FV}$ (psf)	Measured Remolded $s_{u\text{-}FV,\,r}$ (psf)	S_t	Plasticity Index (%)	μ	Corrected $s_{u\text{-}FVc}$ (psf)
-3	355	167	2.1	31	0.9	320
-7	532	52	10.2	31	0.9	479
-10	188	21	9.0	31	0.9	169
-13	553	84	6.6	93	0.64	354
-16	637	94	6.8	58	0.75	478
-20	940	157	6.0	35	0.85	799
-23	1128	209	5.4	67	0.68	767
-26	1274	449	2.8	67	0.68	866

5.3.3 Triaxial Testing

Thin-walled tube samples were recovered from a boring immediately adjacent to the field vane shear boring. Twenty unconsolidated-undrained (UU) tests and two consolidated-undrained (CU) tests were performed on specimens from tube samples.

Normalized stress-strain curves are shown for all twenty UU tests in Figure 5.8. The results of four of the UU tests were considered questionable based on their stress-strain behavior and relatively large strains. The stress-strain curves of accepted tests generally showed the principal stress difference reaching a peak value at axial strains of approximately 5 to 6 percent, while the stress-strain curves for the questionable tests showed the principal stress difference continuing to increase to axial strains as high as 15 percent.

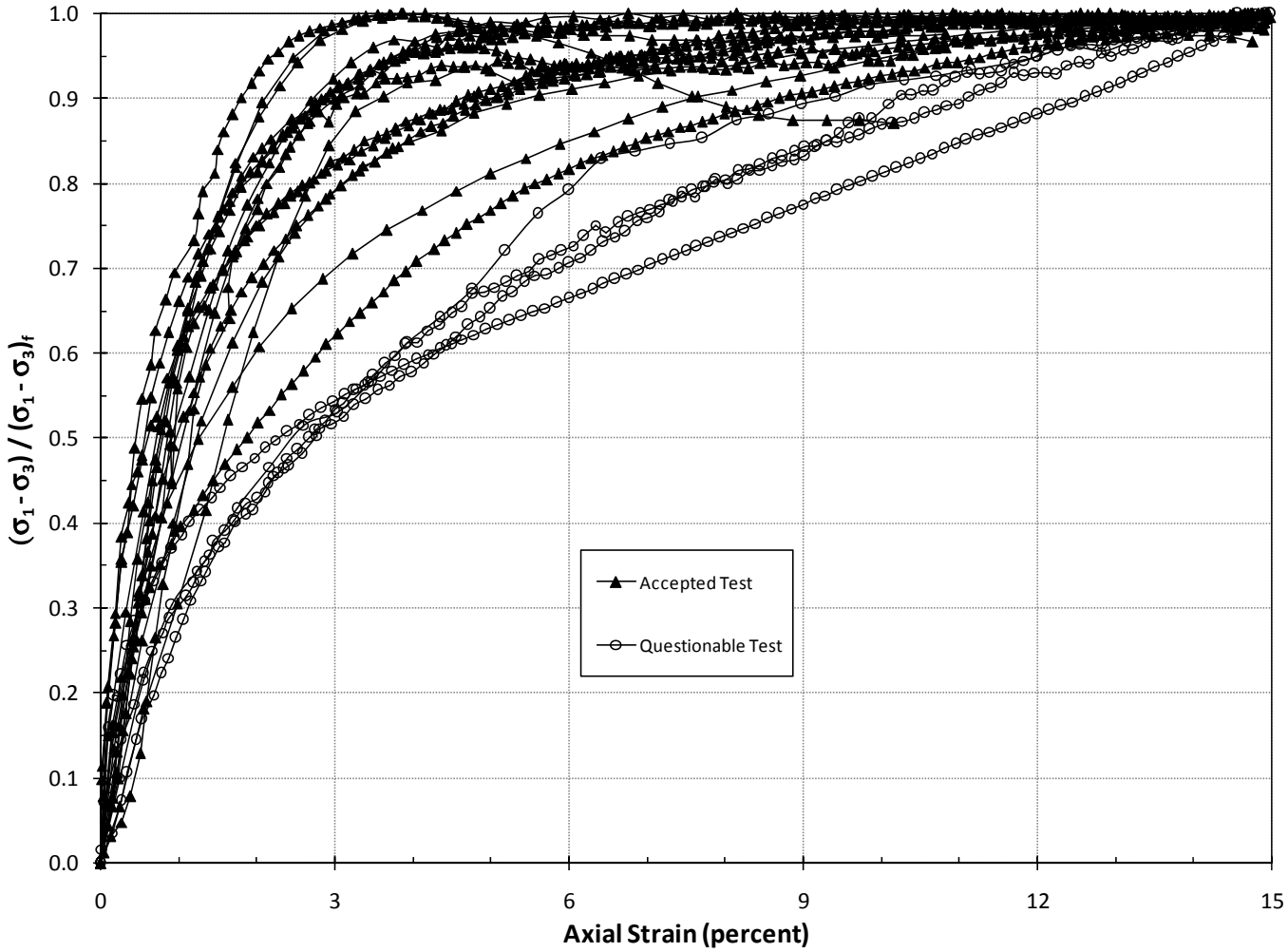

Figure 5.29: Normalized stress-strain curves from accepted and questionable UU tests at Site 2

Values of axial strain at 75 percent of the principal stress difference at failure ($\varepsilon_{75\%}$) are shown for the UU tests in Table 5.5. The questionable tests showed higher strains than the accepted tests. For the questionable tests, $\varepsilon_{75\%}$ values ranged from 5.2 to 8.2 percent, versus 1.2 to 4.6 percent for accepted tests. The stress-strain behavior observed in questionable tests is believed to be due in part to sample disturbance and the presence of sandier material in these specimens.

Table 5.8: Values of axial strain at 75 percent of principal stress difference at failure for UU tests at Site 2

Elevation (ft)	Test Result	$\varepsilon_{75\%}$ (%)
-4	Accepted	3.7
-5	Accepted	2.5
-6	Accepted	1.3
-7	Accepted	1.2
-8	Accepted	1.5
-9	Accepted	1.7
-11	Accepted	2.3
-12	Accepted	1.9
-13	Accepted	1.5
-14	Accepted	1.9
-15	Accepted	1.6
-17	Questionable	6.7
-18	Questionable	5.2
-19	Questionable	6.2
-20	Accepted	2.4
-21	Accepted	1.2
-22	Questionable	8.2
-23	Accepted	1.4
-24	Accepted	4.6
-25	Accepted	1.8

The CU test results are also indicative of disturbed samples based on Andersen and Kolstad's (1979) sample quality criteria. Values of volumetric strain during consolidation ($\varepsilon_{v\text{-}c}$) are shown in Table 5.6. For specimens with an overconsolidation ratio between 1.5 and 2, like those tested, Andersen and Kolstad stipulate specimens are disturbed if the volumetric strain during consolidation exceeds 3.5 percent. The volumetric strain during consolidation for the two CU test specimens was much more than the value of 3.5 suggested by Andersen and Kolstad. Thus, both specimens were likely disturbed, yielding strengths which were too high.

Table 5.9: Values of volumetric strain during consolidation to effective overburden stress for CU tests at Site 2

Elevation (ft)	Sample Quality	$\varepsilon_{v\text{-}c}$ (%)
-13	Disturbed	10.0
-15	Disturbed	12.3

5.3.4 One-Dimensional Consolidation Testing

Two incremental load (IL) and one constant rate of strain (CRS) consolidation tests were performed on specimens from tube samples. Void ratio is plotted versus vertical effective stress for these tests in Figure 5.9. The maximum previous effective stress (σ'_p) for each test was determined using the Casagrande construction and is indicated in the figure. Also, the present in-situ effective overburden stress (σ'_{vo}) was computed using the total unit weights of specimens from tube samples and pore water pressures determined from ground water table observations at the site. The present in-situ effective overburden stress is indicated in the figure.

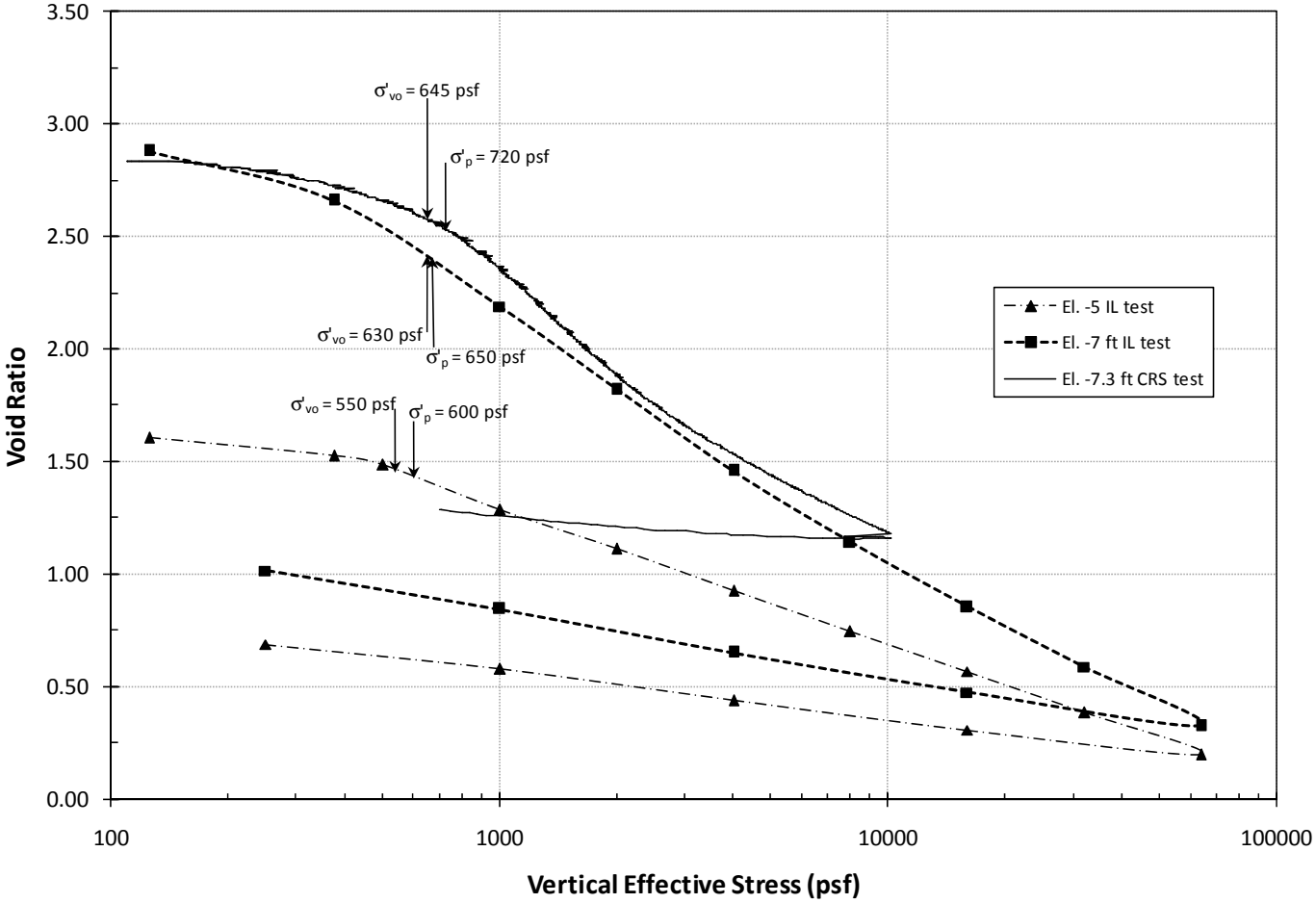

Figure 5.30: One-dimensional consolidation test results for Site 2

The overconsolidation ratios determined from one-dimensional consolidation tests are plotted with the overconsolidation profiles determined using the piezocone penetration test in Figure 5.10. The overconsolidation ratios determined from one-dimensional consolidation tests are slightly lower than those determined from piezocone soundings BH108, BH109, and BH109A. However, the incremental load test on a specimen from El. -7 feet (10 foot depth) and the constant rate of strain test on a specimen from El. -7.3 feet (10.3 foot depth) indicate slightly lower overconsolidation ratios than piezocone soundings BH108, BH109, and BH09A. This may in part be due to sample disturbance or errors associated with the determination of the maximum previous effective stress from the piezocone penetration test. This error may also be the result of using the Casagrande construction to determine the maximum previous effective stress. However, the overconsolidation ratios determined from one-dimensional consolidation tests are still within the scatter of the data from the piezocone soundings.

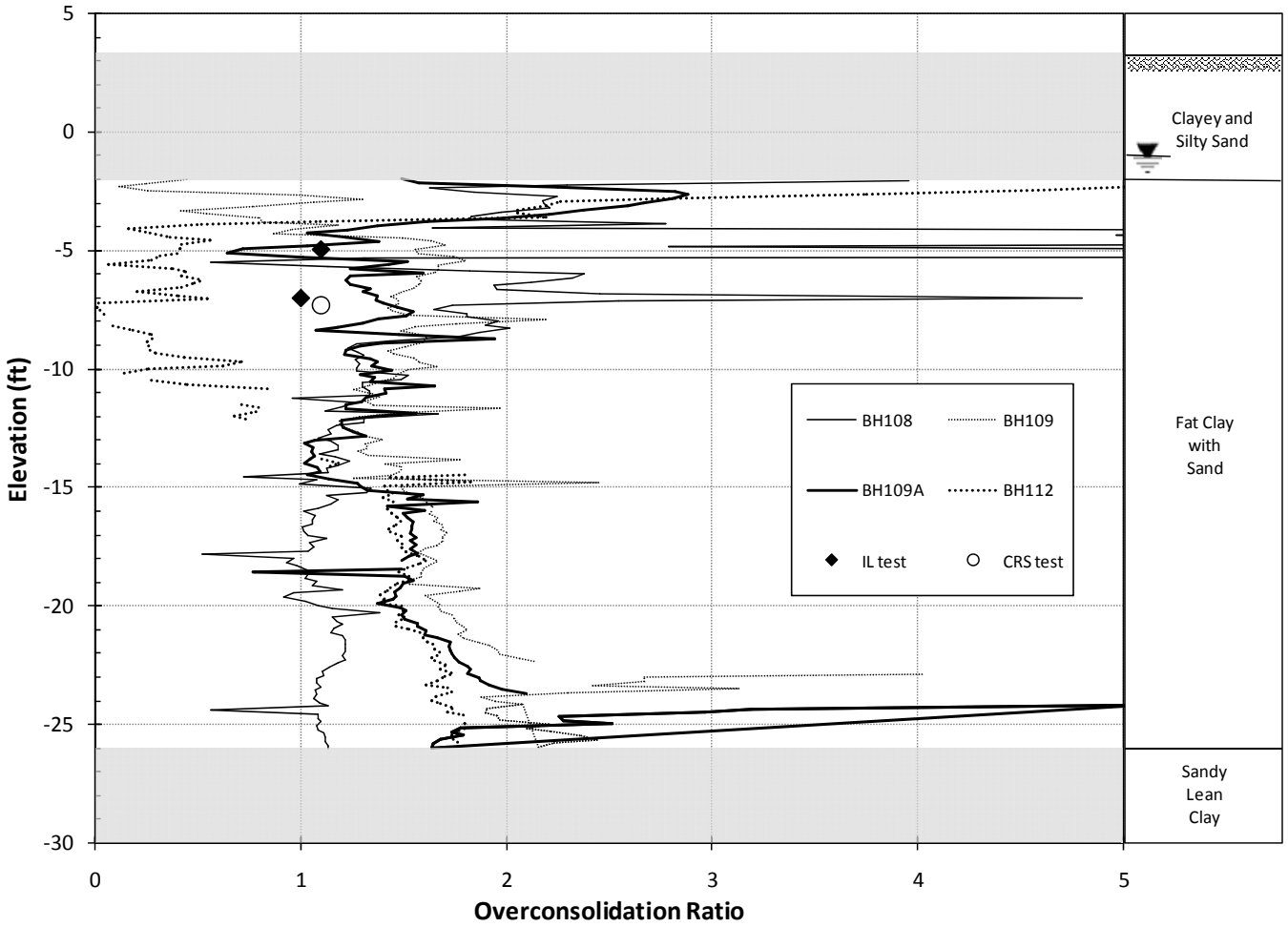

Figure 5.31: Overconsolidation ratios determined from one-dimensional consolidation tests and piezocone penetration tests for Site 2

.

5.3.5 Undrained Shear Strength Profile

Undrained strengths determined from triaxial and field vane shear tests are plotted versus elevation in Figure 5.11. Data in this figure were combined with piezocone penetration data in Figure 5.12. The data were then analyzed and interpreted to determine a representative average undrained shear strength profile, and upper and lower bounds for undrained shear strength, which are also shown in Figure 5.12. In the following sections, the average, upper and lower bound undrained strength profiles, and test results are discussed further for various ranges of elevation.

El. +3 to -2 feet (zero to 5 foot depth)

Soil from these depths is sandy and undrained strengths are not applicable.

El. -2 to -10 feet (5 to 13 foot depth)

Below El. -5 feet, strengths measured in unconsolidated-undrained tests tended to be significantly lower than strengths determined from piezocone soundings BH108, BH109, BH109A, and field vane shear tests. The low strengths measured in laboratory tests are believed to be a result of sample disturbance. Specimens tested in unconsolidated-undrained tests generally failed at axial strains of approximately 6 percent. However, specimens of lightly overconsolidated, undisturbed clay would usually be expected to fail at slightly lower axial strains, suggesting the samples may have been disturbed. In this elevation range, the average undrained strength profile was weighted towards the upper range of unconsolidated-undrained strengths and the lower range of strengths based on piezocone soundings BH108, BH109, and BH109A.

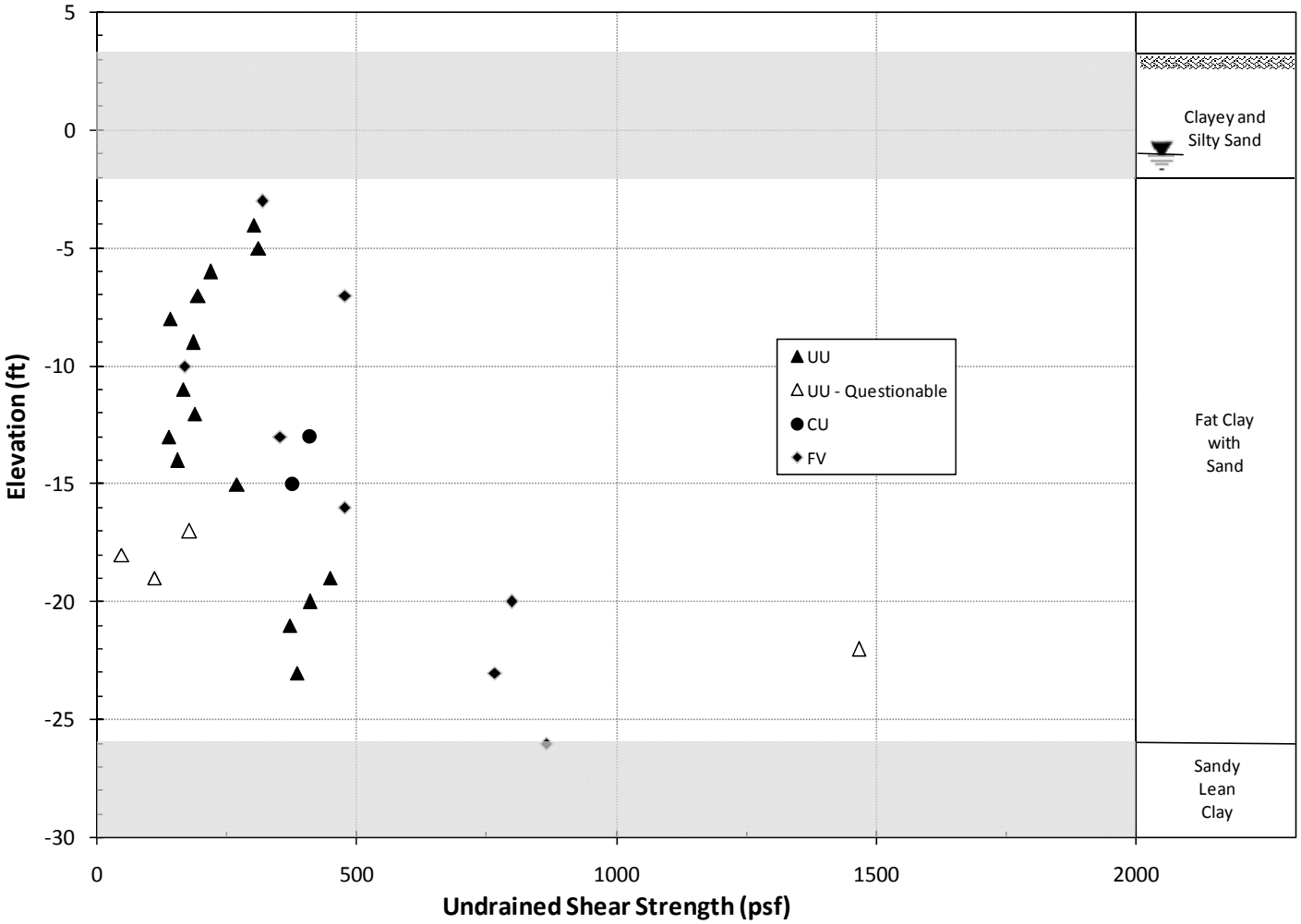

Figure 5.32: Undrained shear strengths from triaxial and field vane tests at Site 2

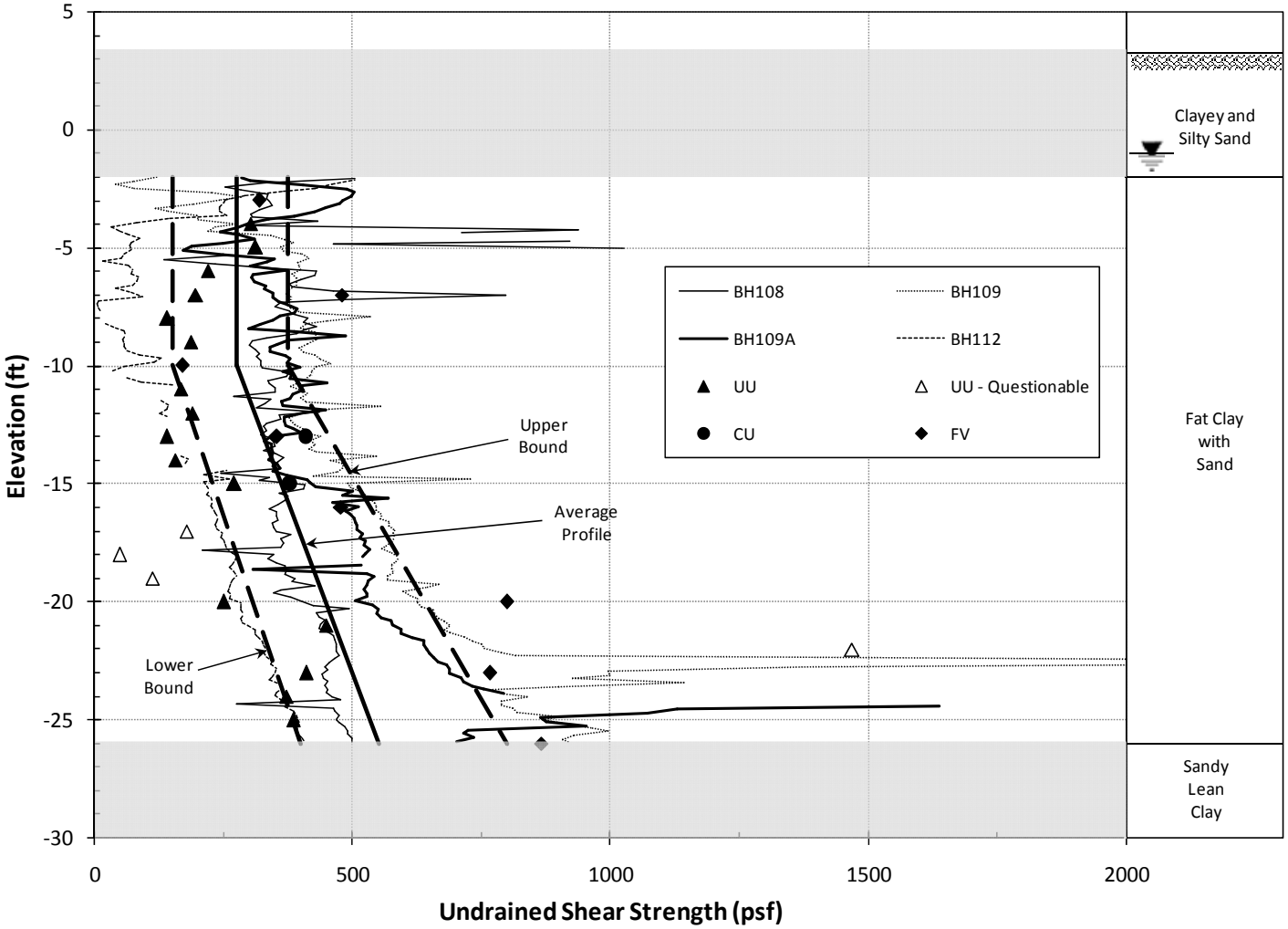

Figure 5.33: Undrained shear strength profile and bounds with piezocone, vane, and triaxial test strengths for Site 2

El. -10 to -26 feet (13 to 29 foot depth)

In this elevation range, strengths from unconsolidated-undrained tests tended to be significantly lower than strengths determined from piezocone soundings BH109, BH109, BH109A, and field vane shear tests. These low strengths are believed to be the result of sample disturbance.

The undrained strengths from the consolidated-undrained tests were significantly higher than the strengths from unconsolidated-undrained tests. This was expected given the large amount of volume change that occurred during consolidation and the probable large amount of disturbance of the unconsolidated-undrained test specimens. The strengths from the consolidated-undrained tests did agree well with strengths from the field vane and piezocone soundings.

Significantly lower strengths were measured in piezocone sounding BH112 compared to soundings BH108, BH109, and BH109A. While the strengths from BH112 did agree somewhat with unconsolidated-undrained tests, this seems fortuitous given that the strength of the unconsolidated-undrained test specimens was probably too low due to disturbance. The relatively low strengths measured from sounding BH112 may also be indicative of local variability at the site.

Below El. -15 feet (18 foot depth), the strengths from piezocone soundings BH109 and BH109A were markedly higher than the strengths from sounding BH108 and the average strength profile. Vane tests performed below El. -20 (23 foot depth) feet also indicated strengths substantially higher than the average strength profile and sounding BH108. The vane strengths did agree to some extent with soundings BH109 and BH109A. However, the field vane strengths seem high and given the extreme increase in strength measured with piezocone soundings BH109 and BH109A between El. -22 and -26 feet (25 to 29 foot depth), it is believed that sandier material was encountered in these tests. Considering the relatively high vane strengths, this may be explained by the fact that these tests were also performed in sandier material.

In this elevation range, the representative undrained strength profile was selected primarily based on strengths from piezocone sounding BH108, which showed good agreement with strengths from consolidated-undrained tests and several unconsolidated-undrained tests. The lower bound was governed by strengths from unconsolidated-undrained tests, while the upper bound was governed by strengths from piezocone soundings BH109A and BH109, and field vane shear tests.

5.4 Site 3

Site 3 is located north of FM 1942 and west of Cedar Bayou in Mont Belvieu, Texas. The subsurface profile consists of an 18-foot-thick layer of fat and lean tan and gray clay with varying amounts of silt and sand. The clay layer is underlain by tan and gray clayey sand. The ground surface at the site is fairly level, with the ground surface located at approximately El. +31 feet for all piezocone soundings and the boring where tube samples were taken. During the field investigation, the water table was observed to be 4 feet below the ground surface. No one-dimensional consolidation tests were performed for Site 3.

5.4.1 Piezocone Penetration Testing

Four piezocone soundings, labeled CPT25, CPT26, CPT27, and CPTB9, were performed at Site 3. Three soundings (CPT25, CPT26, and CPT27) were spaced at approximately 120°

around the circumference of an approximately 130-foot diameter circle with the fourth sounding (CPTB9) located near the center of the circle. The profiles of overconsolidation ratio determined from the four piezocone soundings are shown in Figure 5.13 The results show the presence of a heavily overconsolidated crust extending to El +25 feet. Below this elevation, all 4 soundings show an overconsolidation ratio gradually decreasing from approximately 10 to 8. For each piezocone sounding, undrained shear strengths were computed using Equation 5.1 and are plotted versus depth in Figure 5.14.

The piezocone soundings show very limited horizontal spatial variation in undrained shear strength in the upper 18 feet of clay. At greater depths, soil classification determined from the piezocone soundings indicates the presence of sandier soil. The presence of a higher portion of sand in this material also leads to the piezocone indicating higher and more variable strengths.

5.4.2 Field Vane Shear Testing

The field vane device could not be advanced through the stiff soils which were encountered at Site 3. As a result, vane shear tests were not performed at the site.

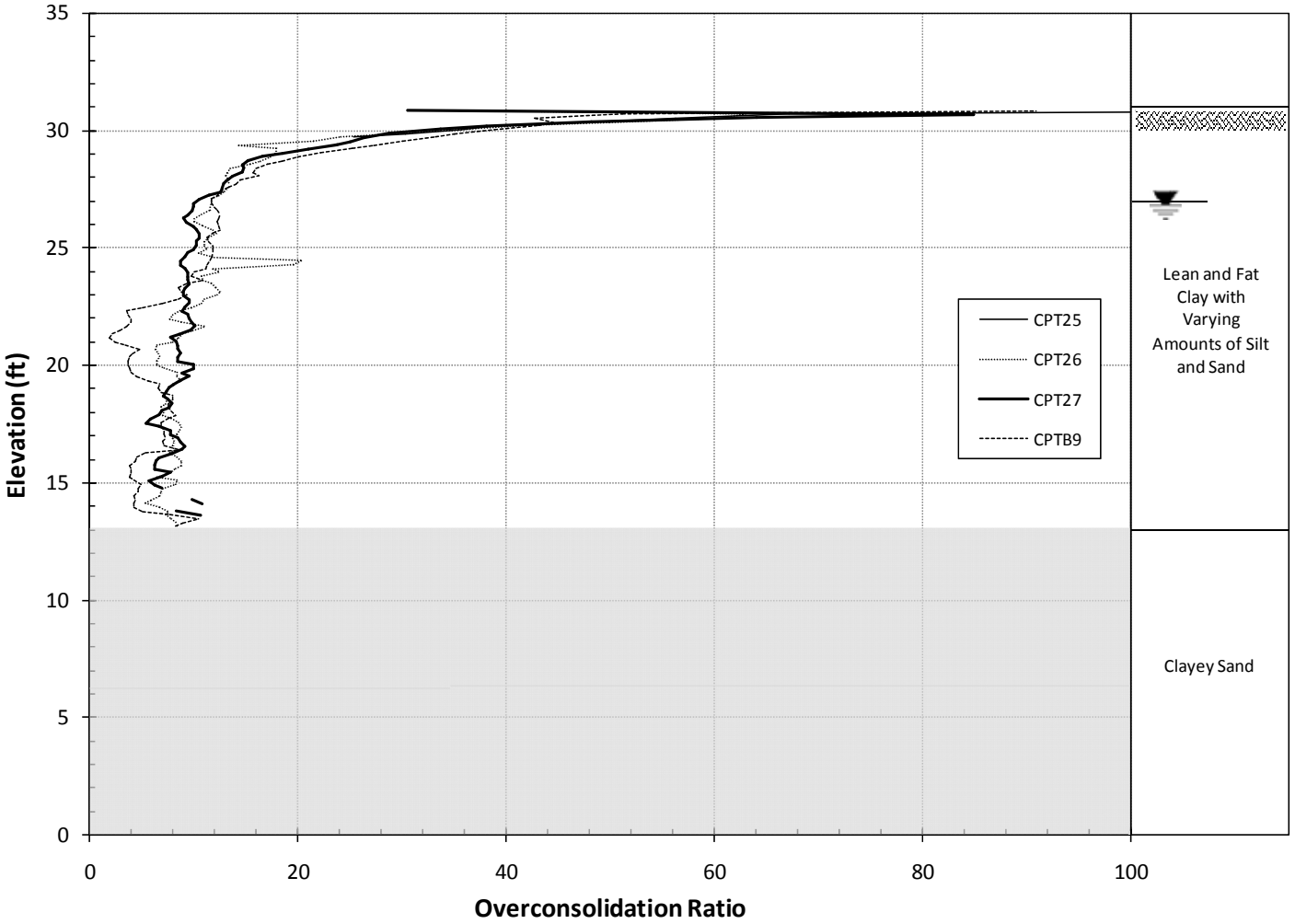

Figure 5.34: Overconsolidation ratio profiles determined from piezocone soundings at Site 3

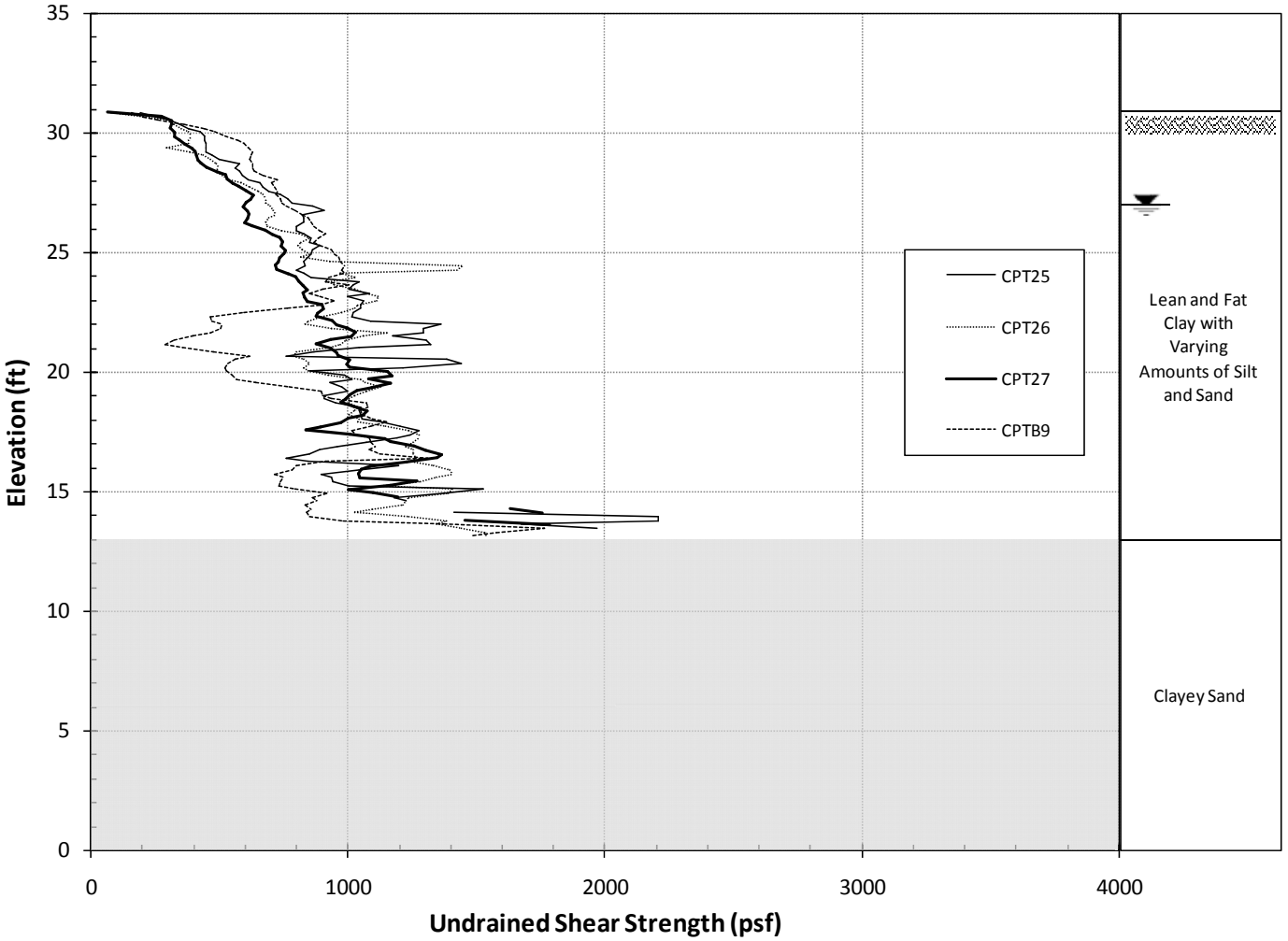

Figure 5.35: Undrained shear strength profiles determined from piezocone soundings at Site 3

5.4.3 Triaxial Testing

Thin-walled tube samples were taken in a boring located near the center of the circle on which piezocone soundings CPT25, CPT26, and CPT27 were located and about 30 feet from sounding CPTB9. Fifteen unconsolidated-undrained (UU) tests and four consolidated-undrained (CU) tests were performed on specimens from the tube samples.

Normalized stress-strain curves from the UU tests are plotted in Figure 5.15. The results of four of the UU tests were considered questionable due to the relatively large strains in these tests. These tests exhibited stress-strain curves with the principal stress difference continuing to increase for axial strains as high as 15 percent.

Values of axial strain at 75 percent of the principal stress difference at failure ($\varepsilon_{75\%}$) are shown for the UU tests in Table 5.7. The accepted tests had $\varepsilon_{75\%}$ values less than 3.1 percent, while the questionable tests showed $\varepsilon_{75\%}$ values greater than 6.1 percent. All of the specimens from questionable tests had a large portion of sand, which may explain their stress-strain behavior. Three of the specimens came from the layer of clayey sand located below El. 13 feet.

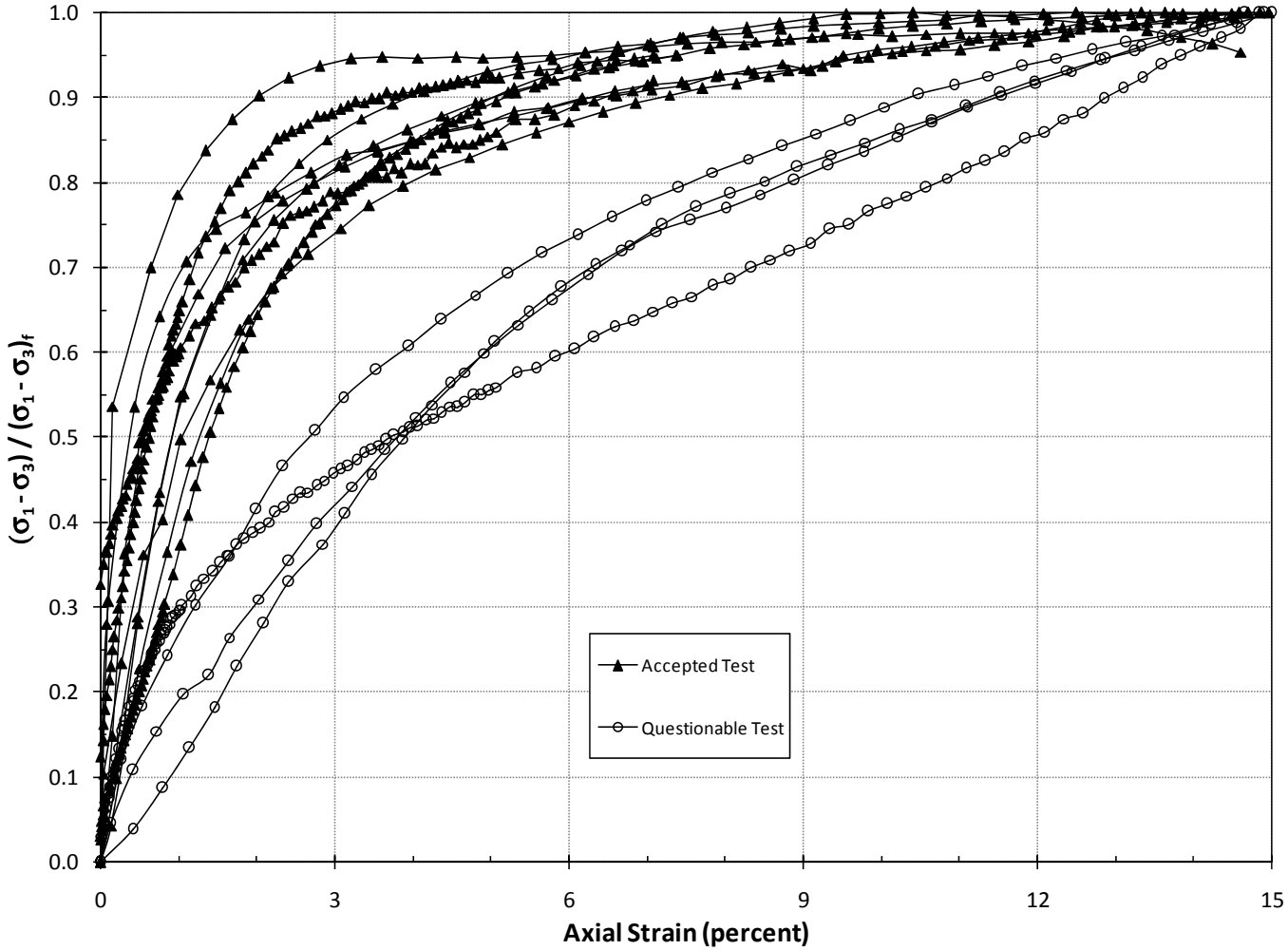

Figure 5.36: Normalized stress-strain curves from UU tests at Site 3

Table 5.10: Values of axial strain at 75 percent of principal stress difference at failure for UU tests at Site 3

Elevation (ft)	Test Result	$\varepsilon_{75\%}$ (%)
+29	Accepted	2.7
+28	Accepted	3.1
+27	Accepted	1.8
+26	Accepted	1.6
+25	Accepted	1.8
+24	Accepted	2.2
+21	Accepted	0.6
+20	Questionable	9.6
+18	Accepted	1.4
+16	Accepted	1.5
+8	Questionable	6.8
+7	Questionable	6.1
+6	Questionable	7.1
+5	Accepted	2.4

The results of a consolidated-undrained test performed on a specimen from the clayey sand layer (El. +13 feet) also suggest the effect of the presence of a greater portion of sand in specimens. This specimen exhibited a significantly higher strength than measured in unconsolidated-undrained tests on specimens from similar depths. This is believed to be due to the fact that the sandy material drained quickly and experienced substantial stress relief after sampling and during specimen preparation. As a result, the effective stress in the specimens tested in unconsolidated-undrained tests was probably very low, leading to low undrained shear strengths. Such loss in effective stress was removed in the consolidated-undrained test and an undrained strength more representative of a sandy material was measured. Based on the results of laboratory testing, the clayey sand below El. +13 feet (18 foot depth) did not exhibit clay-like behavior and undrained strengths are not applicable to this material.

Values of volumetric strain during consolidation ($\varepsilon_{v\text{-}c}$) are shown in Table 5.8. Based on Andersen and Kolstad's sample quality criteria, the values of volumetric strain during consolidation of the consolidated-undrained test specimens indicate one of the four specimens was disturbed. They suggest specimens with an overconsolidation ratio of 3 to 8, like those tested, are disturbed if the volumetric strain during consolidation exceeds 1 percent. One test (El +23 feet) had a value of 1.3 percent, while the others had values less than 0.7 percent.

Table 5.11: Values of volumetric strain during consolidation to effective overburden stress for CU tests at Site 3

Elevation (ft)	Sample Quality	$\varepsilon_{v\text{-}c}$ (%)
+23	Disturbed	1.3
+19	Acceptable	0.7
+17	Perfect	0.2
+14	Acceptable	0.7

5.4.4 Undrained Shear Strength Profile

Undrained strengths determined from triaxial tests are plotted versus elevation in Figure 5.16. Data from this figure were combined with strengths derived from piezocone penetration data in Figure 5.17. The data were then analyzed and interpreted to determine a representative average undrained shear strength profile, and upper and lower bounds for undrained shear strength, which are also shown in Figure 5.17. In the following sections, the average, upper and lower bound undrained strength profiles, and test results are discussed further for various ranges of elevation.

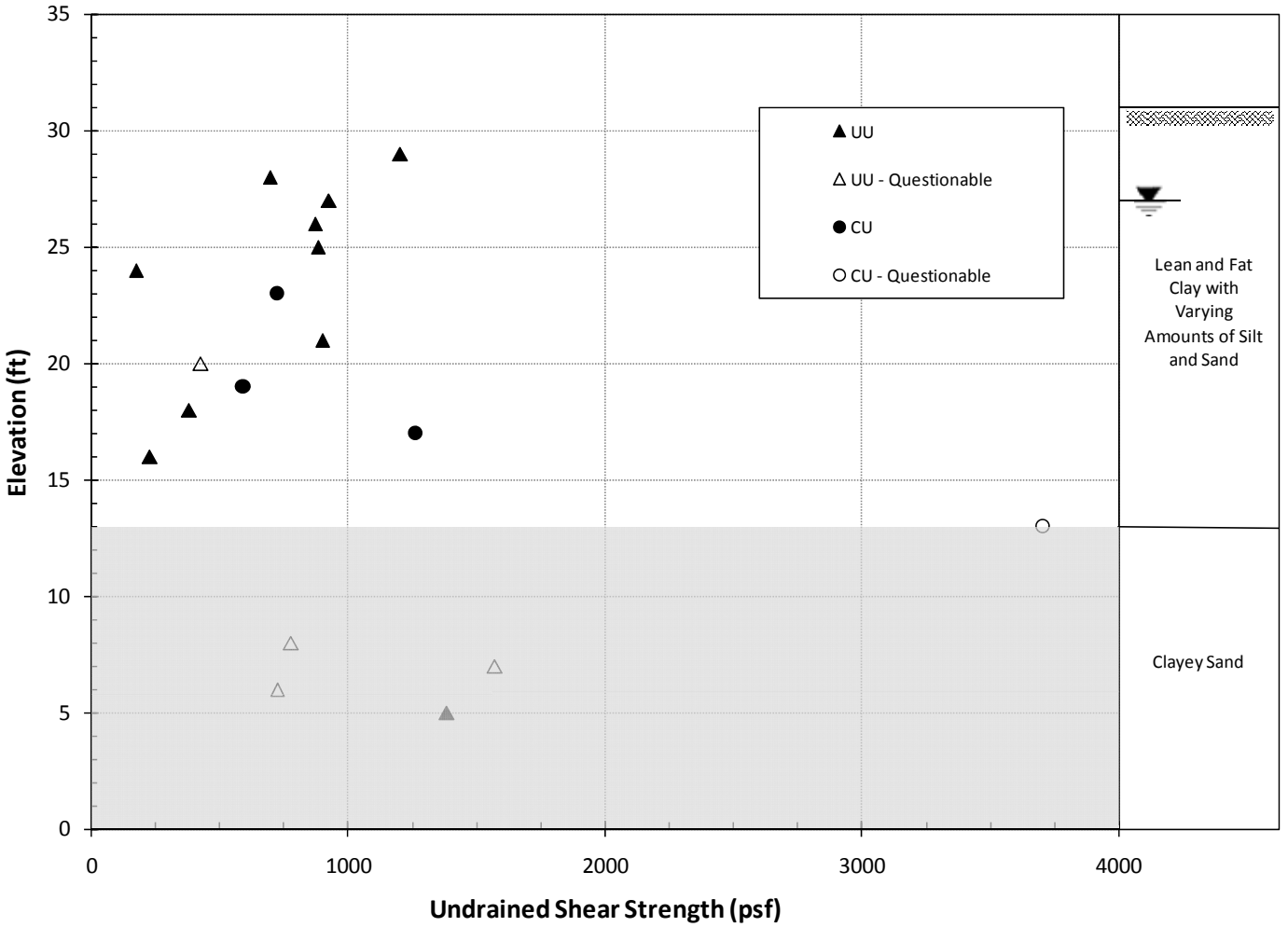

Figure 5.37: Undrained shear strengths from triaxial tests at Site 3

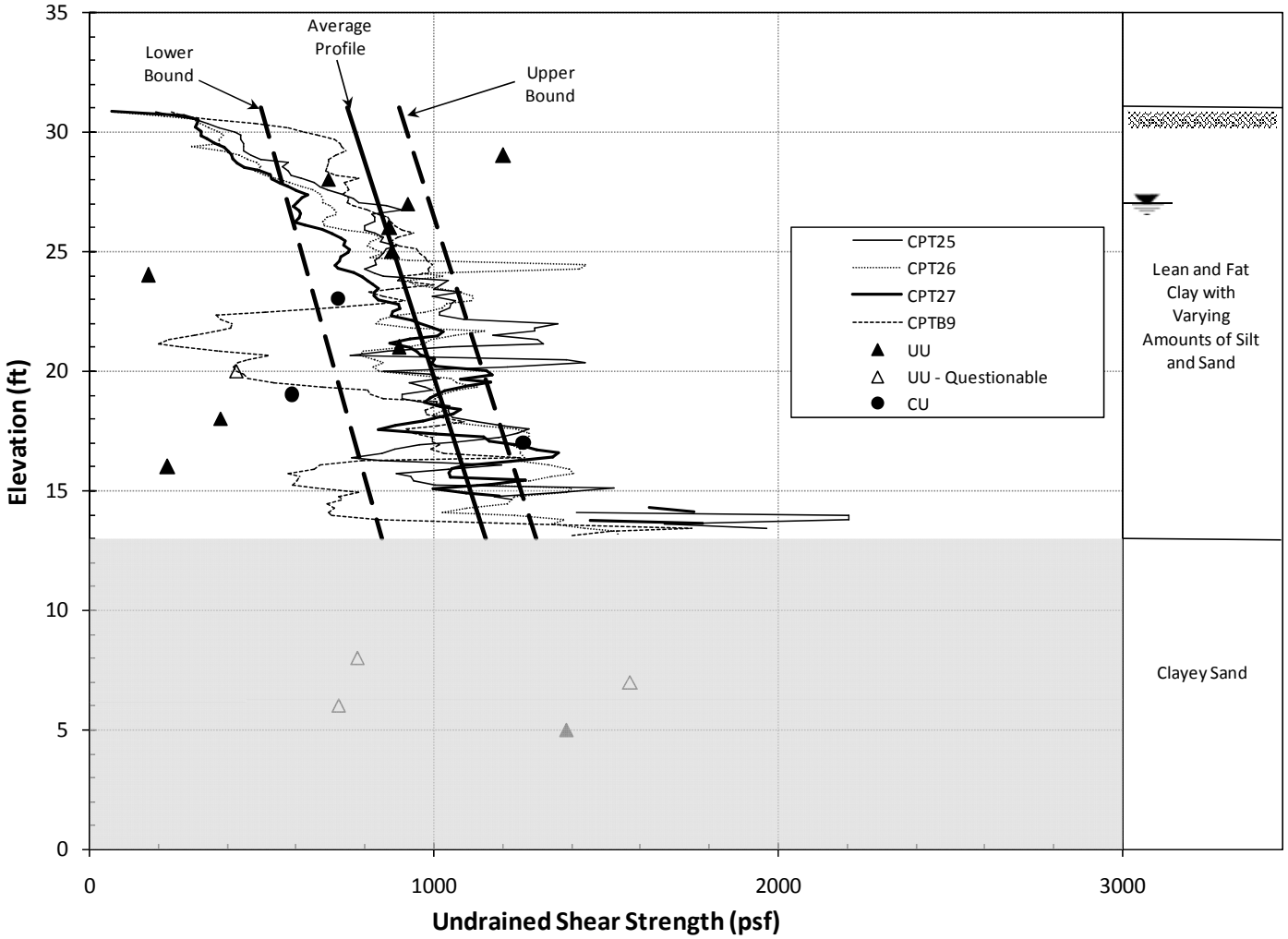

Figure 5.38: Undrained shear strength profile and bounds with piezocone, vane, and triaxial test strengths for Site 3

El. +31 to +25 feet (zero to 6 foot depth)

In the crust (El. +31 to +25 feet), the piezocone soundings show the undrained shear strength increasing linearly from a value of approximately 100 psf at the ground surface. However, laboratory tests indicated the strength in the crust is significantly higher, ranging from about 900 to 1,200 psf. Ladd and DeGroot (2003) noted that the SHANSEP method may not accurately predict undrained strengths of heavily overconsolidated clays in which the primary mechanism of overconsolidation is not mechanical. This may explain the discrepancy between the undrained strengths determined for the crust with the piezocone and the triaxial tests. In this elevation range, strengths from unconsolidated-undrained tests were the basis for the representative average strength profile. One unconsolidated-undrained test (El. +29 feet) did yield strength significantly higher than the upper bound undrained strength profile. The lower bound strength profile was based on strengths from the piezocone soundings.

El. +25 to +13 feet (6 to 18 foot depth)

The sounding (CPTB9) located closest to the boring where tube samples were taken indicated the presence of two thin layers (El. +23 to +19 feet and El. +16 to +14 feet) of material with strengths notably lower than the average profile. Several triaxial tests performed on specimens from El +24 to +16 feet also showed strengths notably lower than the average undrained shear strength profile. However, for each triaxial test that yielded such lower strengths, there was at least one other test on a specimen from the immediate vicinity that gave a strength that agreed relatively well with the representative average profile. The relatively low strengths measured in some of the triaxial tests may be due either to sample disturbance or to local variability in the soil strength and type. Even with several measures of undrained shear strength, there still remains some uncertainty in defining an appropriate strength profile. In this elevation range, the representative average strength profile was driven primarily by strengths determined from piezocone penetration tests. For the most part, unconsolidated-undrained tests tended to underestimate strengths.

El. +13 to +5 feet (18 to 26 foot depth)

Below El. +13 feet, the soil became significantly sandier and undrained shear strengths are not applicable.

5.5 Site 4

Site 4 is located just north of the intersection of US 287 and TX 347W in Beaumont, Texas. Beginning at the ground surface, the subsurface profile consists of a 4-foot-thick layer of tan sandy clay fill, a 7-foot-thick layer of medium sand, an 11.5-foot-thick layer of gray organic clay, and a layer of sandy fat clay in which the subsurface exploration was terminated. The ground surface at the site was nearly level. The ground surface is located at approximately El. +10 feet for all piezocone soundings, the boring where field vane shear tests were performed, and the boring where tube samples were taken. During the subsurface investigation, the groundwater table was observed to be 2.5 feet below the ground surface of the boring where tube samples were taken.

During testing in the laboratory, soil in several samples from this site appeared to contain a significant portion of organic matter. In order to determine the organic content of the soil,

specimens were tested in general accordance with ASTM standard D2974 (2007c). Specimens were heated in a muffle furnace to combust the organic matter. The organic content was then determined by weight and found to range from approximately 10 to 20 percent.

5.5.1 Piezocone Penetration Testing

Three piezocone soundings, labeled 21, 21A, and 21B, were performed at Site 4. The three soundings were spaced at approximately 120° on the circumference of an approximately 40-foot diameter circle. The overconsolidation ratio profiles determined from the three piezocone soundings are shown in Figure 5.18. The soundings indicate the upper 4 feet of sandy lean clay fill is heavily overconsolidated. Below a layer of medium sand (El. +10 to +6 feet), layers of gray organic clay (El. -1 to -12.5 feet) and sandy fat clay (El. -12.5 to -16 feet) are indicated to have an overconsolidation ratio of slightly less than 2. Undrained shear strengths determined from the piezocone soundings using Equation 5.1 are shown in Figure 5.19.

5.5.2 Field Vane Shear Testing

Field vane shear tests were performed in a boring located near the center of the circle on whose circumference the piezocone soundings were located. Four vane tests were performed, three in the gray organic clay layer and one in the sandy fat clay layer. Test results are reported in Table 5.9. The remolded strength was measured in all tests except the test performed at El. -16 feet. In addition to Bjerrum's correction based on plasticity, an additional reduction factor of 0.85 was applied to the strength measured in the organic clay as suggested by Terzaghi, Peck, and Mesri (1996). The vane tests suggest that the organic clay is significantly sensitive, with sensitivities ranging from approximately 6.5 to 12.

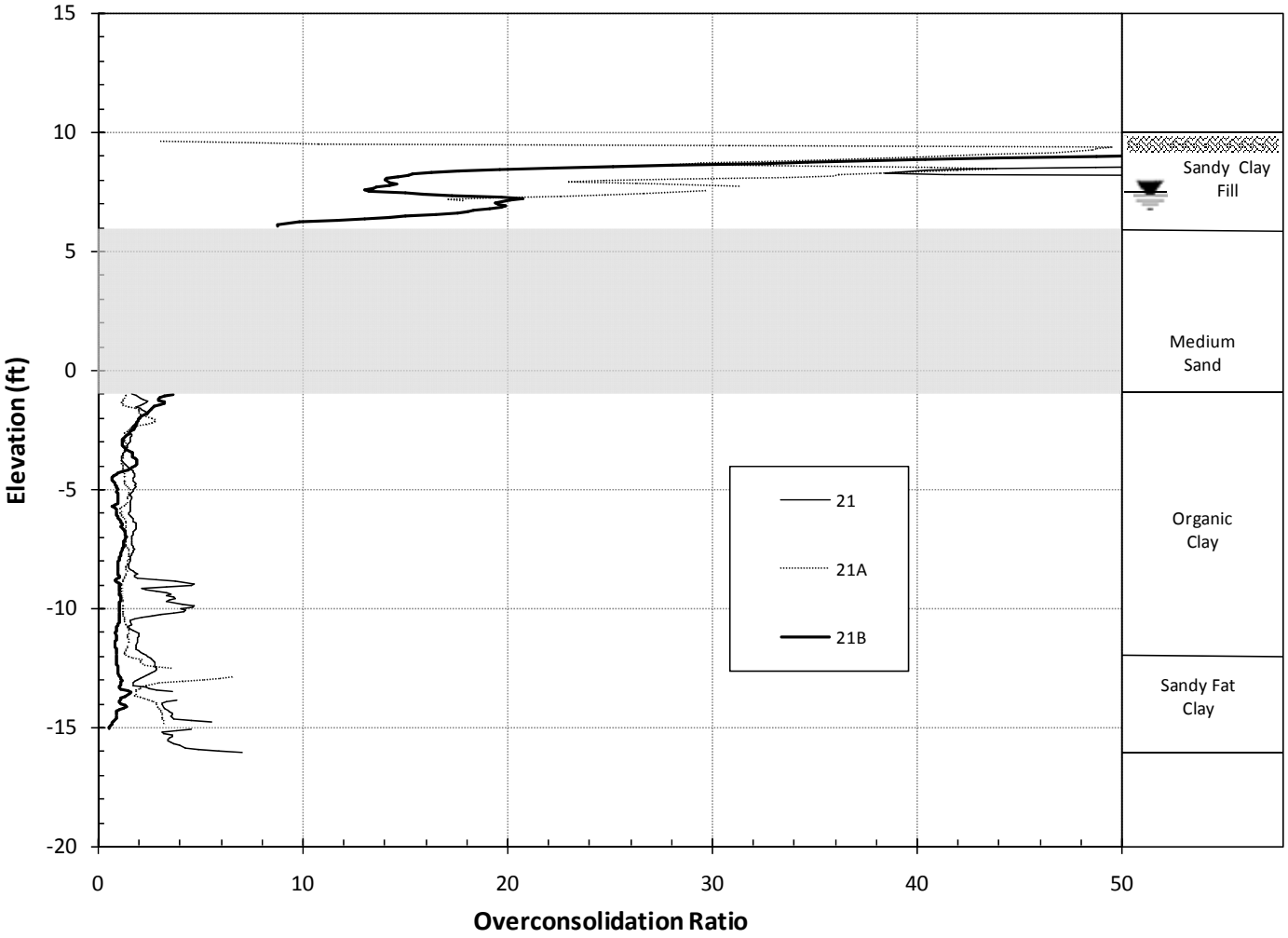

Figure 5.39: Overconsolidation ratio profiles determined from piezocone soundings at Site 4

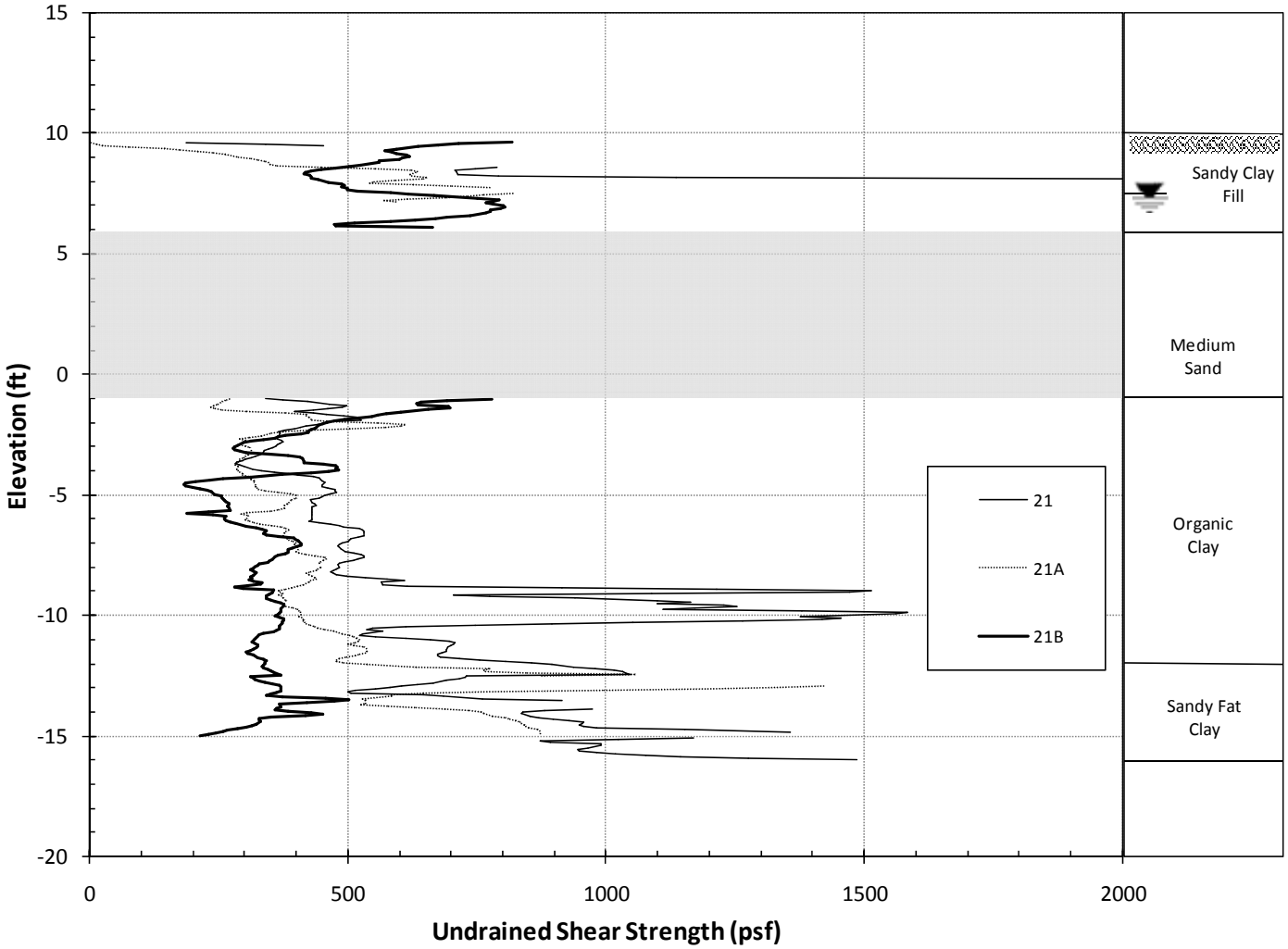

Figure 5.40: Undrained shear strength profiles determined from piezocone soundings at Site 4

.

Table 5.12: Summary of field vane shear test results at Site 4.

Elevation (ft)	Measured Peak $s_{u\text{-}FV}$ (psf)	Measured Remolded $s_{u\text{-}FV,\,r}$ (psf)	S_t	Plasticity Index (%)	μ	Corrected $s_{u\text{-}FVc}$ (psf)
-3	814	125	6.5	93	0.53	429
-7	1044	157	6.6	206	0.51	532
-11.5	1274	104	12.3	105	0.52	661
-16	1336	-	-	62	0.70	935

5.5.3 Triaxial Testing

Thin-walled tube samples were recovered from a boring located approximately 10 feet from the field vane boring. Sixteen unconsolidated-undrained (UU) tests and six consolidated-undrained (CU) tests were performed on specimens from tube samples.

Normalized stress-strain curves from the UU tests are plotted in Figure 5.20. The peak principal stress difference was generally reached at an axial strain ranging from approximately 3 to 6 percent. Several of the tests also showed notable strain-softening, with post-peak reductions in strength ranging from approximately 20 to 30 percent.

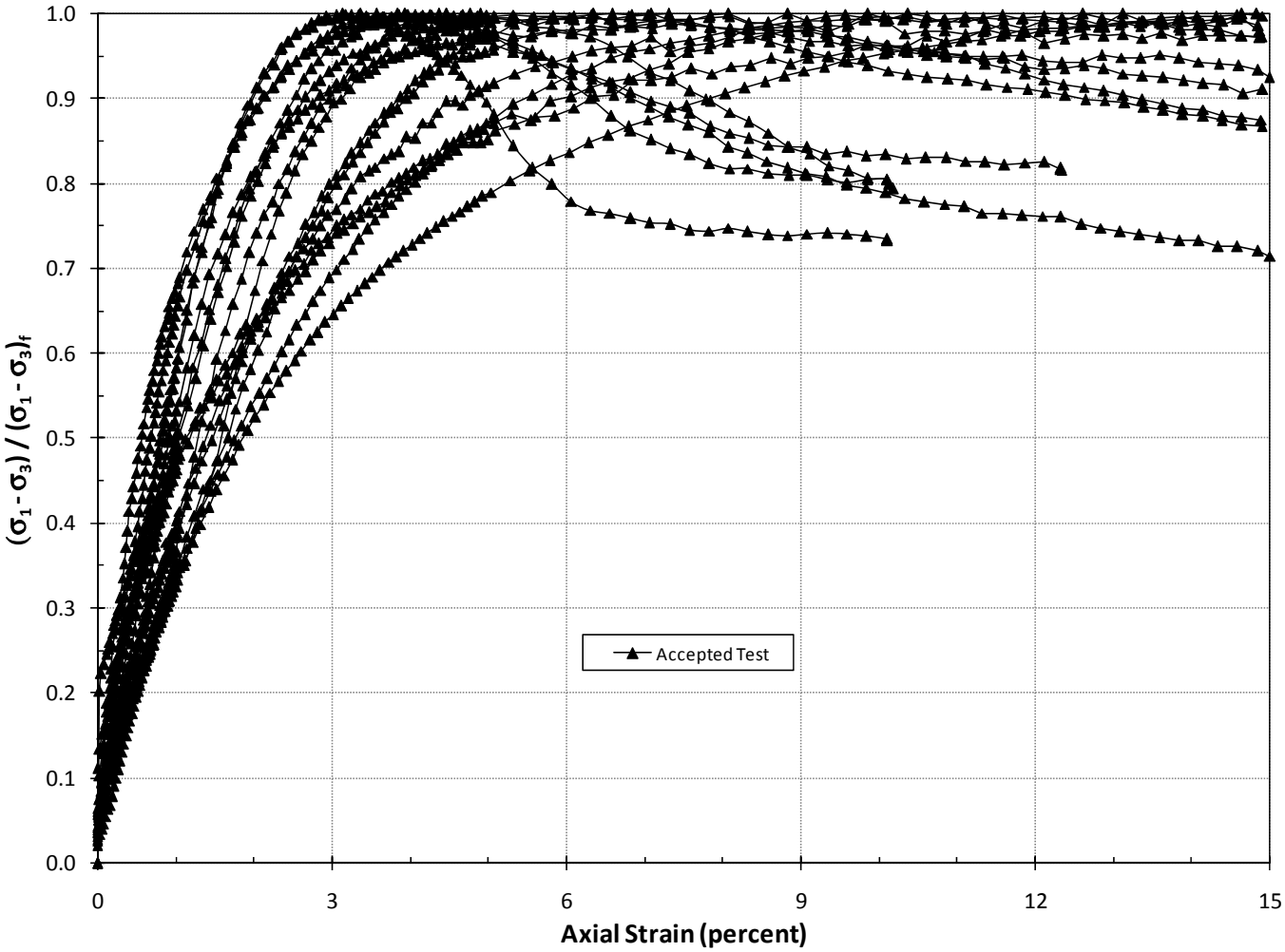

Figure 5.41: Normalized stress-strain curves from UU tests at Site 4

Values of axial strain at 75 percent of the principal stress difference at failure ($\varepsilon_{75\%}$) are shown for the UU tests in Table 5.10. The values ranged from 1.2 to 4 percent, with an average value of 2.3 percent. The stress-strain behavior and relatively low strains for these tests suggests high-quality samples.

Table 5.13: Values of axial strain at 75 percent of principal stress difference at failure for UU tests at Site 4.

Elevation (ft)	Test Result	$\varepsilon_{75\%}$ (%)
+8	Accepted	4.3
+7	Accepted	2.2
+6.5	Accepted	1.3
-2.5	Accepted	2.7
-3	Accepted	1.7
-4	Accepted	1.6
-5	Accepted	3.5
-6	Accepted	1.8
-7	Accepted	2.0
-8	Accepted	2.6
-9	Accepted	2.9
-10	Accepted	2.8
-11	Accepted	3.2
-12	Accepted	1.3
-13.5	Accepted	1.2
-14	Accepted	1.3

Values of volumetric strain during consolidation ($\varepsilon_{v\text{-}c}$) in CU tests are shown in Table 5.11. Volumetric strains during consolidation of the consolidated-undrained test specimens were relatively low. Of the six consolidated-undrained tests performed, four specimens had less than 3.5 percent volumetric strain during consolidation. The values for the other two specimens (El. -9.5 and -13.5 feet) were 4.4 and 5.9 percent. Andersen and Kolstad suggest specimens with an overconsolidation ratio of 1.5 to 2, like those tested, are disturbed if the volumetric strain during consolidation exceeds 3.5 percent. Based on this criterion, four of the six specimens were of "acceptable" quality.

Table 5.14: Values of volumetric strain during consolidation to effective overburden stress for CU tests at Site 4.

Elevation (ft)	Sample Quality	$\varepsilon_{v\text{-}c}$ (%)
-3.5	Acceptable	3.5
-5.5	Acceptable	3.0
-7.5	Acceptable	2.1
-9.5	Disturbed	4.4
-11.5	Acceptable	2.9
-13	Disturbed	5.9

5.5.4 One-Dimensional Consolidation Testing

A single one-dimensional, constant rate of strain (CRS) consolidation test was performed on a specimen of organic clay from El. -11.3 feet (21.3 foot depth). Void ratio is plotted versus vertical effective stress for this test in Figure 5.21. The maximum previous effective stress (σ'_p) was determined using the Casagrande construction and is indicated in the figure. Also, the present in-situ effective overburden stress (σ'_{vo}) was computed using the total unit weights of specimens from tube samples and pore water pressures determined from ground water table observations at the site. The present in-situ effective overburden stress is indicated in the figure.

An overconsolidation ratio was calculated from the one-dimensional consolidation test and found to be approximately 1.8. This value is plotted with the profiles of overconsolidation ratio determined from the piezocone penetration tests in Figure 5.22. The results of the piezocone tests agree well with the consolidation test.

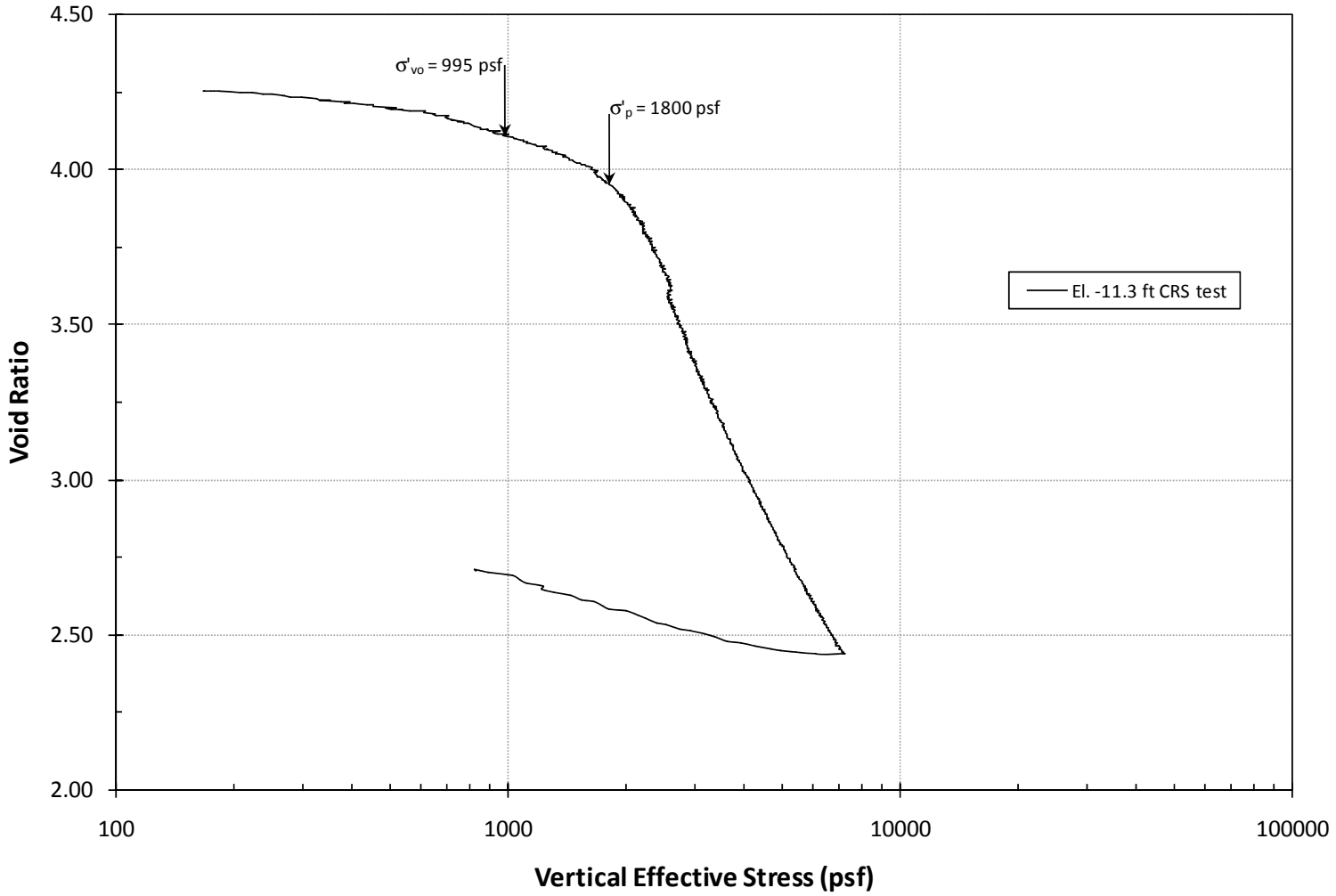

Figure 5.42: One-dimensional consolidation test results for Site 4

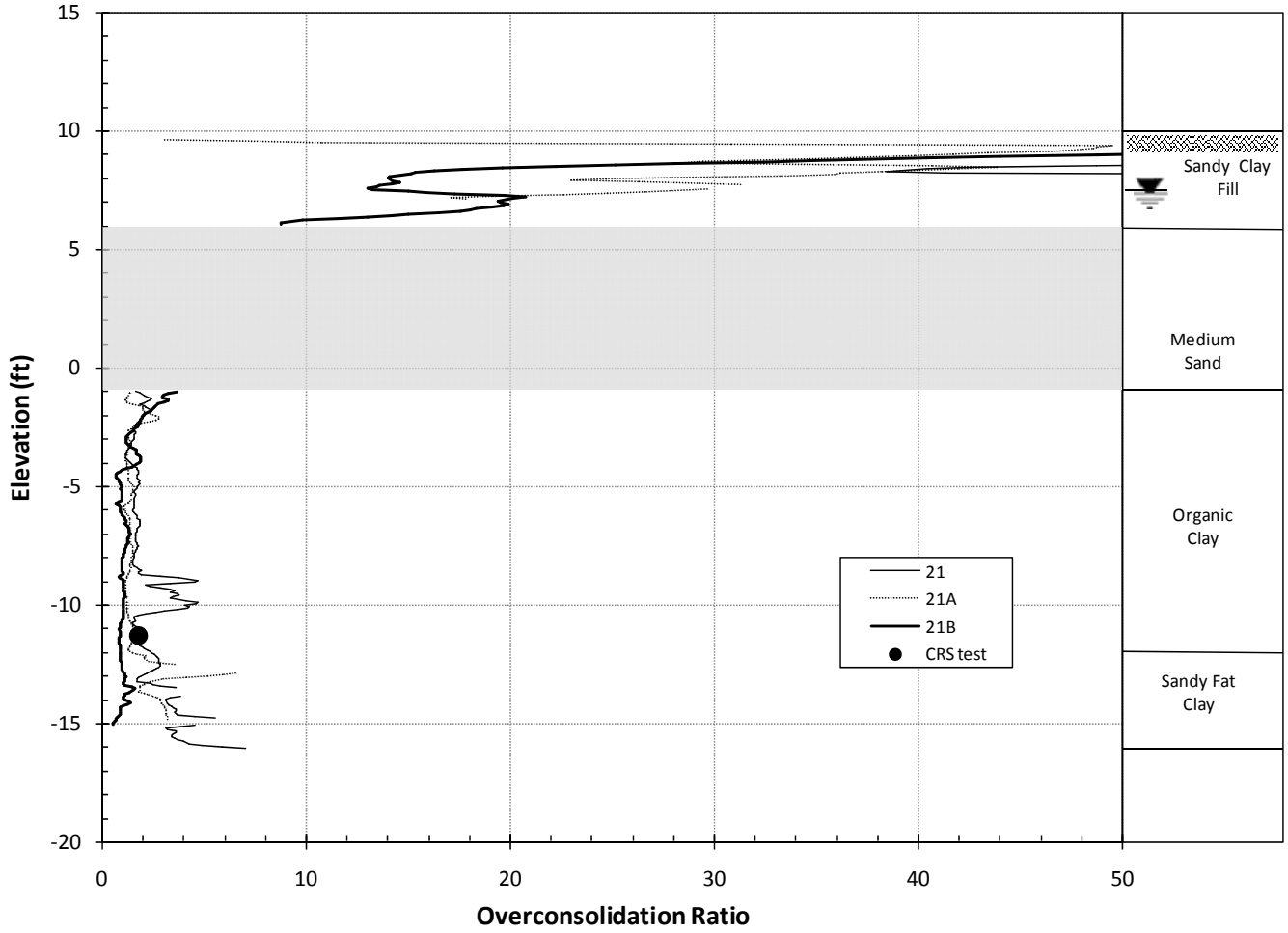

Figure 5.43: Overconsolidation ratios determined from one-dimensional consolidation test and piezocone penetration tests for Site 4

.

5.5.5 Undrained Shear Strength Profile

Undrained strengths determined from triaxial and field vane shear tests are plotted versus elevation in Figure 5.23. Data from this figure were combined with strengths derived from piezocone penetration data in Figure 5.24. The data were then analyzed and interpreted to determine a representative average undrained shear strength profile and upper and lower bounds for undrained shear strength, which are also shown in Figure 5.24. In the following sections, the average, upper and lower bound undrained strength profiles, and test results are discussed further for various ranges of elevation.

El. +10 to +6 feet (0 to 4 foot depth)

In the upper 4 feet of fill material, there was a broad range in the undrained shear strength measured using unconsolidated-undrained tests, with the strengths ranging from approximately 600 to 1,900 psf. The undrained strength determined from piezocone soundings tended to range from approximately 500 to 800 psf. However, sounding 21 did indicate higher strengths, which agree with the unconsolidated-undrained tests performed at El. +8 feet (2 foot depth). The strengths from the unconsolidated-undrained tests were used as a basis for the average strength, upper and lower bound undrained strength profiles.

El. +6 to -1 feet (4 to 11 foot depths)

Soil from these depths is sandy and undrained strengths are not applicable.

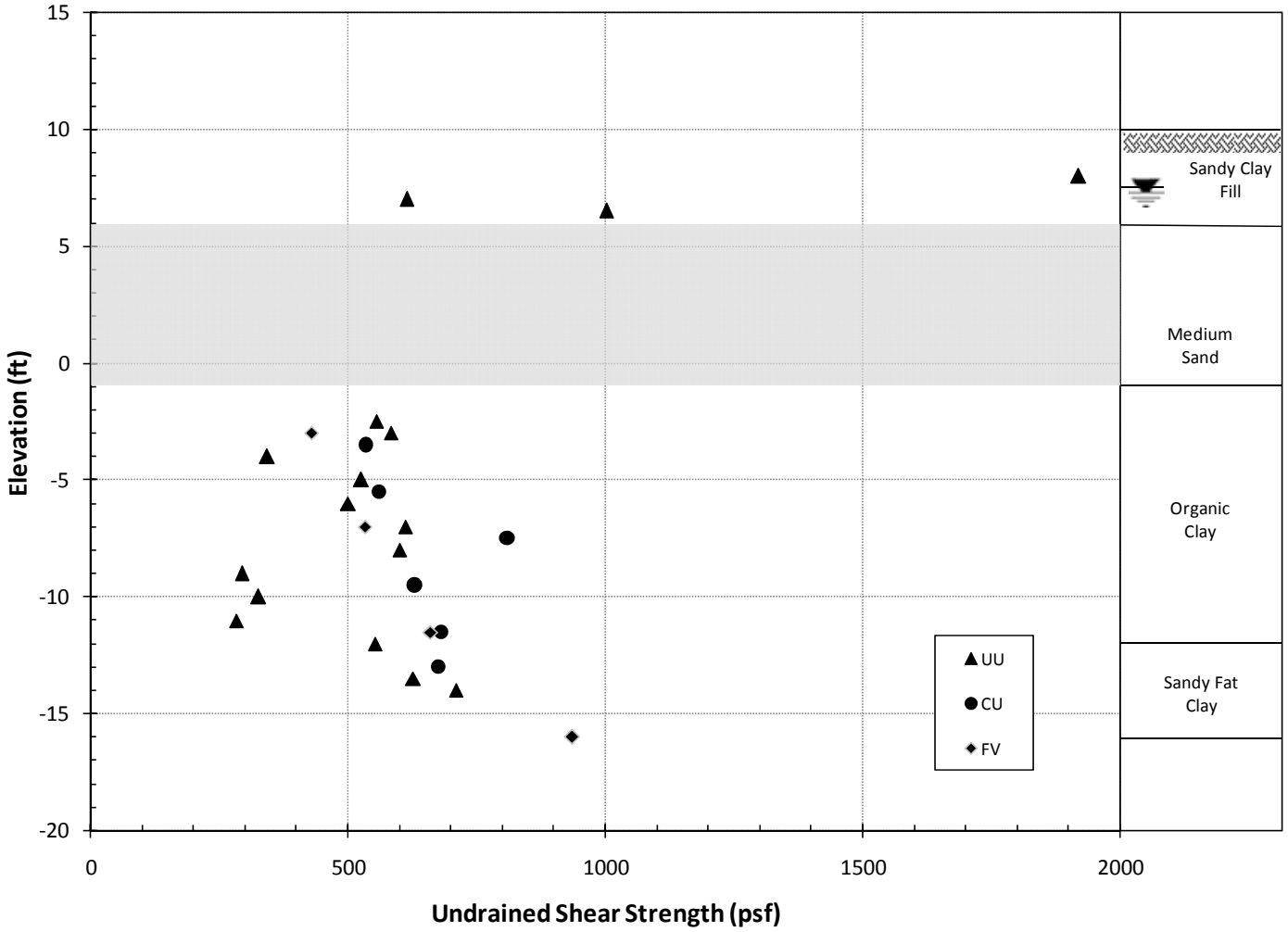

Figure 5.44: Undrained shear strengths from triaxial and field vane tests at Site 4

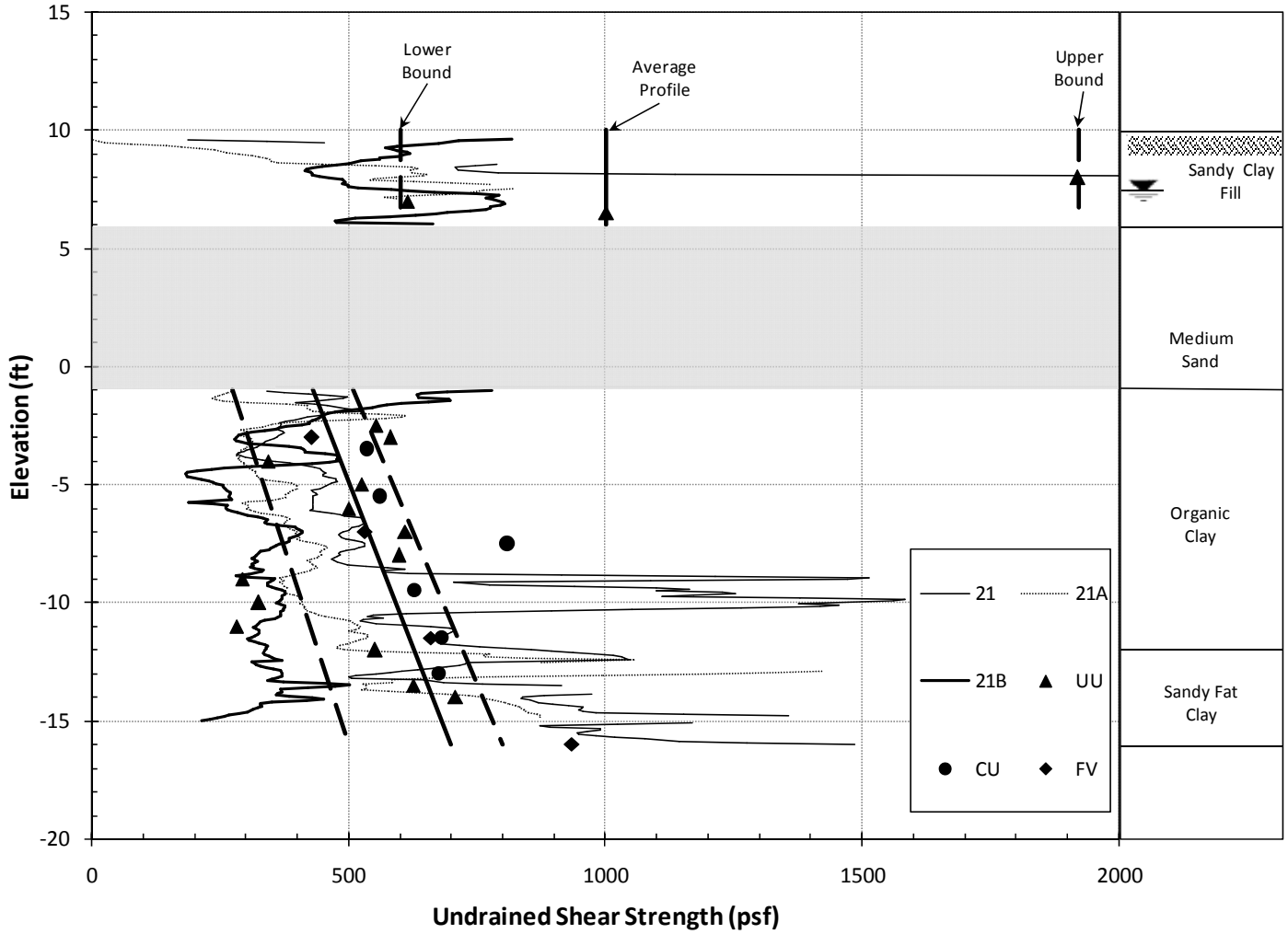

Figure 5.45: Undrained shear strength profile and bounds with piezocone, vane, and triaxial test strengths for Site 4

El. -1 to -16 feet (11 to 26 foot depth)

In this range of elevations, there was very good agreement among the undrained shear strengths measured using unconsolidated-undrained, consolidated-undrained, and field vane shear tests. The majority of the unconsolidated-undrained and consolidated-undrained tests yielded strengths that were within 50 psf of the strength for the average profile. From El. -9 to -11 feet (19 to 21 foot depth), three unconsolidated-undrained tests were performed. These yielded strengths approximately 50 percent lower than strengths for the average profile. However, in all three tests the axial strains (represented by $\varepsilon_{75\%}$ values) were greater than the average value (2.2 percent) for the unconsolidated-undrained tests performed on specimens for this interval. These larger strains may be indicative of some sample disturbance. Although the strengths from these three tests agree with strengths determined from piezocone soundings 21A and 21B, this agreement may be fortuitous. A consolidated-undrained performed on a specimen from between two of the three unconsolidated-undrained test specimens in question yielded a strength which agreed with the average profile.

Comparing the results of the piezocone penetration tests to the average undrained shear strength profile, the strengths derived from the piezocone tests tended to be less than strengths from the average profile below El. -1 feet (11 foot depth), especially soundings 21A and 21B. Sounding 21B did agree somewhat with the unconsolidated-undrained tests performed between El. -9 to -11 feet (19 to 21 foot depth). However, as previously discussed, this agreement seems fortuitous given the fact that the results from these triaxial tests seem to be questionable. Piezocone sounding 21 also tended to produce strengths less than the average profile, but to a much lesser degree. Below El. -8 feet (18 foot depth), the shape of the undrained strength profile determined from sounding 21 became much more erratic and inconsistent, suggesting the cone was penetrating through a more variable soil and possibly also a sandier soil. These strengths are significantly higher than those measured in the laboratory and with the vane, as well as significantly higher than the upper bound on the strength profile.

In this elevation range, the representative undrained shear strength profile agreed very well with strengths from field vane shear, unconsolidated-undrained, and consolidated-undrained tests. The lower bound undrained strength profile was selected on the basis of strengths from piezocone soundings 21A and 21B, while the upper bound profile was selected based primarily on strengths from sounding 21.

5.6 Site 5

Site 5 is located south of the Gulf Coast Highway and slightly east of Sabine Pass in Cameron Parish, Louisiana. Beginning at the ground surface, the subsurface profile consists of a 2-foot-thick layer of sandy clay fill, underlain by fat clay and sandy fat clay to a depth of 26 feet. The ground surface at the site is nearly level, with the ground surface located at approximately El. 0 feet. During the subsurface investigation, the groundwater was observed to be 8 feet below the ground surface of the boring where tube samples were taken. No piezocone penetration tests were performed at Site 5.

5.6.1 Field Vane Shear Testing

Field vane shear tests were performed in a boring located within 10 feet of the tube sample boring. Seven tests were performed in the layer of fat clay and sandy fat clay. Test results

are reported in Table 5.12. The sensitivities at this site ranged from 3.6 to 9.5, with the majority of tests showing sensitivities between 4.5 and 6.7.

Table 5.15: Summary of field vane shear test results at Site 5.

Elevation (ft)	Measured Peak $s_{u\text{-}FV}$ (psf)	Measured Remolded $s_{u\text{-}FV,\,r}$ (psf)	S_t	Plasticity Index (%)	μ	Corrected $s_{u\text{-}FVc}$ (psf)
-3	188	52	3.6	52	0.80	150
-6.5	397	42	9.5	52	0.80	318
-9.5	282	63	4.5	52	0.80	226
-12.5	271	42	6.5	60	0.72	195
-16	292	52	5.6	60	0.72	210
19.5	334	63	5.3	31	0.89	297
-22.5	282	42	6.7	43	0.82	231
-26	397	73	5.4	43	0.82	326

5.6.2 Triaxial Testing

Tube samples were recovered from a boring located within 10 feet of the boring where field vane shear tests were performed. Sixteen unconsolidated-undrained (UU) tests and five consolidated-undrained (CU) tests were performed on specimens from the tube samples.

Normalized stress-strain curves are presented for the UU tests in Figure 5.25. The results of eight UU tests were considered questionable due to their stress strain behavior. The accepted tests showed principal stress difference generally peaking at axial strains less than 9 percent, while the questionable tests showed the principal stress difference continuing to increase to axial strains as high as 15 percent. This behavior is believed to be primarily due to sample disturbance.

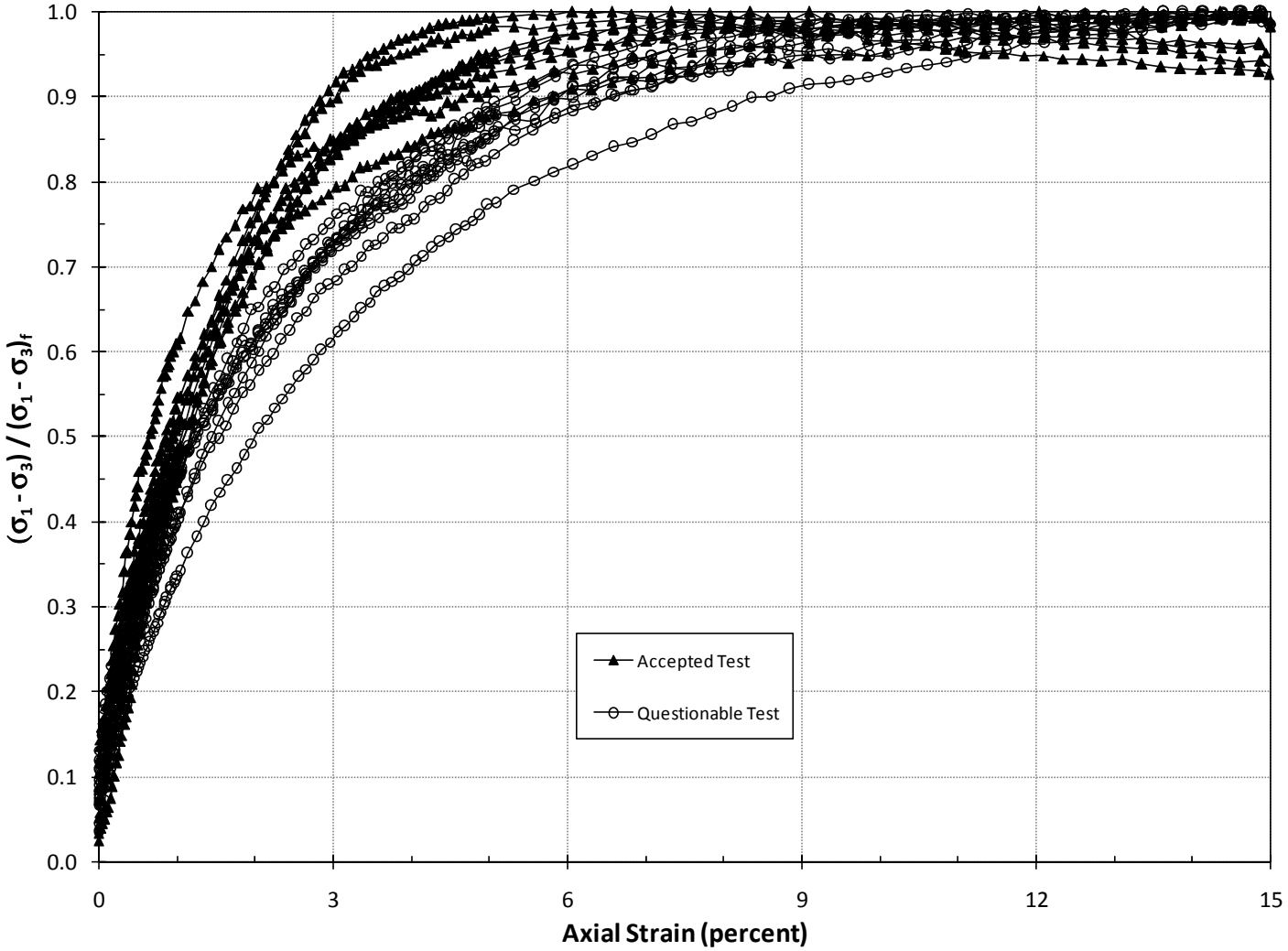

Figure 5.46: Normalized stress-strain curves from accepted and questionable UU tests at Site 5

Values of axial strain at 75 percent of the principal stress difference at failure ($\varepsilon_{75\%}$) are shown for the UU tests at Site 5 in Table 5.13. The questionable tests showed higher strains than the accepted tests. For the questionable tests, $\varepsilon_{75\%}$ values ranged from 2.9 to 5.7 percent, versus 1.7 to 2.3 percent for accepted tests. Half of the UU tests were considered questionable. It is believed that these specimens were badly disturbed.

Table 5.16: Values of axial strain at 75 percent of principal stress difference at failure for UU tests at Site 5

Elevation (ft)	Test Result	$\varepsilon_{75\%}$ (%)
-3	Accepted	1.9
-3.5	Accepted	2.1
-5	Accepted	2.1
-5.5	Questionable	4.7
-6.5	Accepted	2.2
-7.5	Questionable	3.4
-8.0	Accepted	2.3
-9.5	Accepted	1.8
-10.5	Accepted	1.7
-11.5	Questionable	3.3
-13.5	Questionable	3.3
-14.5	Questionable	3.9
-15	Questionable	3.3
-16.5	Questionable	2.9
-17	Questionable	3.2
-17.5	Accepted	2.3

The results of the consolidated-undrained tests were also indicative of badly disturbed samples. Values of volumetric strain during consolidation ($\varepsilon_{v\text{-}c}$) are shown in Table 5.14. Of the five CU tests performed, four experienced volumetric strain during consolidation greater than 8.1 percent. One test (El. -7 feet) had a volumetric strain during consolidation of 4.8 percent. For specimens having an overconsolidation ratio of 1.3, like those tested, Andersen and Kolstad (1979) suggest samples are disturbed if they experience greater than 4 percent volumetric strain during consolidation. Based on this, all five CU test specimens were disturbed, therefore likely yielding strengths that were too high.

Table 5.17: Values of volumetric strain during consolidation to effective overburden stress for CU tests at Site 5

Elevation (ft)	Sample Quality	$\varepsilon_{v\text{-}c}$ (%)
-7	Disturbed	4.8
-9	Disturbed	13.4
-11	Disturbed	15.3
-15.5	Disturbed	8.1
-24	Disturbed	9.7

5.6.3 One-Dimensional Consolidation Testing

A single one-dimensional, constant rate of strain (CRS) consolidation test was performed on a specimen from El. -16.5 feet (16.5 foot depth). Void ratio is plotted versus vertical effective stress in Figure 5.26. The maximum previous effective stress (σ'_p) was determined using the Casagrande construction and is indicated in the figure. Also, the present in-situ effective overburden stress (σ'_{vo}) was computed using the total unit weights of specimens from tube samples and pore water pressures determined from ground water table observations at the site. The present in-situ effective overburden stress is indicated in the figure.

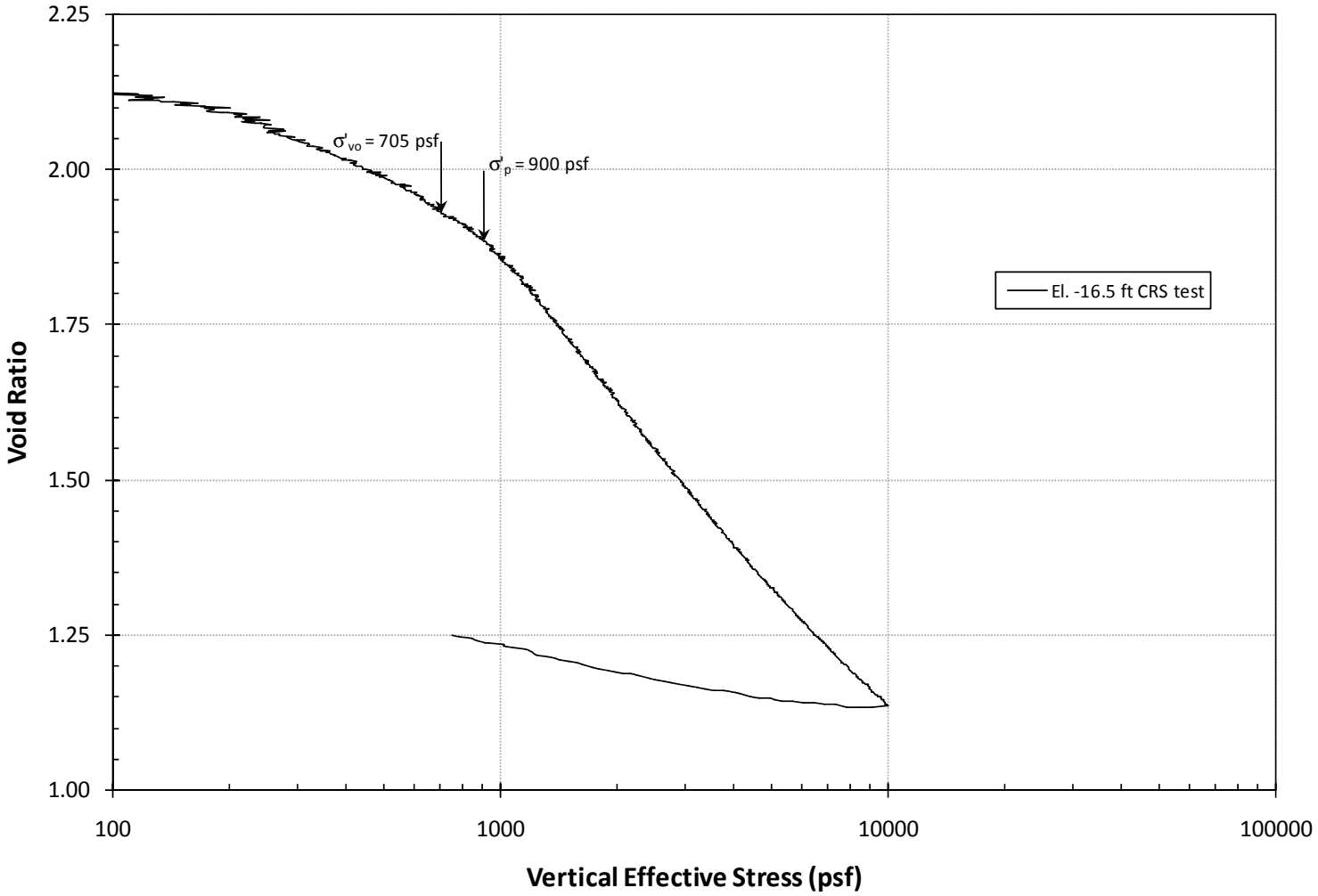

Figure 5.47: One-dimensional consolidation test results for Site 5

Given the relatively large change in void ratio during consolidation to σ'_{vo}, which corresponds with an axial strain of 7.9 percent, the test specimen was disturbed based on Andersen and Kolstad's (1979) sample quality criterion. Based on the results of this test, the layer of fat clay and sandy fat clay is lightly overconsolidated, with an overconsolidation ratio of approximately 1.3 at El. -16.5 feet. However, because the test specimen was fairly disturbed, this may be an underestimation of the overconsolidation ratio.

5.6.4 Undrained Shear Strength Profile

Undrained strengths determined from undrained triaxial and field vane shear tests are plotted versus elevation in Figure 5.27. Data in this figure were analyzed and interpreted to determine a representative average undrained shear strength profile, and upper and lower bounds for undrained shear strength, which are also shown in Figure 5.27. In the following sections, the average, upper and lower bound undrained strength profiles, and test results are discussed further for two ranges of elevation.

El. 0 to -2 feet (0 to 2 foot depth)

In this elevation range, undrained shear strengths are not applicable.

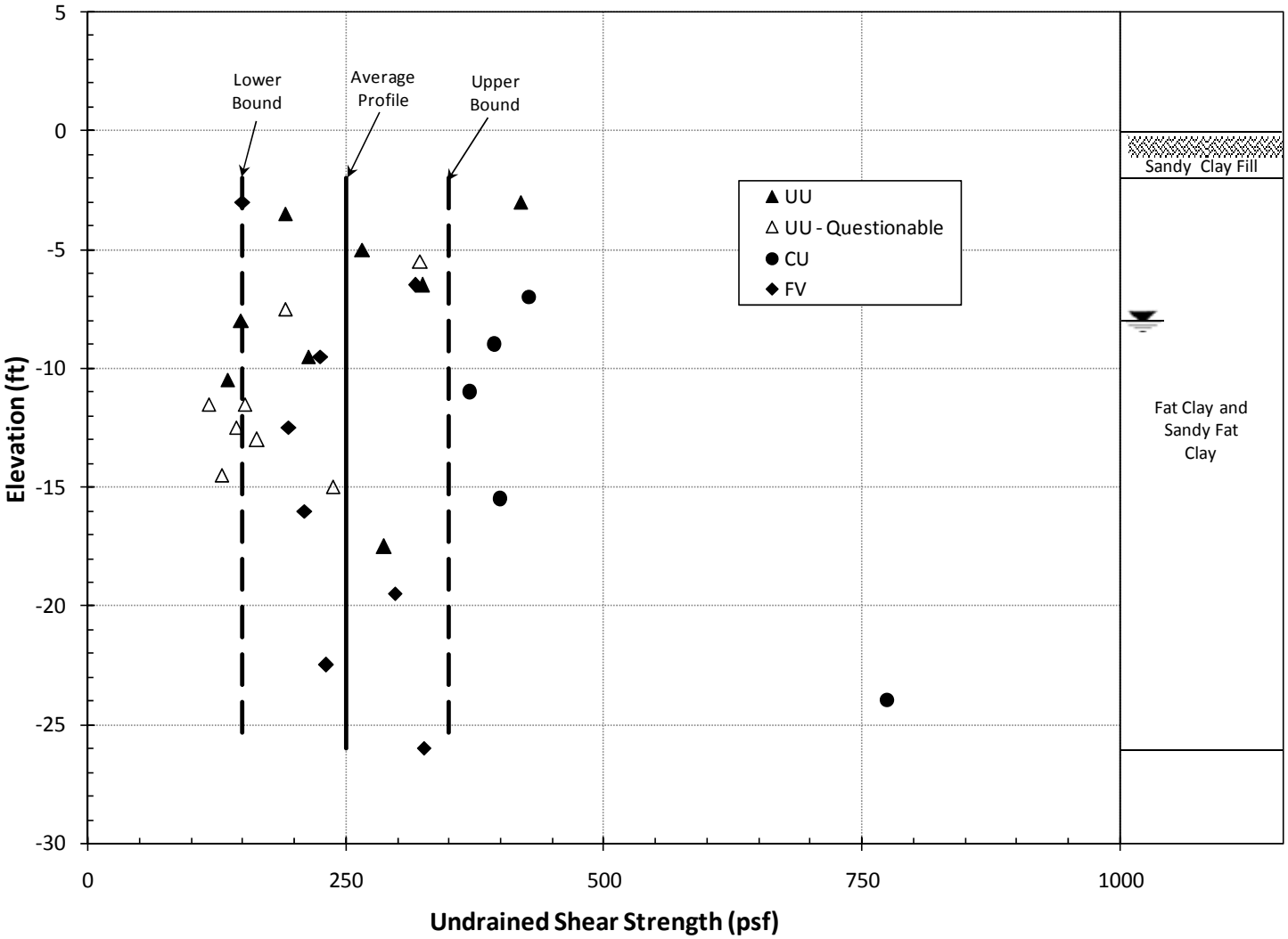

Figure 5.48: Undrained shear strength profile and bounds with vane and triaxial test strengths for Site 5

El. -2 to -26 feet (2 to 26 foot depth)

In this range of elevations, the strengths measured in unconsolidated-undrained tests ranged from approximately 130 to 420 psf. The bulk of the tests yielded strengths significantly lower than those from the representative average profile. This is believed to be largely the result of sample disturbance. The strengths from these tests also did not show a clear increase in undrained strength with depth. Strengths from consolidated-undrained tests in this range yielded strengths notably greater than those from the upper bound strength profile. This was expected, given the relatively large volumetric strains the specimens experienced during consolidation.

The best data for this layer came from field vane shear tests. Strengths from field vane shear showed a relatively constant strength with depth. The average corrected field vane shear strength was approximately 244 psf, which agrees well with the strength of 250 psf that was selected for the average profile. Since most unconsolidated-undrained and consolidated-undrained test specimens appeared to be significantly disturbed, vane shear strengths were used as the primary basis for the average strength profile in this range of elevations.

5.7 Site 6

Site 6 is located approximately one mile southeast of Site 5 in Cameron Parish, Louisiana. Beginning at the ground surface, the subsurface profile consists of a 2-foot-thick layer of sandy clay fill, underlain by fat clay and sandy fat clay to a depth of 26 feet. The ground surface at the site is nearly level, with the ground surface located at approximately El. 0 feet. During the subsurface investigation, the groundwater table was observed to be 8 feet below the ground surface of the boring where tube samples were taken. No piezocone penetration tests were performed at Site 6.

5.7.1 Field Vane Shear Testing

Field vane shear tests were performed in a boring located within 10 feet of the boring where tube samples were taken. Seven tests were performed in the layer of fat clay and sandy fat clay. Test results are reported in Table 5.15. The remolded strength was measured in all tests except the test performed at El. -26 feet. Two tests (El. -3 and -16 feet) indicated relatively sensitive soil, with sensitivities of 9.4 and 17.2, respectively.

Table 5.18: Summary of field vane shear test results at Site 6

Elevation (ft)	Measured Peak $s_{u\text{-}FV}$ (psf)	Measured Remolded $s_{u\text{-}FV,\,r}$ (psf)	S_t	Plasticity Index (%)	μ	Corrected $s_{u\text{-}FVc}$ (psf)
-3	793	84	9.4	48	0.78	619
-6.5	219	63	3.5	48	0.78	171
-9.5	125	63	2.0	48	0.78	98
-12.5	459	63	7.3	49	0.79	362
-16	532	31	17.2	49	0.78	415
19.5	574	84	6.8	40	0.80	459
-22.5	407	94	4.3	40	0.80	326
-26	887	-	-	30	0.90	798

5.7.2 Triaxial Testing

Tube samples were recovered from a boring located within 10 feet of the boring where field vane shear tests were performed. Seventeen unconsolidated-undrained and four consolidated-undrained tests were performed on specimens from tube samples.

Normalized stress-strain curves are plotted for the UU tests in Figure 5.28. Eight of the UU tests were considered questionable due to their stress-strain behavior. Nine tests were accepted. These tests generally showed the peak principal stress difference being reached at between approximately 6 to 9 percent axial strain. The questionable tests showed higher strains, with principal stress difference continuing to increase to axial strains as high as 15 percent. This behavior is believed to be primarily due to sample disturbance.

Values of axial strain at 75 percent of the principal stress difference at failure ($\varepsilon_{75\%}$) are shown for the UU tests at Site 6 in Table 5.16 The questionable tests generally showed higher strains than the accepted tests. For questionable tests, $\varepsilon_{75\%}$ values ranged from 2.3 to 6.8 percent, with most tests showing values greater than 3 percent. The values of $\varepsilon_{75\%}$ ranged from 1.6 to 2.3 for accepted tests. The higher strains and stress-strain behavior seen in questionable tests is believed to be due to sample disturbance.

Table 5.19: Values of axial strain at 75 percent of principal stress difference at failure for UU tests at Site 6

Elevation (ft)	Test Result	$\varepsilon_{75\%}$ (%)
-3.5	Accepted	1.8
-4.5	Accepted	1.6
-5.5	Questionable	3.6
-7.0	Questionable	5.0
-7.5	Questionable	6.8
-8.5	Questionable	5.8
-9.5	Accepted	3.4
-11.5	Accepted	2.5
-12.5	Accepted	2.3
-13.0	Accepted	1.6
-14.5	Accepted	1.9
-15	Accepted	2.2
-16.5	Questionable	2.3
-17.5	Questionable	2.9
-20.5	Questionable	3.3
-21.5	Accepted	2.3
-23	Questionable	6.1

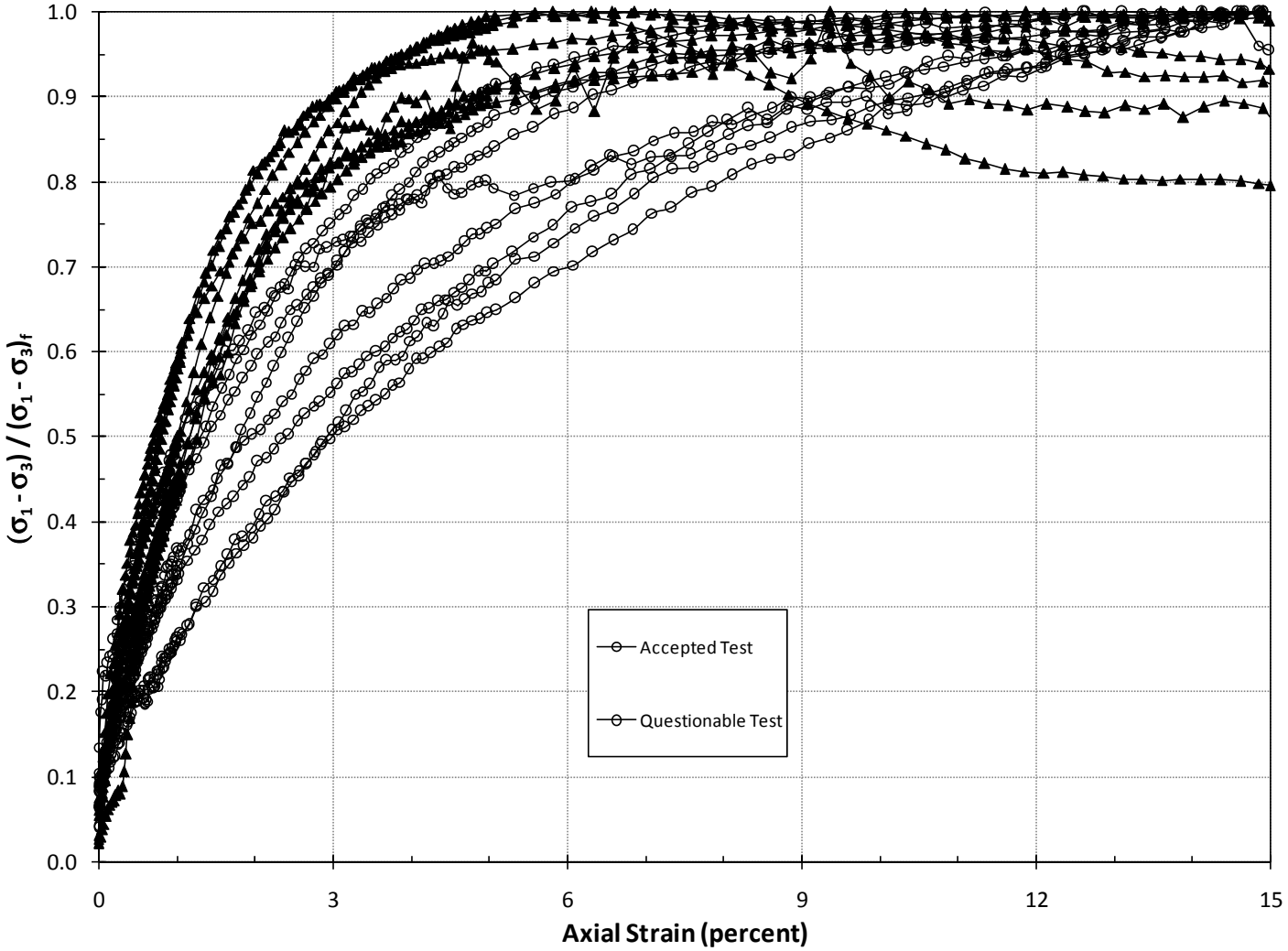

Figure 5.49: Normalized stress-strain curves from accepted and questionable UU tests at Site 6

The results of consolidated-undrained (CU) tests also suggested badly disturbed samples. Values of volumetric strain during consolidation ($\varepsilon_{v\text{-}c}$) are shown in Table 5.17. Volumetric strains during consolidation were relatively high for all four CU test specimens, the values ranging from 6.1 to 23.2 percent. Although an overconsolidation ratio of less than was computed from the results of a one-dimensional consolidation test, Andersen and Kolstad suggest specimens with an overconsolidation of 1 to 1.2 are disturbed if volumetric strain during consolidation exceeds 5 percent. Based on this criterion, all four CU test specimens were judged to be disturbed, therefore likely yielding strengths that are too high.

Table 5.20: Values of volumetric strain during consolidation to effective overburden stress for CU tests at Site 6.

Elevation (ft)	Sample Quality	$\varepsilon_{v\text{-}c}$ (%)
-5	Disturbed	19.7
-13.5	Disturbed	6.1
-17.5	Disturbed	23.2
-21	Disturbed	7.7

5.7.3 One-Dimensional Consolidation Testing

A single one-dimensional, constant rate of strain (CRS) consolidation test was performed on a specimen from El. -20.5 (20.5 foot depth). Void ratio is plotted versus vertical effective stress in Figure 5.29. The maximum previous effective stress (σ'_p) was determined using the Casagrande construction and is indicated in the figure. Also, the present in-situ effective overburden stress (σ'_{vo}) was computed using the total unit weights of specimens from tube samples and pore water pressures determined from ground water table observations at the site and is indicated in the figure.

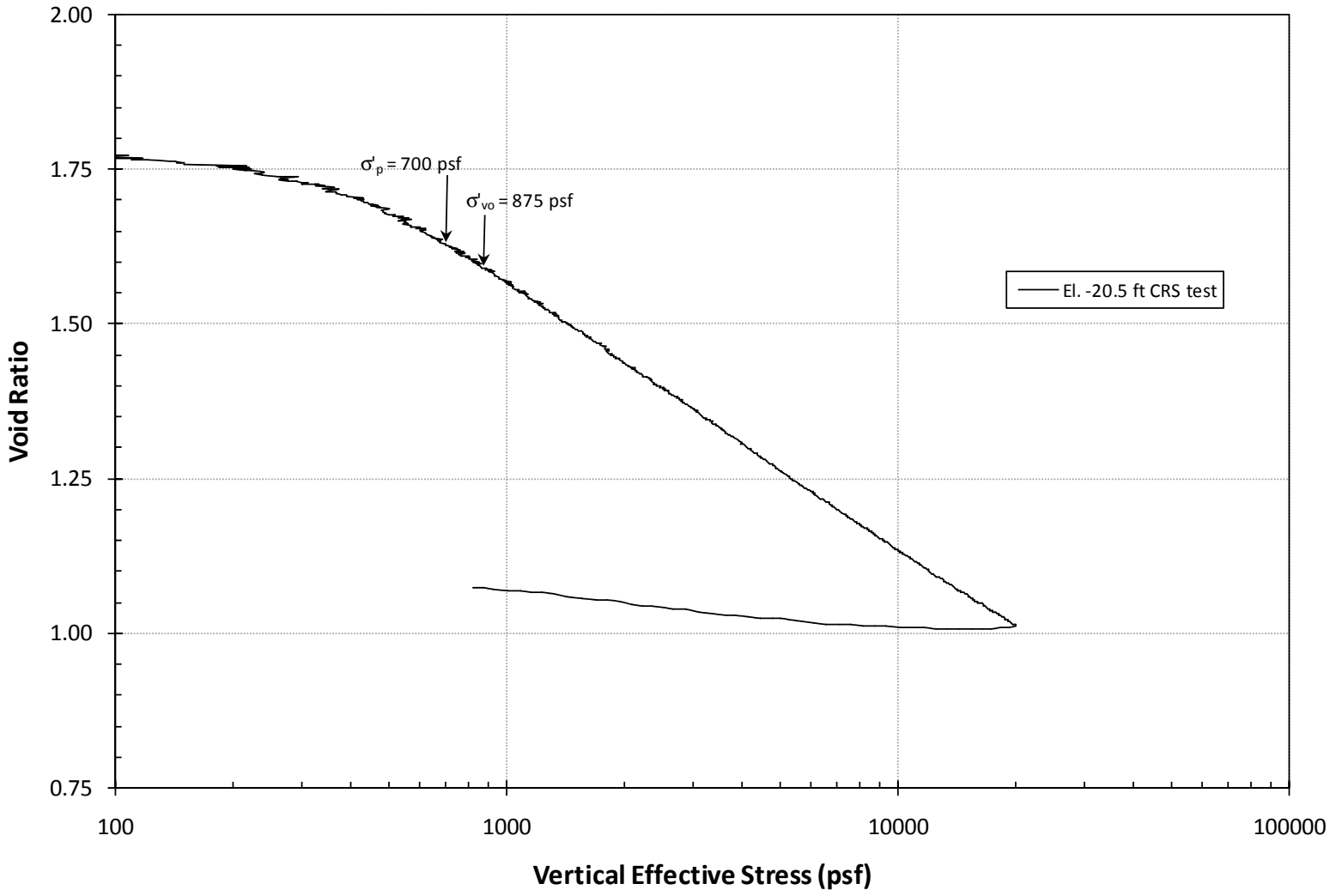

Figure 5.50: One-dimensional consolidation test results for Site 6

An overconsolidation ratio was calculated using the maximum previous effective stress from the one-dimensional consolidation test and found to be 0.8. This overconsolidation ratio of less than one was likely the result of sample disturbance. The relatively large change in void ratio during consolidation to σ'_{vo}, which corresponds with an axial strain of 8.8 percent, is also indicative of sample disturbance based on Andersen and Kolstad's (1979) sample quality criterion.

5.7.4 Undrained Shear Strength Profile

Undrained strengths determined from undrained triaxial and field vane shear tests are plotted versus depth in Figure 5.30. Data in this figure were analyzed and interpreted to determine a representative average undrained shear strength profile, and upper and lower bounds for undrained shear strength, which are also shown in Figure 5.27. In the following sections, the average, upper and lower bound undrained strength profiles, and test results are discussed further for two ranges of elevation.

El. 0 to -2 feet (0 to 2 foot depth)

In this range of elevations, undrained shear strengths are not applicable.

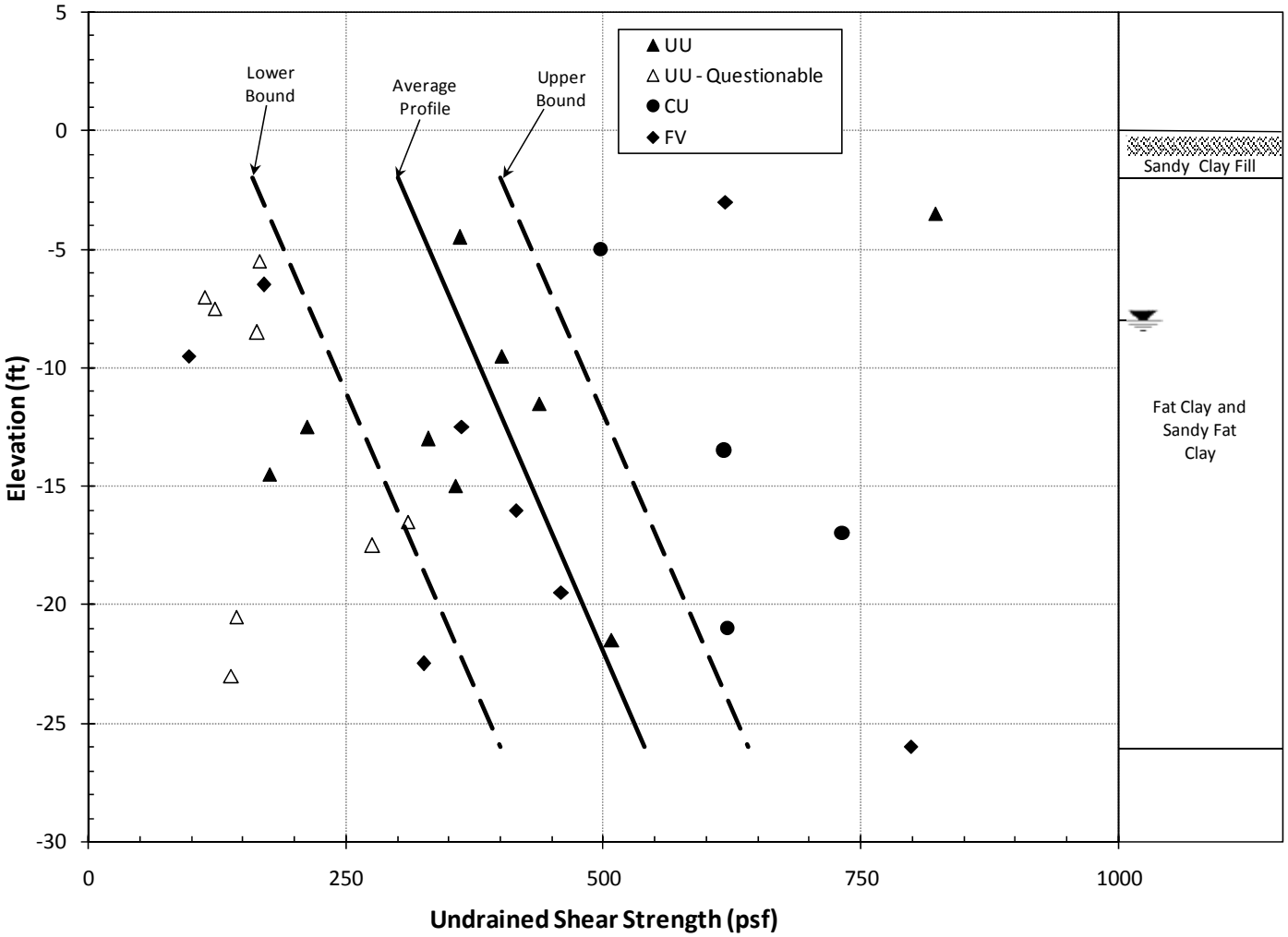

Figure 5.51: Undrained shear strength profile and bounds with vane and triaxial strengths for Site 6

El. -2 to -26 feet (2 to 26 foot depth)

In this range of elevations, the majority of undrained shear strengths from unconsolidated-undrained tests agree relatively well with the representative average strength profile. However, there were two tests (El. -12.5 and -14.5 feet) that yielded strengths less than the corresponding strengths from the lower bound. Strengths from field vane shear tests at similar elevations yielded strengths in agreement with the representative average profile.

Strengths from consolidated-undrained tests were much higher than corresponding strengths from the average profile and strengths from field vane shear and unconsolidated-undrained tests. This was expected given the large amount of volume change that occurred during consolidation. Given that these strengths were likely too high, they were used as a basis for the upper bound undrained shear strength profile.

Strengths from field vane shear tests tended to agree with the representative average profile. However, two vane shear tests (El. -6.5 and -9.5) did give strengths nearly equal to strengths from the lower bound. Unconsolidated-undrained tests at similar elevations gave strengths which agreed with the average profile. The cause of these low strengths measured with the field vane is uncertain, but it may be the result of spatial variability at the site. Since strengths from field vane shear and unconsolidated-undrained tests agreed well with one another for the most part, these strengths were used as the basis to establish the representative average undrained shear strength profile.

Chapter 6. Analysis of Undrained Shear Strength Data

In this study, undrained strengths have been determined for six sites using several different types of field and laboratory tests. The types of tests included:

- unconsolidated-undrained triaxial compression,
- consolidated-undrained triaxial compression,
- field vane shear, and
- piezocone penetration.

The results of these tests were analyzed and evaluated in Chapter 5 to determine representative average undrained shear strength profiles for each site. In this chapter, the undrained shear strengths measured in the various types of tests are compared to the average undrained strength profile and discussed.

6.1 Unconsolidated-Undrained Triaxial Compression Tests

For each site, undrained strengths from unconsolidated-undrained (UU) tests, $s_{u\text{-}UU}$, were normalized with respect to corresponding undrained strengths from the average undrained strength profile, $s_{u\text{-}Avg}$. These normalized values are plotted versus the axial strain at 75 percent of the peak principal stress difference, $\varepsilon_{75\%}$, in Figure 6.1 to assess the effects of sample disturbance. Although the data show significant scatter, the values of $s_{u\text{-}UU}/s_{u\text{-}Avg}$ tend to decrease with increasing strains, suggesting increasing amounts of sample disturbance with higher axial strains. At $\varepsilon_{75\%}$ values greater than 4 percent, over 75 percent (13 of 17) of UU tests gave strengths that were only 25 to 75 percent of the strengths from the average profiles.

At $\varepsilon_{75\%}$ values less than 4 percent, over 65 percent (52 of 78) of UU tests still underestimate strengths. Although in this range of strains the strengths are still very scattered, the UU tests on average yielded strengths approximately 75 percent of the strengths from the average profiles. A number of tests with $\varepsilon_{75\%}$ values less than 4 percent did show strengths greater than the strengths from the average profiles. This could be due to the average strengths being somewhat low. However, the relatively higher strengths for some UU test specimens were not considered justification for increasing the average strength profile adopted based on all the data.

6.2 Consolidated-Undrained Triaxial Compression Tests

Undrained strengths from consolidated-undrained (CU) tests, $s_{u\text{-}CU}$, were also normalized with respect to corresponding undrained strengths from the average undrained strength profile ($s_{u\text{-}Avg}$). These values are plotted versus the volumetric strain during consolidation, $\varepsilon_{v\text{-}c}$, in the CU tests for all sites in Figure 6.2. All specimens were consolidated to the in-situ effective overburden stress. While there is significant scatter in the data, the figure shows that at volumetric strains greater than approximately 4 percent, all CU tests overestimated strengths, with the average overestimate being approximately 50 percent. This is consistent with Berre and Bjerrum's (1973) sample quality criterion that suggests samples are disturbed if the volumetric strain during consolidation exceeds 4 percent.

Eliminating the data from Site 3 which consisted of stiff clays, the data for soft clays show that strengths from CU tests generally overestimate strengths by approximately 10 percent when the volumetric strain during consolidation is less than 4 percent. This may be due to the strengths from the average profiles being somewhat low. However, the relatively higher strengths for some CU test specimens were not considered justification for increasing the average strength profile adopted based on all the data.

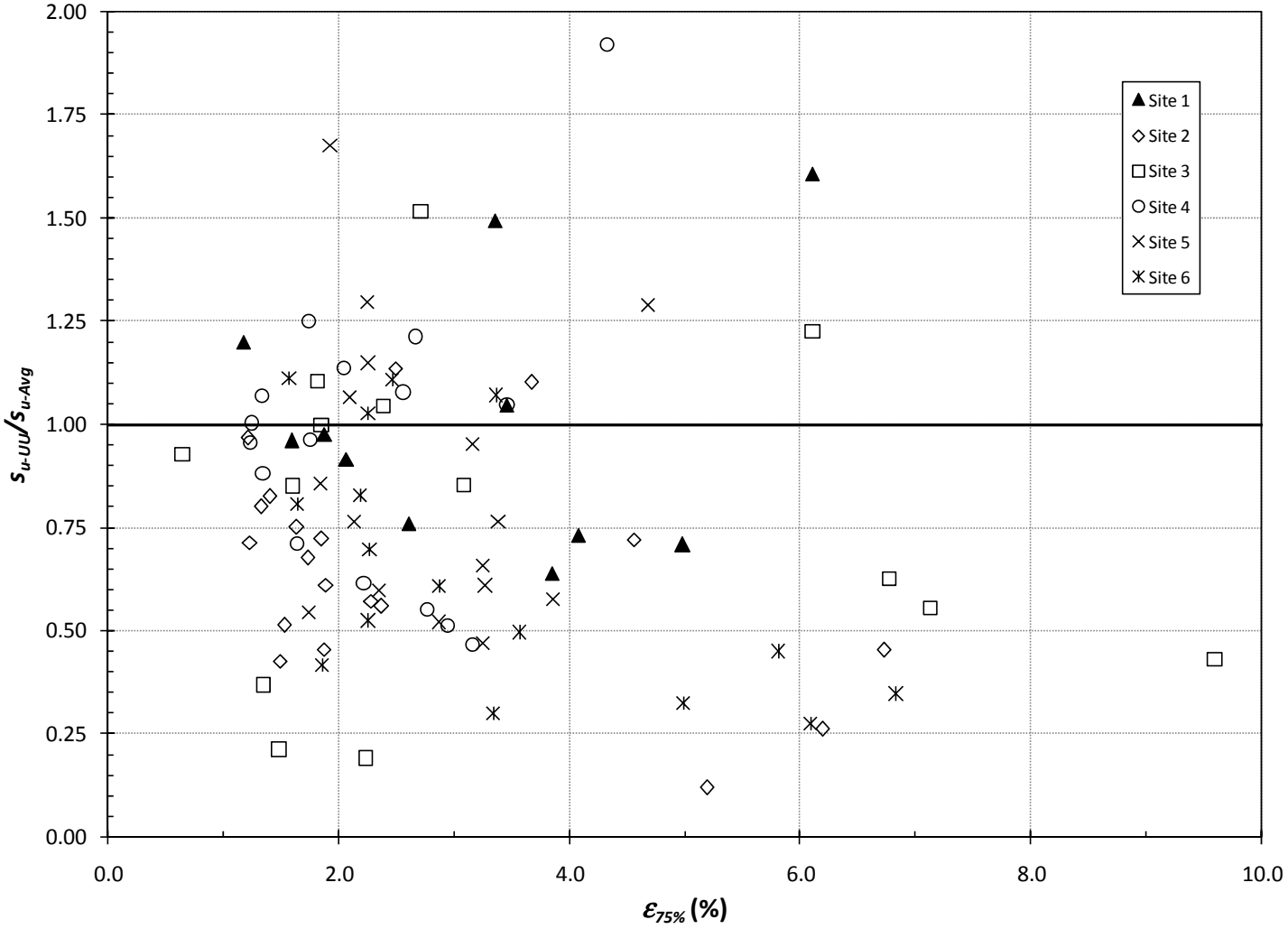

Figure 6.52: Values of normalized UU strengths versus axial strain at 75 percent of peak principal stress difference

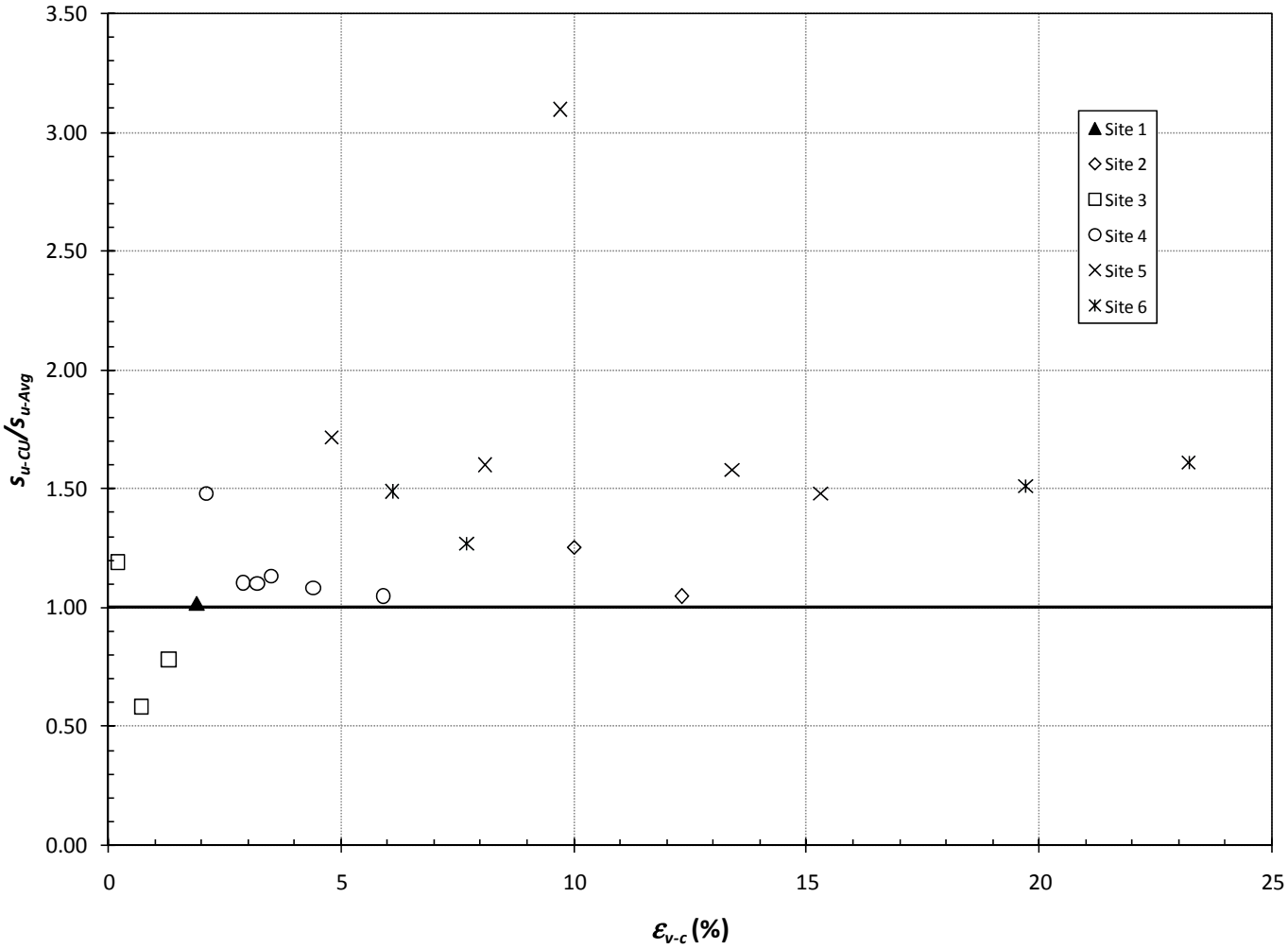

Figure 6.53: Values of normalized CU strengths plotted versus volumetric during consolidation to in-situ effective overburden stress

6.3 Field Vane Shear Tests

In Figure 6.3, corrected field vane strengths, $s_{u\text{-}FVc}$, are plotted versus corresponding strengths from the representative average strength profile ($s_{u\text{-}Avg}$) for the sites where field vane tests were performed. For most sites, the corrected field vane strengths agree relatively well with the average strengths, particularly where the soil is predominantly clay with little sand. However, the figure shows that the vane tests at Sites 2 and 6 tended to overestimate strengths. This is believed to be caused by the presence of sandier clays at these sites.

6.4 Piezocone Penetration Tests

Undrained strengths determined from piezocone soundings, $s_{u\text{-}PCPT}$, normalized with respect to corresponding strengths from the average strength profile ($s_{u\text{-}Avg}$) are plotted versus depth in Figure 6.4. In the upper 5 feet, the data show that the piezocone tends to underestimate strengths by approximately 40 percent. At greater depths, the piezocone tests at Sites 1, 2, and 3 tend to overestimate strengths by approximately 20 percent, while the piezocone tests at Site 4 tended to underestimate strengths by approximately 30 percent. These overestimates in strength generally correspond with the cone penetrating through sandy clays. The cause of the underestimates in strengths at Site 4 is uncertain.

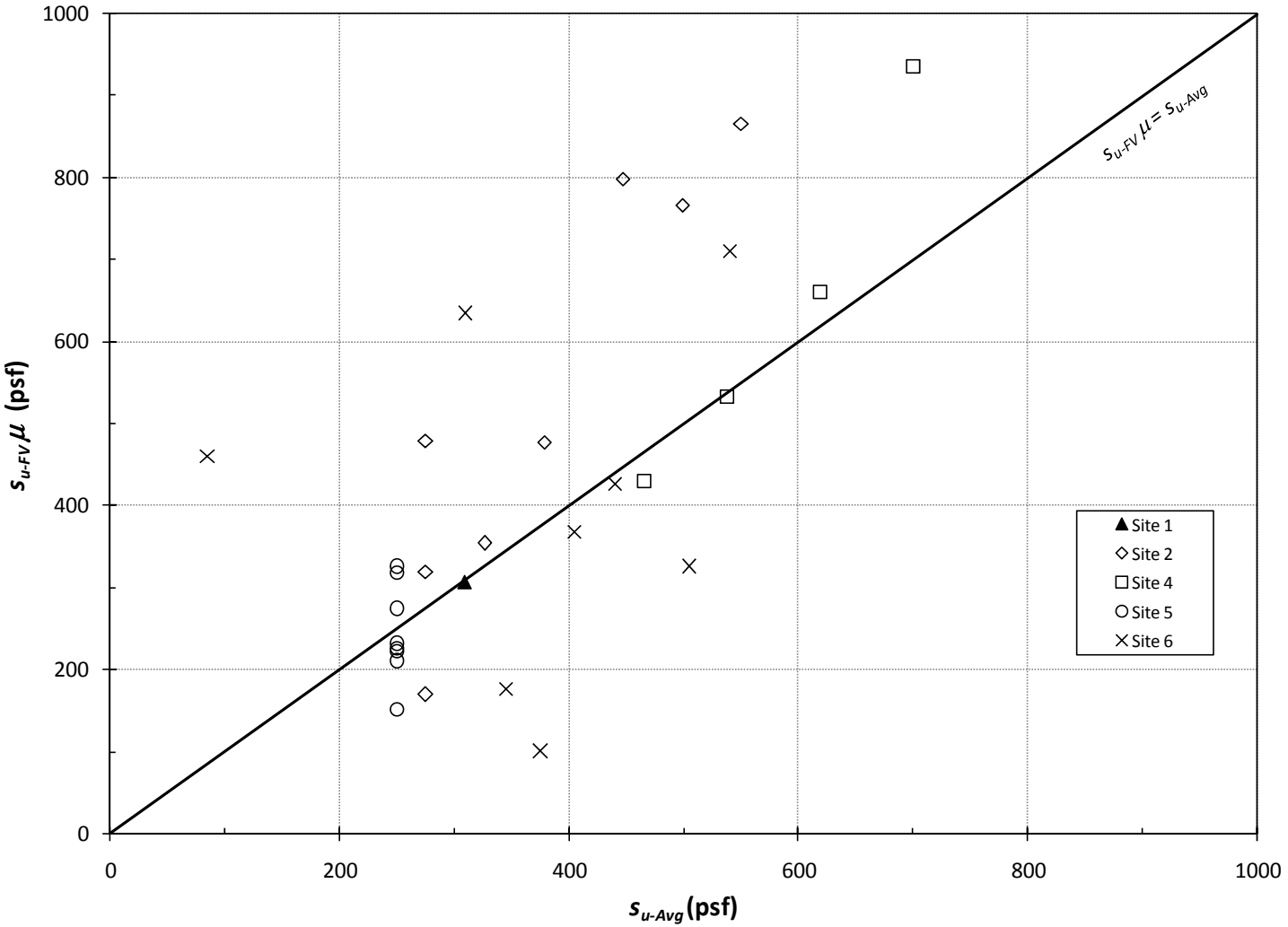

Figure 6.54: Corrected field vane strengths plotted versus corresponding strengths from average undrained strength profiles

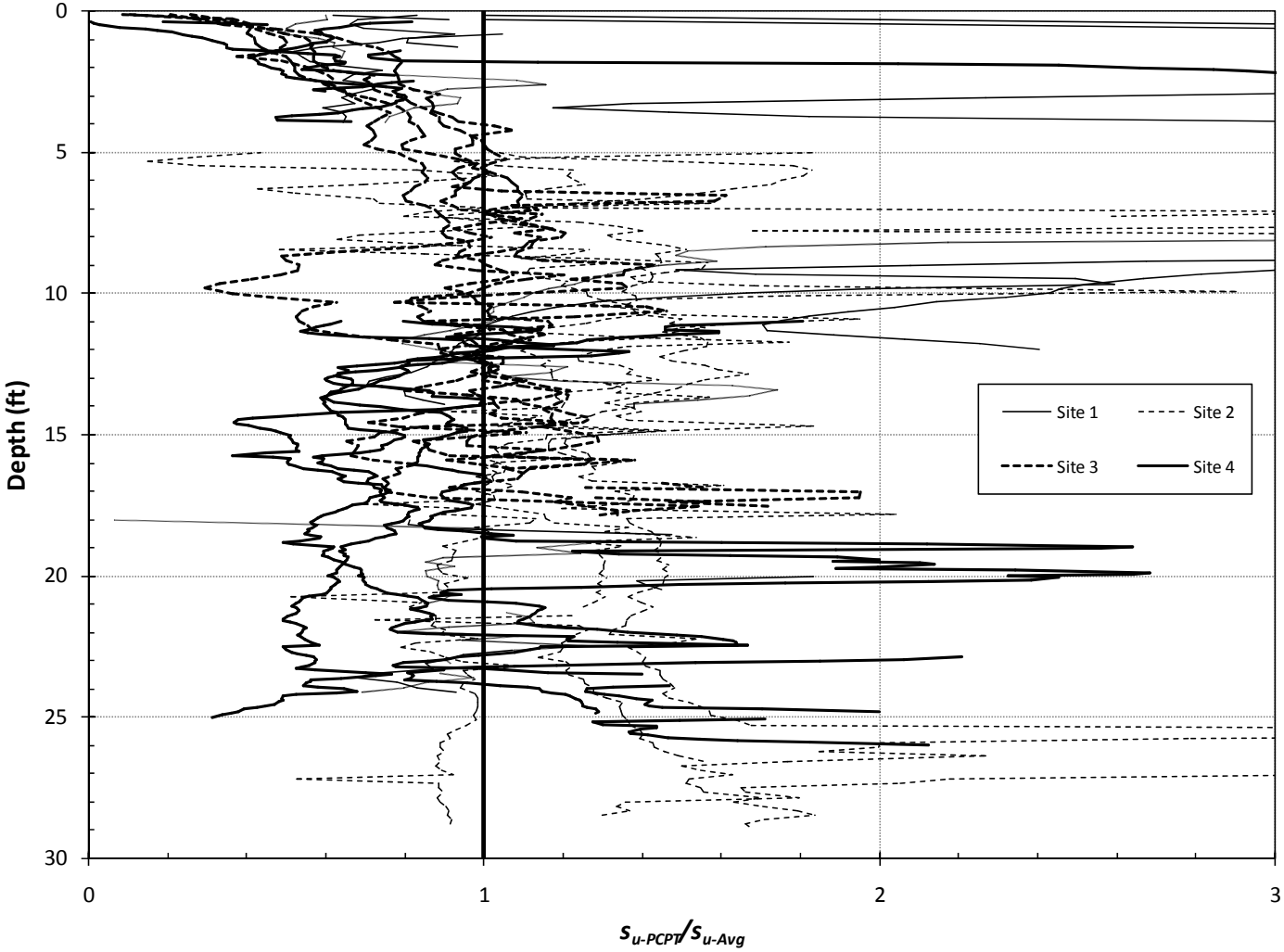

Figure 6.55: Normalized strengths determined from piezocone penetration tests plotted versus depth

6.5 Summary

Although an average undrained strength profile was determined for each site, no single undrained shear strength profile exists for a number of the reasons discussed in Chapter 3. However, the shear strengths represented by the average shear strength profiles that were developed show the expected and logical relationships with the values from the various types of tests performed for this study and are believed to be reasonable.

Chapter 7. Summary, Conclusions, and Recommendations

Recently, there has been a desire to update existing correlations between Texas Cone Penetrometer resistance and undrained shear strength to better estimate the shear strength of shallow, soft soils for the design of embankments and earth retaining structures. Existing correlations between Texas Cone Penetrometer resistance and undrained shear strength have been developed primarily for soils significantly stronger than those encountered at shallow depths. Considering the uncertainty associated with these correlations, the primary objective of this study was to characterize the undrained shear strength profiles of six sites with strengths generally less than 750 psf. The undrained shear strength profiles developed in this study have been used by Garfield (2008) to develop and assess the reliability of correlations between Texas Cone Penetrometer resistance and undrained shear strength.

7.1 Summary

Representative average undrained shear strength profiles, as well as upper and lower bound strength profiles, have been determined for six Texas sites. These profiles were determined based on judgment and the analysis and interpretation of results from a variety of field and laboratory tests. Field tests included piezocone penetration and vane shear tests. Laboratory tests included unconsolidated-undrained triaxial compression, consolidated-undrained triaxial compression, and one-dimensional consolidation tests.

Undrained strengths were determined from undrained triaxial tests and assuming that the undrained shear strength is one-half the principal stress difference at failure. Undrained strengths measured using field vane shear tests were corrected using Bjerrum's (1972) correction factor. Finally, undrained shear strengths were determined from piezocone penetration tests by first determining the maximum previous effective stress based on the net cone resistance and then using this value in existing normalized undrained strength relationships to compute undrained shear strengths.

7.2 Conclusions

The following conclusions are drawn from this study:

- Unconsolidated-undrained tests generally underestimate strengths. This is believed to be in large part due to sample disturbance. The degree of sample disturbance can be assessed by relative values of axial strain at 75 percent of peak principal stress difference ($\varepsilon_{75\%}$). Although there is significant scatter in the data, the level of sample disturbance seems unacceptable at $\varepsilon_{75\%}$ greater than approximately 3 percent. Unconsolidated-undrained tests on poor quality samples gave strengths that were as low as 25 percent of the strengths from the average profiles. Unconsolidated-undrained tests on high-quality samples gave strengths that were comparable to the strengths from the average profiles.
- Consolidated-undrained tests can be used to overcome some of the effects of sample disturbance present in unconsolidated-undrained tests. In the case of consolidated-undrained tests, sample quality can be evaluated based on the volumetric strain during consolidation to the in-situ effective overburden stress. Strengths of soft clay specimens experiencing greater than 4 percent volumetric

strain were approximately 50 percent higher than strengths from the average profiles. Strengths of specimens experiencing less than 4 percent volumetric strain during consolidation were to strengths from the average profiles.

- Field vane shear strengths corrected using Bjerrum's (1972) correction factor produce reasonable strengths in soft-to-medium, homogenous clays. However, in sandy clays, field vane strengths are likely to be too high.
- Piezocone penetration tests can be used to develop reasonably accurate overconsolidation ratio profiles in intact clays without the use of site-specific correlations. Although the data are limited, the overconsolidation ratios determined from the results of one-dimensional consolidation tests agreed favorably with the results of piezocone penetration tests.
- A good first- or second-order approximation of undrained shear strength can be made by combining the overconsolidation ratio and effective overburden stress determined from piezocone penetration tests with normalized strength relationships. Strengths determined using this approach are a useful supplement to field vane shear, unconsolidated-undrained, and consolidated-undrained test data. For example, the strengths determined using this method can be used to identify questionable laboratory test results, to locate seams of weak material, to establish trends in the rate of increase in undrained strength, or to quantify lateral variability at a site.

7.3 Recommendations

Different test methods for determining undrained shear strengths produce potentially widely ranging strengths. These differences have been well-identified by past research, and the findings of this study are generally consistent with this past research. For critical sites, it is recommended that more than one technique be used to determine an undrained shear strength profile. Utilizing multiple test methods helps to account for issues such as sample disturbance, strain rate effects, and anisotropy. Even when different measures of undrained strength are available, there remains a degree of uncertainty; selecting appropriate design strengths still requires exercising careful judgment.

Appendix A

Undrained shear strength profiles, including upper and lower bounds, were developed for each site based on the results of laboratory and field tests. Representative undrained shear strength profiles were selected based on judgment and the evaluation and interpretation of results of field and laboratory tests. These profiles are referred to as the *average* undrained shear strength profiles. The coordinates of the lines representing these profiles are presented in tables in this Appendix. Elevation ranges where undrained strengths were not considered applicable are indicated by gaps in these tables.

Table A.1: Site 1 undrained shear strength profile bounds

Lower Bound		Average Profile		Upper Bound	
El. (ft)	s_u (psf)	El. (ft)	s_u (psf)	El. (ft)	s_u (psf)
+10	800	+10	1200	+10	1600
+4	800	+4	1200	+4	1600
Non-Clay		Non-Clay		Non-Clay	
0	225	0	250	0	400
-6	375	-6	600	-6	900
Non-Clay		Non-Clay		Non-Clay	
-10	1550	-10	1900	-10	2200
-16	2100	-16	2400	-16	2700

Table A.2: Site 2 undrained shear strength profile bounds

Lower Bound		Average Profile		Upper Bound	
El. (ft)	s_u (psf)	El. (ft)	s_u (psf)	El. (ft)	s_u (psf)
-2	150	-2	275	-2	375
-10	150	-10	275	-10	375
-26	400	-26	550	-26	800

Table A.3: Site 3 undrained shear strength profile bounds

Lower Bound		Average Profile		Upper Bound	
El. (ft)	s_u (psf)	El. (ft)	s_u (psf)	El. (ft)	s_u (psf)
+31	500	+31	750	+31	900
+13	850	+13	1150	+13	1300

Table A.4: Site 4 undrained shear strength profile bounds

Lower Bound		Average Profile		Upper Bound	
El. (ft)	s_u (psf)	El. (ft)	s_u (psf)	El. (ft)	s_u (psf)
+10	600	+10	1000	+10	1920
+6	600	+6	1000	+6	1920
Non-Clay		Non-Clay		Non-Clay	
-2	275	-2	430	-2	510
-16	500	-16	700	-16	800

Table A.5: Site 5 undrained shear strength profile bounds

Lower Bound		Average Profile		Upper Bound	
El. (ft)	s_u (psf)	El. (ft)	s_u (psf)	El. (ft)	s_u (psf)
-2	150	-2	250	-2	350
-27	150	-27	250	-27	350

Table A.6: Site 6 undrained shear strength profile bounds

Lower Bound		Average Profile		Upper Bound	
El. (ft)	s_u (psf)	El. (ft)	s_u (psf)	El. (ft)	s_u (psf)
-2	160	-2	300	-2	400
-26	400	-26	540	-26	640

Appendix B

Results of unconsolidated-undrained, consolidated-undrained, field vane shear, and Atterberg limit tests are presented in this Appendix. The depth, elevation, confining pressure (σ_{cell}), principal stress difference at failure $(\sigma_1 - \sigma_3)_f$, undrained shear strength (s_u), axial strain at failure ($\varepsilon_{a\text{-}f}$), and initial and at failure water contents are given for unconsolidated-undrained tests. The depth, elevation, effective consolidation stress (s'3c), the principal stress difference at failure $(\sigma_1 - \sigma_3)_f$, the undrained shear strength (s_u), the axial strain at failure ($\varepsilon_{a\text{-}f}$), volumetric strain during consolidation ($\varepsilon_{v\text{-}c}$), pore water pressure at failure (u_f), pore pressure coefficient at failure ($\bar{A}_f$), and initial and at failure water contents are given for consolidated-undrained tests. The depth, elevation, vane size, measured peak strength ($s_{u\text{-}FV}$), measured remolded strength ($s_{u\text{-}FV,r}$), sensitivity (S_t), plasticity index (I_p), Bjerrum's (1972) correction factor (μ), and corrected undrained strength ($s_{u\text{-}FVc}$) are given for field vane shear tests. Elevation, depth, plastic limit (PL), liquid limit (LL), and plasticity index (I_p) are given for Atterberg limit tests.

Table B.1: Unconsolidated-undrained test results for Site 1

						Water Content			
							At Failure		
Depth (ft)	Elevation (ft)	σ_{cell} (psi)	$(\sigma_1 - \sigma_3)_f$ (psf)	s_u (psf)	$\varepsilon_{a\text{-}f}$ (%)	Initial (%)	Top (%)	Middle (%)	Bottom (%)
2	8	2.0	2342	1171	8.4	23.5	21.7	25.9	25.9
3	7	2.5	1818	909	14.5	25.4	24.5	27.5	27.2
4	6	3.0	2510	1255	15.0	108.9	24.7	19.3	30.3
5	5	4.2	2880	1440	8.1	22.1	26.6	21.8	31.4
11	-1	9.2	592	296	8.1	81.1	47.2	77.8	81.9
12.5	-2.5	10.4	670	335	7.3	71.8	31.3	37.9	73.6
13	-3	10.9	1270	635	15.0	30.2	27.9	26.4	30.7
15	-5	11.5	1742	871	15.0	19.9	28.7	29.4	26.9
21	-11	17.5	2902	1451	15.0	27.2	23.6	25.6	26.8
23	-13	18.0	3044	1522	15.0	26.7	28.3	29.4	27.6
24	-14	18.0	2858	1429	14.9	13.9	30.4	32.0	27.8

Table B.2: Consolidated-undrained test results for Site 1

									Water Content			
										At Failure		
Depth (ft)	Elevation (ft)	σ'_{3c} (psi)	$(\sigma_1 - \sigma_3)_f$ (psf)	s_u (psf)	$\varepsilon_{a\text{-}f}$ (%)	$\varepsilon_{v\text{-}c}$ (%)	u_f (psf)	$\bar{A}_f$	Initial (%)	Top (%)	Middle (%)	Bottom (%)
12.25	-2.25	5.1	746	373	7.2	1.9	4340	0.61	81.0	69.7	79.5	79.9

Table B.3: Field vane shear test results for Site 1

Depth (ft)	Elevation (ft)	Vane Size (mm)	$s_{u\text{-}FV}$ (psf)	$s_{u\text{-}FV,r}$ (psf)	S_t	I_p (%)	μ	$s_{u\text{-}FVc}$ (psf)
4	6	55 x 110	>1441	-	-	26	0.90	>1297
11	-1	55 x 110	439	167	2.6	69	0.70	307
17	-7	55 x 110	>1441	-	-	26	0.90	>1297

Table B.4: Atterberg limit test results for Site 1

Depth (ft)	Elevation (ft)	*PL* (%)	*LL* (%)	I_p (%)
11.5	-1.5	27	96	69
12.5	-2.5	22	49	27

Table B.5: Unconsolidated-undrained test results for Site 2

						Water Content			
							At Failure		
Depth (ft)	Elevation (ft)	σ_{cell} (psi)	$(\sigma_1 - \sigma_3)_f$ (psf)	s_u (psf)	$\varepsilon_{a\text{-}f}$ (%)	Initial (%)	Top (%)	Middle (%)	Bottom (%)
7	-4	4.9	606	303	15.0	40.7	37.8	36.5	42.5
8	-5	5.3	624	312	15.0	33.7	36.9	37.8	38.4
9	-6	6.3	440	220	4.2	100.4	91.8	66.4	61.5
10	-7	7.6	392	196	3.9	68.2	55.2	54.1	49.4
11	-8	8.4	282	141	14.9	100.5	129.6	116.0	93.6
12	-9	9.2	372	186	6.8	76.0	77.0	65.3	113.5
14	-11	10.7	334	167	10.7	51.6	49.7	48.0	53.7
15	-12	11.8	378	189	15.0	76.1	89.3	89.9	80.5
16	-13	12.6	278	139	12.6	86.1	92.8	89.9	79.9
17	-14	12.7	312	156	11.5	93.6	90.3	90.1	93.8
18	-15	13.6	542	271	8.2	93.4	94.5	72.8	89.3
20	-17	14.9	358	179	15.0	61.8	60.8	63.5	51.5
21	-18	15.8	98	49	14.6	59.3	94.8	100.0	76.9
22	-19	16.4	224	112	15.0	59.9	63.3	68.8	68.2
23	-20	17.3	500	250	10.9	72.5	76.1	57.8	69.6
24	-21	18.0	898	449	3.9	67.6	57.7	61.2	71.1
25	-22	18.8	2936	1468	15.0	35.2	29.1	27.9	29.2
26	-23	19.5	822	411	15.0	35.8	33.2	61.9	48.6
27	-24	20.6	744	372	14.8	36.6	30.1	47.9	28.1
28	-25	21.0	770	385	15.0	65.0	41.0	64.3	46.1

Table B.6: Consolidated-undrained test results for Site 2

Depth (ft)	Elevation (ft)	σ'_{3c} (psi)	$(\sigma_1 - \sigma_3)_f$ (psf)	s_u (psf)	$\varepsilon_{a\text{-}f}$ (%)	$\varepsilon_{v\text{-}c}$ (%)	u_f (psf)	$\bar{A}_f$	Water Content			
									Initial (%)	At Failure		
										Top (%)	Middle (%)	Bottom (%)
16	-13	6.0	820	410	8.3	10.0	1975	0.68	85.6	78.8	76.8	69.7
18	-15	6.5	756	378	9.8	12.3	1416	0.84	70.6	48	56.9	57.8

Table B.7: Field vane shear test results for Site 2

Depth (ft)	Elevation (ft)	Vane Size (mm)	$s_{u\text{-}FV}$ (psf)	$s_{u\text{-}FV,r}$ (psf)	S_t	I_p (%)	μ	$s_{u\text{-}FVc}$ (psf)
6	-3	65 x 130	355	167	2.1	31	0.90	320
10	-7	65 x 130	532	52	10.2	31	0.90	479
13	-10	65 x 130	188	21	9.0	31	0.90	169
16	-13	65 x 130	553	84	6.6	93	0.64	354
19	-16	65 x 130	637	94	6.8	58	0.75	478
23	-20	65 x 130	940	157	6.0	35	0.85	799
26	-23	65 x 130	1128	209	5.4	67	0.68	767
29	-26	65 x 130	1274	449	2.8	67	0.68	866

Table B.8: Atterberg limit test results for Site 2

Depth (ft)	Elevation (ft)	*PL* (%)	*LL* (%)	I_p (%)
8	-5	21	52	31
13	-10	34	101	67
16.5	-13.5	17	110	93
18	-15	29	94	65
20.5	-17.5	21	79	58
21.5	-18.5	27	62	35

Table B.9: Unconsolidated-undrained test results for Site 3

Depth (ft)	Elevation (ft)	σ_{cell} (psi)	$(\sigma_1 - \sigma_3)_f$ (psf)	s_u (psf)	$\varepsilon_{a\text{-}f}$ (%)	Water Content			
						Initial (%)	At Failure Top (%)	At Failure Middle (%)	At Failure Bottom (%)
2	+29	1.4	2407	1204	13.1	31.0	33.7	32.6	32.2
3	+28	2.5	1391	695	15.0	32.2	31.9	32.3	33.2
4	+27	3.1	1850	925	15.0	32.0	32.8	30.0	30.6
5	+26	4.2	1464	732	8.0	30.0	30.3	29.4	29.6
6	+25	4.7	1762	881	15.0	29.7	29.8	31.6	34.4
7	+24	5.8	344	172	15.0	42.3	46.9	45.5	43.2
10	+21	8.1	1800	900	6.0	25.6	30.7	21.7	33.2
11	+20	9.2	854	427	15.0	25.4	30.1	28.3	26.7
13	+18	10.8	762	381	13.4	41.2	42.3	40.1	41.0
15	+16	12.5	456	228	15.0	40.3	44.1	42.0	36.8
23	+8	19.2	1578	789	15.0	28.8	27.3	25.1	27.4
24	+7	19.7	3144	1572	15.0	28.3	26.0	24.9	23.3
25	+6	20.8	1448	724	15.0	27.2	26.1	29.1	29.0
26	+5	19.6	2770	1385	10.4	25.4	28.3	28.6	27.5

Table B.10: Consolidated-undrained test results for Site 3

Depth (ft)	Elevation (ft)	σ'_{3c} (psi)	$(\sigma_1 - \sigma_3)_f$ (psf)	s_u (psf)	$\varepsilon_{a\text{-}f}$ (%)	$\varepsilon_{v\text{-}c}$ (%)	u_f (psf)	$\bar{A}_f$	Water Content			
									Initial (%)	At Failure Top (%)	At Failure Middle (%)	At Failure Bottom (%)
8	+23	4.9	1446	723	14.5	1.3	7902	0.30	29.4	32.9	33	35.5
12	+19	6.4	1182	591	4.0	0.7	5516	0.14	32.3	32.7	29.7	24.4
14	+17	7.2	2524	1262	5.8	0.2	9317	0.06	40.8	28.3	26.3	25.0
17.5	+14	8.8	7417	3709	12.3	0.7	5779	-0.29	25	24.3	24.9	23.9

Table B.11: Atterberg limit test results for Site 3

Depth (ft)	Elevation (ft)	PL (%)	LL (%)	I_p (%)
4	+27	22	70	48
7.5	+24	27	72	45
11	+20	16	38	22
11.5	+20	26	74	48
13.5	+18	22	55	33
15.5	+16	21	43	22

Table B.12: Unconsolidated-undrained test results for Site 4

Depth (ft)	Elevation (ft)	σ_{cell} (psi)	$(\sigma_1 - \sigma_3)_f$ (psf)	s_u (psf)	$\varepsilon_{a\text{-}f}$ (%)	Water Content			
						Initial (%)	At Failure		
							Top (%)	Middle (%)	Bottom (%)
2	+8	2.0	3838	1919	15.0	20.2	20.0	18.8	21.1
3	+7	2.5	1228	614	7.3	28.5	41.8	29.6	22.3
4	+6.5	3.1	2004	1002	4.5	25.1	23.5	24.5	25.7
13	-2.5	8.5	1108	554	8.1	83.8	87.8	121.0	107.3
13	-3	8.9	1164	582	3.9	114.9	110.9	108.3	91.0
14	-4	10.3	686	343	8.8	74.1	94.8	96.5	102.7
15	-5	10.5	1050	525	12.6	172.7	208.4	211.5	155.8
16	-6	11.2	1000	500	6.3	94.7	91.9	92.0	101.7
17	-7	11.6	1222	611	4.8	127.5	114.3	98.4	94.3
18	-8	12.3	1198	599	6.6	169.7	179.2	164.4	156.9
19	-9	14.3	586	293	13.1	263.9	147.2	152.5	188.1
20	-10	13.7	652	326	10.5	192.7	211.6	214.8	201.4
21	-11	14.4	566	283	14.6	162.7	171.6	147.1	156.3
22	-12	16.6	1104	552	3.4	124.6	110.6	110.6	89.4
24	-13.5	16.1	1252	626	3.9	99.4	112.3	92.2	102.3
24	-14	16.5	1418	709	3.1	96.7	101.9	100.1	106.5

Table B.13: Consolidated-undrained test results for Site 4

Depth (ft)	Elevation (ft)	σ'_{3c} (psi)	$(\sigma_1 - \sigma_3)_f$ (psf)	s_u (psf)	$\varepsilon_{a\text{-}f}$ (%)	$\varepsilon_{v\text{-}c}$ (%)	u_f (psf)	$\bar{A}_f$	Water Content			
									Initial (%)	At Failure		
										Top (%)	Middle (%)	Bottom (%)
13.5	-3.5	5.8	1072	536	4.0	3.5	7574	0.53	113.1	77.6	75.5	111.8
15.5	-5.5	6.0	1122	561	6.0	3.0	6085	0.49	123.1	85.5	94.0	102.1
17.5	-7.5	6.1	1618	809	8.2	2.1	9024	0.48	181.7	176.9	182.4	136.2
19.5	-9.5	6.5	1258	629	6.3	4.4	9852	0.56	162.9	143.1	184	162.0
21.5	-11.5	6.7	1364	682	5.2	2.9	7760	0.57	163.0	165.9	154.3	159.7
23	-13	6.9	1352	676	15.0	5.9	6982	0.06	88.1	80.5	69.7	66.0

Table B.14: Field vane shear test results for Site 4

Depth (ft)	Elevation (ft)	Vane Size (mm)	$s_{u\text{-}FV}$ (psf)	$s_{u\text{-}FV,r}$ (psf)	S_t	I_p (%)	μ	$s_{u\text{-}FVc}$ (psf)
13	-3	65 x 130	814	125	6.5	93	0.53	429
17	-7	65 x 130	1044	157	6.6	206	0.51	532
21.5	-11.5	65 x 130	1274	104	12.3	105	0.52	661
26	-16	65 x 130	1336	-	-	62	0.70	935

Table B.15: Atterberg limit test results for Site 4

Depth (ft)	Elevation (ft)	PL (%)	LL (%)	I_p (%)
12.5	-2.5	49	138	89
15.5	-5.5	45	138	93
17.5	-7.5	49	255	206
22.5	-12.5	45	150	105
25	-15	21	91	62

Table B.16: Unconsolidated-undrained test results for Site 5

						Water Content			
							At Failure		
Depth (ft)	Elevation (ft)	σ_{cell} (psi)	$(\sigma_1 - \sigma_3)_f$ (psf)	s_u (psf)	$\varepsilon_{a\text{-}f}$ (%)	Initial (%)	Top (%)	Middle (%)	Bottom (%)
3	-3	2.3	838	419	6.1	48.4	59.8	52.0	45.0
4	-3.5	2.7	382	191	14.4	57.2	74.6	73.8	50.1
5	-5	3.6	532	266	12.0	41.6	66.0	65.2	40.6
6	-5.5	4.7	644	322	14.9	10.6	54.6	41.1	39.1
7	-6.5	4.6	648	324	8.3	53.8	63.4	62.0	40.9
8	-7.5	5.8	382	191	14.1	43.0	59.4	61.1	66.4
8	-8.0	5.8	298	149	14.9	92.6	98.9	93.0	100.2
10	-9.5	7.1	428	214	7.3	92.7	82.8	94.1	91.5
11	-10.5	7.2	272	136	13.4	97.6	103.5	96.5	98.6
12	-11.5	7.4	234	117	14.6	105.1	68.4	100.9	107.5
14	-13.5	9.1	304	152	14.1	88.3	92.8	87.0	95.5
15	-14.5	10.4	288	144	14.9	65.1	78.8	59.6	72.8
15	-15	10.9	328	164	14.6	52.5	69.1	72.7	76.0
17	-16.5	11.9	260	130	14.9	83.0	97.6	97.6	87.8
17	-17	12.4	476	238	13.6	78.0	172.1	41.1	78.8
18	-17.5	12.9	574	287	9.1	51.3	66.4	83.3	70.5

Table B.17: Consolidated-undrained test results for Site 5

									Water Content			
										At Failure		
Depth (ft)	Elevation (ft)	σ'_{3c} (psi)	$(\sigma_1 - \sigma_3)_f$ (psf)	s_u (psf)	$\varepsilon_{a\text{-}f}$ (%)	$\varepsilon_{v\text{-}c}$ (%)	u_f (psf)	$\bar{A}_f$	Initial (%)	Top (%)	Middle (%)	Bottom (%)
7	-7	5.1	856	428	9.7	4.8	6051	0.44	48.1	64.6	46.3	37.5
9	-9	6.1	788	394	6.3	13.4	5482	0.71	95.8	93.2	91.1	88.1
11	-11	6	740	370	7.5	15.3	6250	0.92	96.1	71.3	78.2	75.2
15.5	-15.5	8.1	800	400	6.7	8.1	6237	0.88	58	72.5	68.8	89.8
24	-24	10.5	1548	774	10.2	9.7	7146	0.65	68.5	57.5	54.5	55.9

Table B.18: Field vane shear test results for Site 5

Depth (ft)	Elevation (ft)	Vane Size (mm)	$s_{u\text{-}FV}$ (psf)	$s_{u\text{-}FV,r}$ (psf)	S_t	I_p (%)	μ	$s_{u\text{-}FVc}$ (psf)
3	-3	65 x 130	188	52	3.6	52	0.80	150
6.5	-6.5	65 x 130	397	42	9.5	52	0.80	318
9.5	-9.5	65 x 130	282	63	4.5	52	0.80	226
12.5	-12.5	65 x 130	271	42	6.5	60	0.72	195
16	-16	65 x 130	292	52	5.6	60	0.72	210
-19.5	19.5	65 x 130	334	63	5.3	31	0.89	297
22.5	-22.5	65 x 130	282	42	6.7	43	0.82	231
26	-26	65 x 130	397	73	5.4	43	0.82	326

Table B.19: Atterberg limit test results for Site 5

Depth (ft)	Elevation (ft)	*PL* (%)	*LL* (%)	I_p (%)
6.5	-6.5	27	79	52
16.5	-16.5	38	98	60
22	-22	51	20	31
26	-26	75	32	43

Table B.20: Unconsolidated-undrained triaxial tests for Site 6

						Water Content			
							At Failure		
Depth (ft)	Elevation (ft)	σ_{cell} (psi)	$(\sigma_1 - \sigma_3)_f$ (psf)	s_u (psf)	$\varepsilon_{a\text{-}f}$ (%)	Initial (%)	Top (%)	Middle (%)	Bottom (%)
4	-3.5	2.6	1644	822	8.6	52.7	55.1	53.1	52.5
5	-4.5	3.3	722	361	6.9	49.0	64.5	41.9	43.6
6	-5.5	4.1	332	166	13.1	37.5	44.2	29.6	61.7
7	-7.0	5.1	226	113	14.9	50.5	45.1	44.9	43.0
8	-7.5	5.6	246	123	14.9	37.5	40.8	40.7	39.2
9	-8.5	6.1	328	164	14.9	40.7	38.8	37.8	39.1
10	-9.5	7.1	802	401	14.6	45.0	39.9	44.3	45.1
12	-11.5	8.5	874	437	11.9	50.7	55.3	42.1	46.3
13	-12.5	8.8	424	212	14.1	69.7	70.4	74.2	72.2
13	-13.0	9.5	660	330	13.6	78.7	71.2	68.6	74.3
15	-14.5	10.4	352	176	14.9	67.5	71.9	74.2	85.2
15	-15	10.9	712	356	14.1	89.2	78.7	68.0	59.4
17	-16.5	12.0	620	310	9.4	79.0	77.2	63.9	65.3
18	-17.5	12.9	552	276	14.1	48.7	78.0	38.6	62.3
21	-20.5	14.8	288	144	14.6	83.2	58.6	63.8	67.4
22	-21.5	15.8	1016	508	5.8	62.7	70.4	71.7	77.5
23	-23	16.8	278	139	14.9	25.4	33.4	59.5	48.1

Table B.21: Consolidated-undrained test results for Site 6

									Water Content			
										At Failure		
Depth (ft)	Elevation (ft)	σ'_{3c} (psi)	$(\sigma_1 - \sigma_3)_f$ (psf)	s_u (psf)	$\varepsilon_{a\text{-}f}$ (%)	$\varepsilon_{v\text{-}c}$ (%)	u_f (psf)	$\bar{A}_f$	Initial (%)	Top (%)	Middle (%)	Bottom (%)
5	-5	3.6	996	498	6.5	19.7	4466	0.25	57.8	54.0	50.7	52.6
13.5	-13.5	7.5	1234	617	3.5	6.1	5633	0.50	76.6	79.0	81.0	72.3
17.5	-17.5	8.5	1464	732	7.0	23.2	5728	0.58	55.5	66.0	69.9	67.4
21	-21	9.7	1242	621	4.6	7.7	6340	0.52	64.6	72.4	79.5	76.7

Table B.22: Field vane shear test results for Site 6

Depth (ft)	Elevation (ft)	Vane Size (mm)	$s_{u\text{-}FV}$ (psf)	$s_{u\text{-}FV,r}$ (psf)	S_t	I_p (%)	μ	$s_{u\text{-}FVc}$ (psf)
3	-3	65 x 130	793	84	9.4	48	0.78	619
6.5	-6.5	65 x 130	219	63	3.5	48	0.78	171
9.5	-9.5	65 x 130	125	63	2.0	48	0.78	98
12.5	-12.5	65 x 130	459	63	7.3	49	0.79	362
16	-16	65 x 130	532	31	17.2	49	0.78	415
-19.5	19.5	65 x 130	574	84	6.8	40	0.80	459
22.5	-22.5	65 x 130	407	94	4.3	40	0.80	326
26	-26	65 x 130	887	-	-	30	0.90	798

Table B.23: Atterberg limit test results for Site 6

Depth (ft)	Elevation (ft)	*PL* (%)	*LL* (%)	I_p (%)
6	-6	28	76	48
15.5	-15.5	35	84	49
21.5	-21.5	29	69	40
25.5	-25.5	22	52	30

Appendix C

Data from piezocone penetration test soundings are presented in this Appendix. Piezocone soundings were performed by Southern Earth Sciences at Sites 1, 2, and 3. Fugro Geosciences performed piezocone soundings at Site 4.

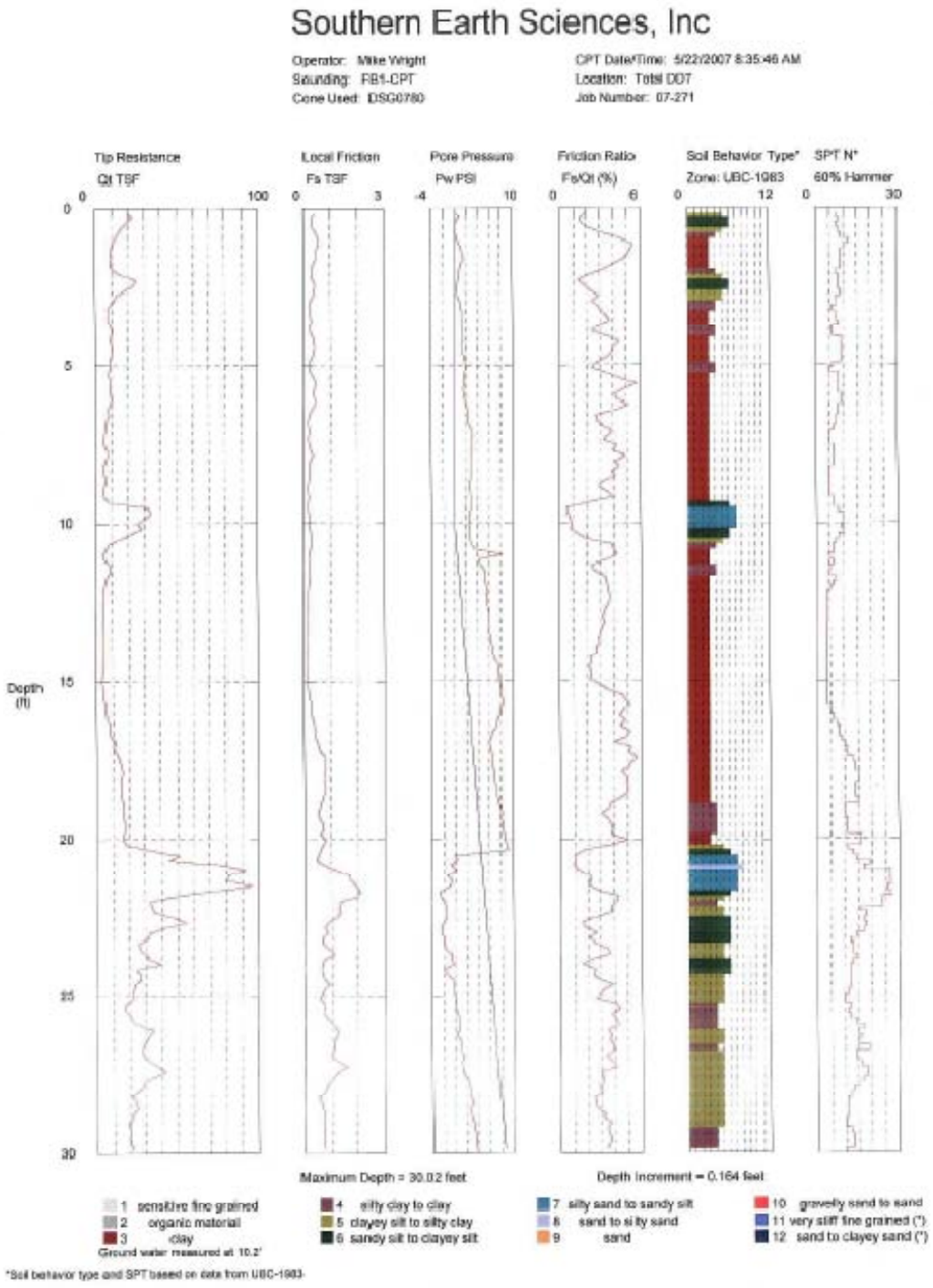

Figure C.1: Site 1 piezocone penetration sounding FB1.

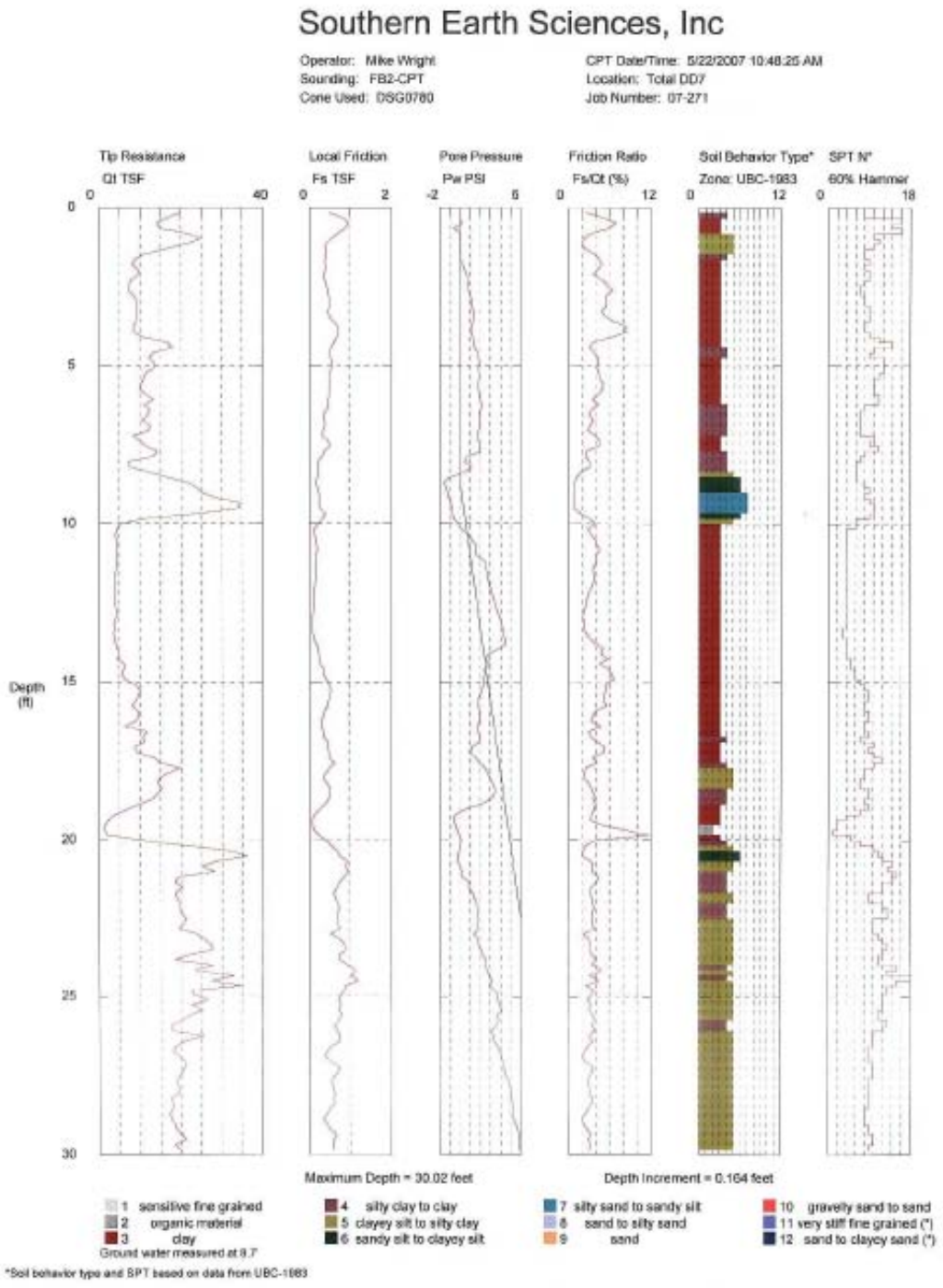

Figure C.2: Site 1 piezocone penetration sounding FB2.

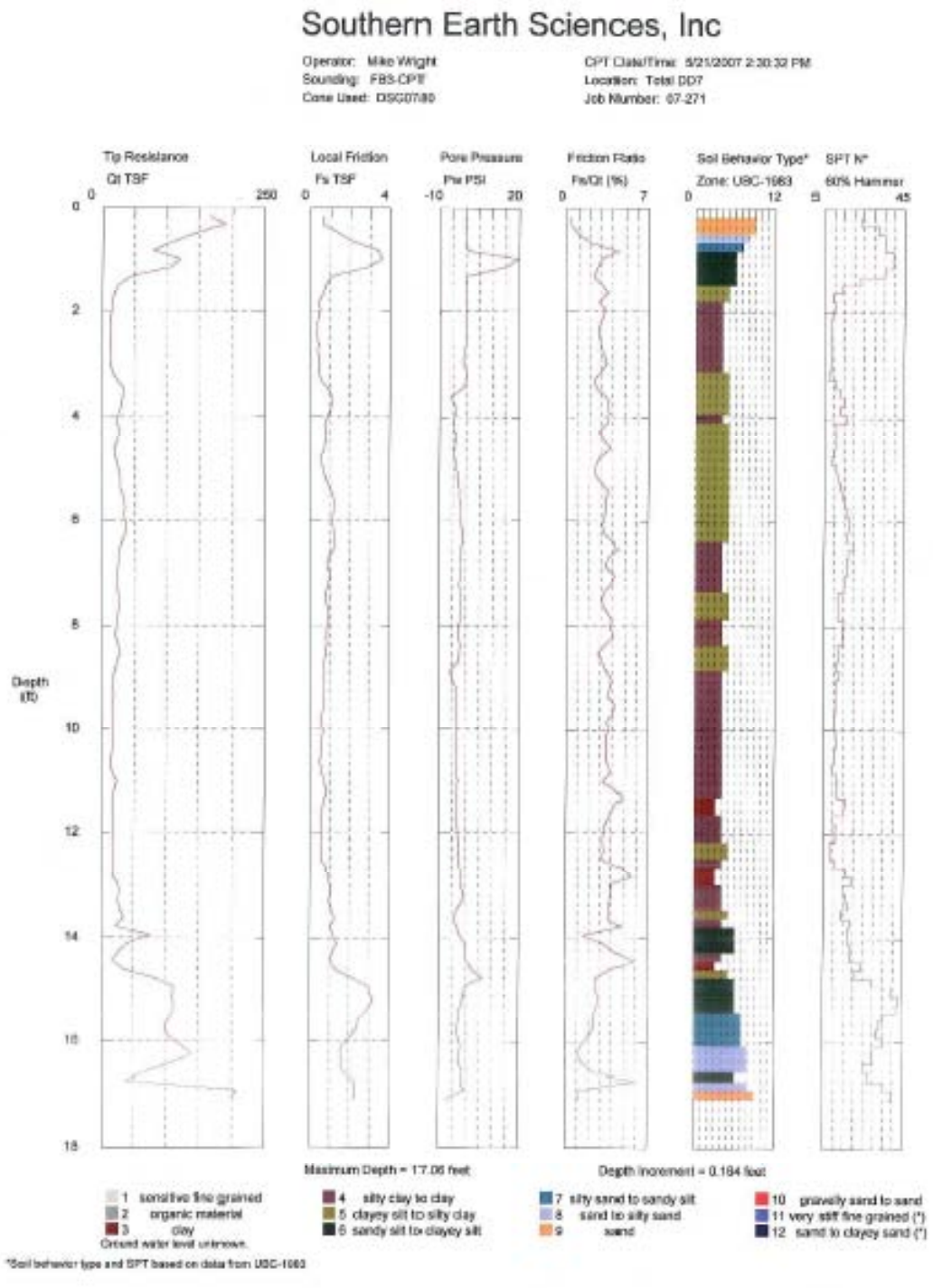

Figure C.3: Site 1 piezocone penetration sounding FB3.

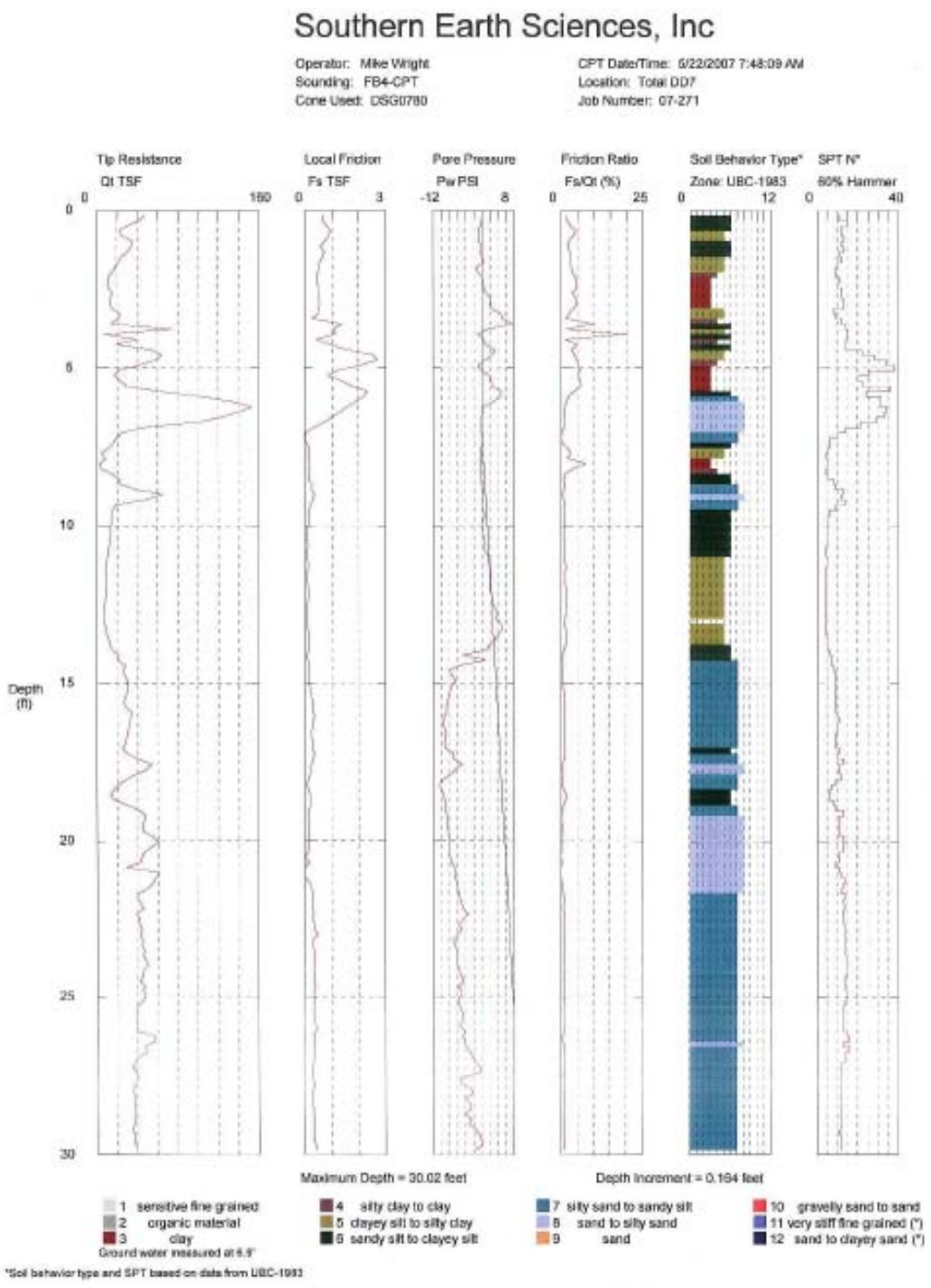

Figure C.4: Site 1 piezocone penetration sounding FB4.

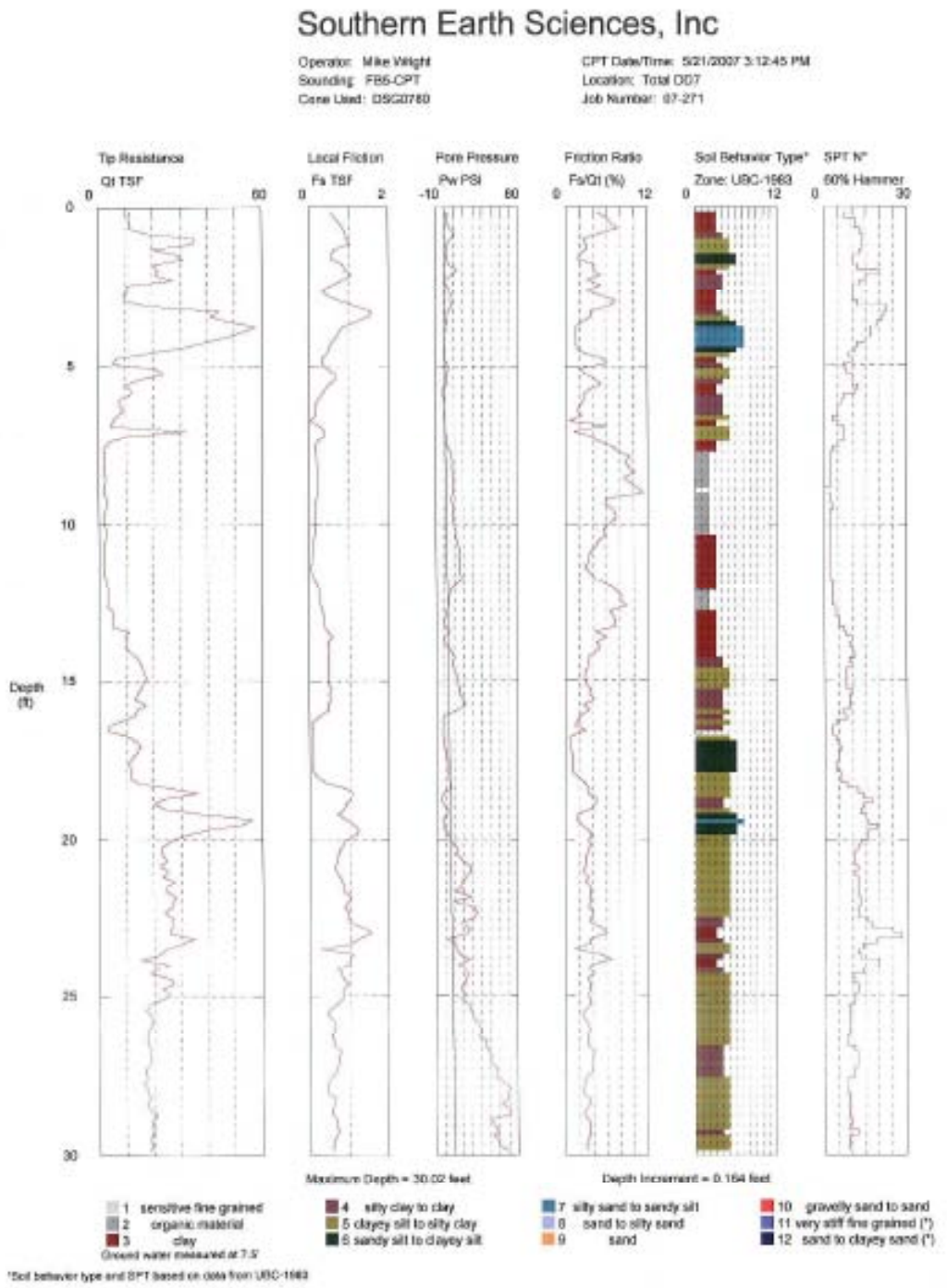

Figure C.5: Site 1 piezocone penetration sounding FB5.

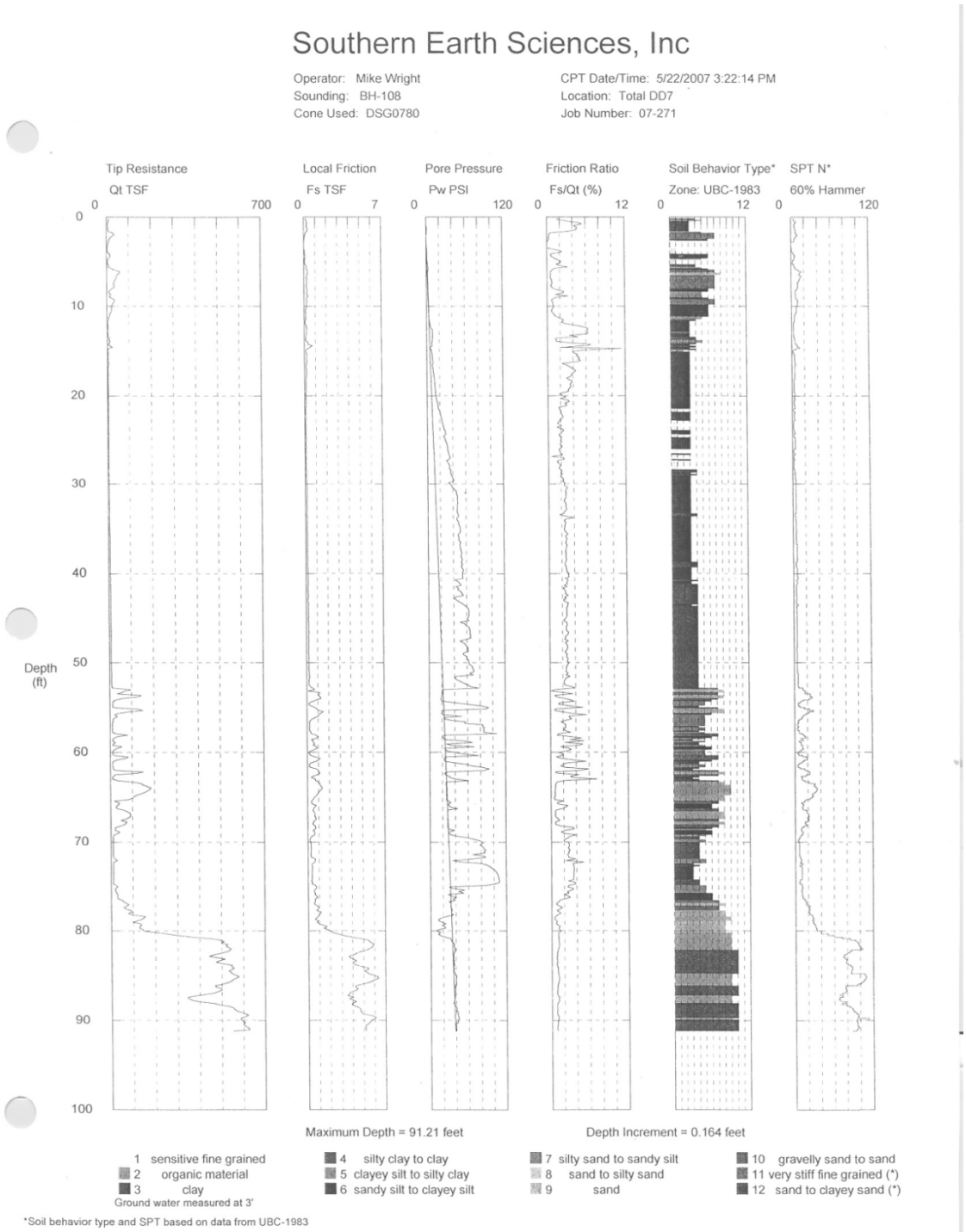

Figure C.6: Site 2 piezocone penetration sounding BH108.

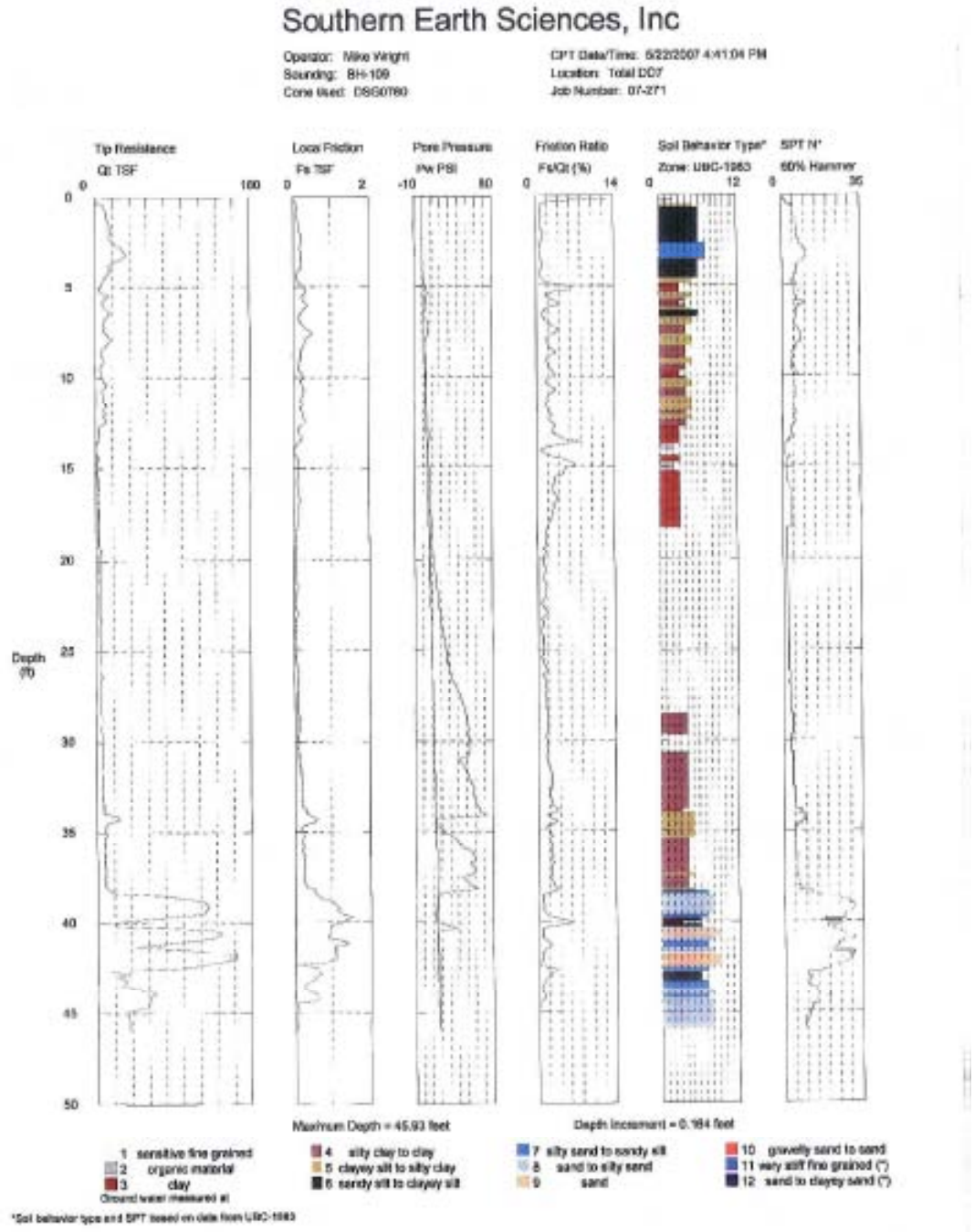

Figure C.7: Site 2 piezocone penetration sounding BH109.

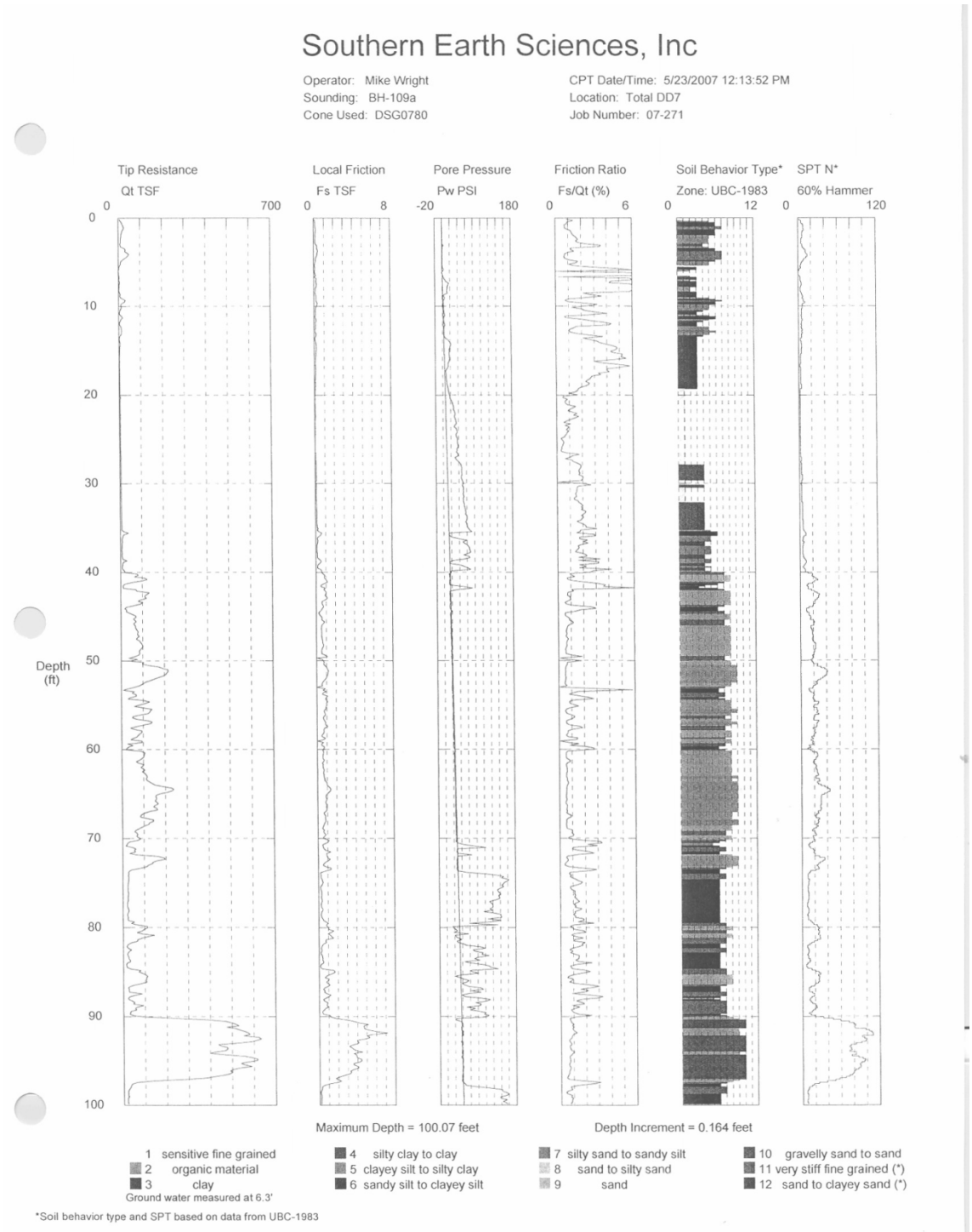

Figure C.8: Site 2 piezocone penetration sounding BH109A.

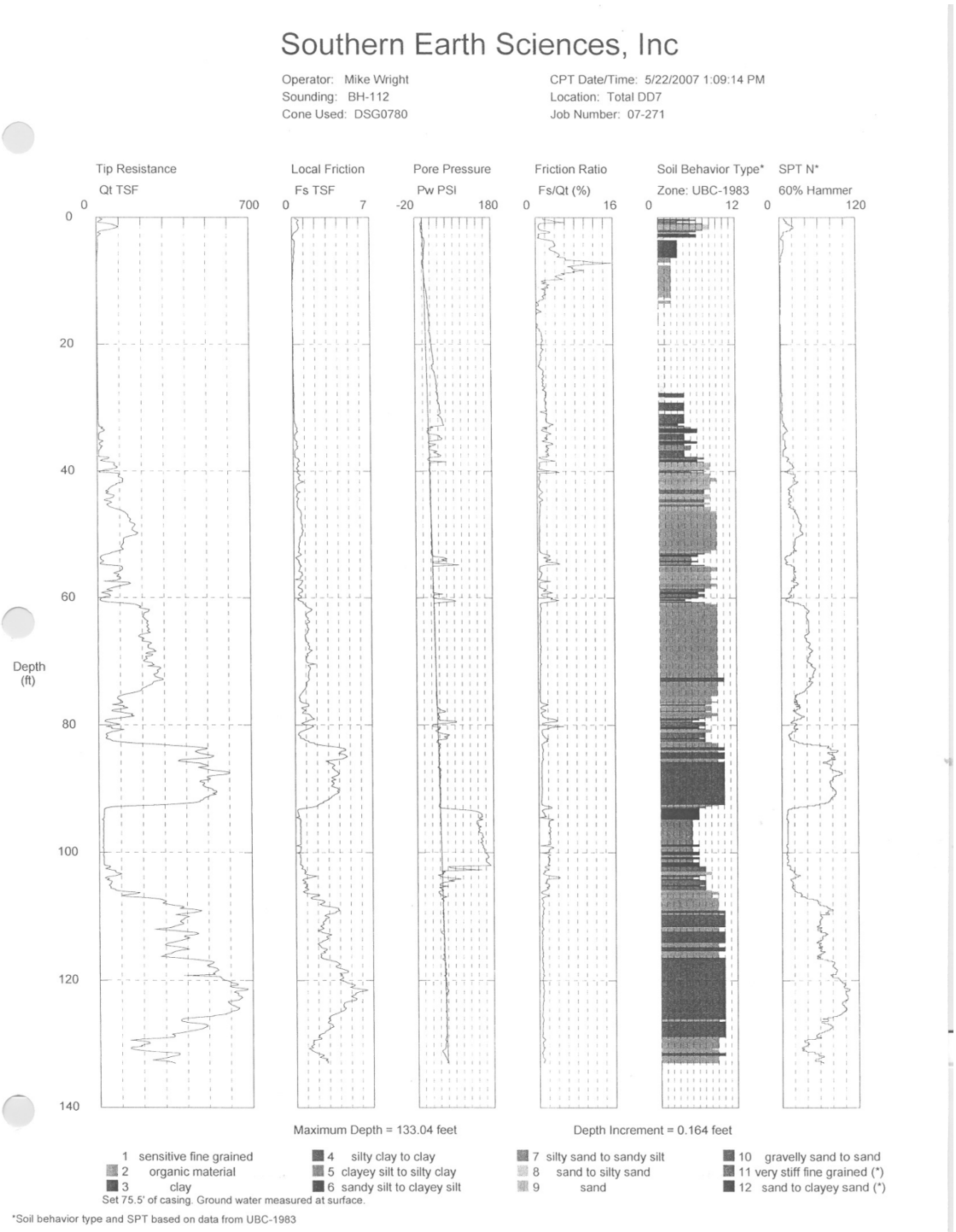

Figure C.9: Site 2 piezocone penetration sounding BH112.

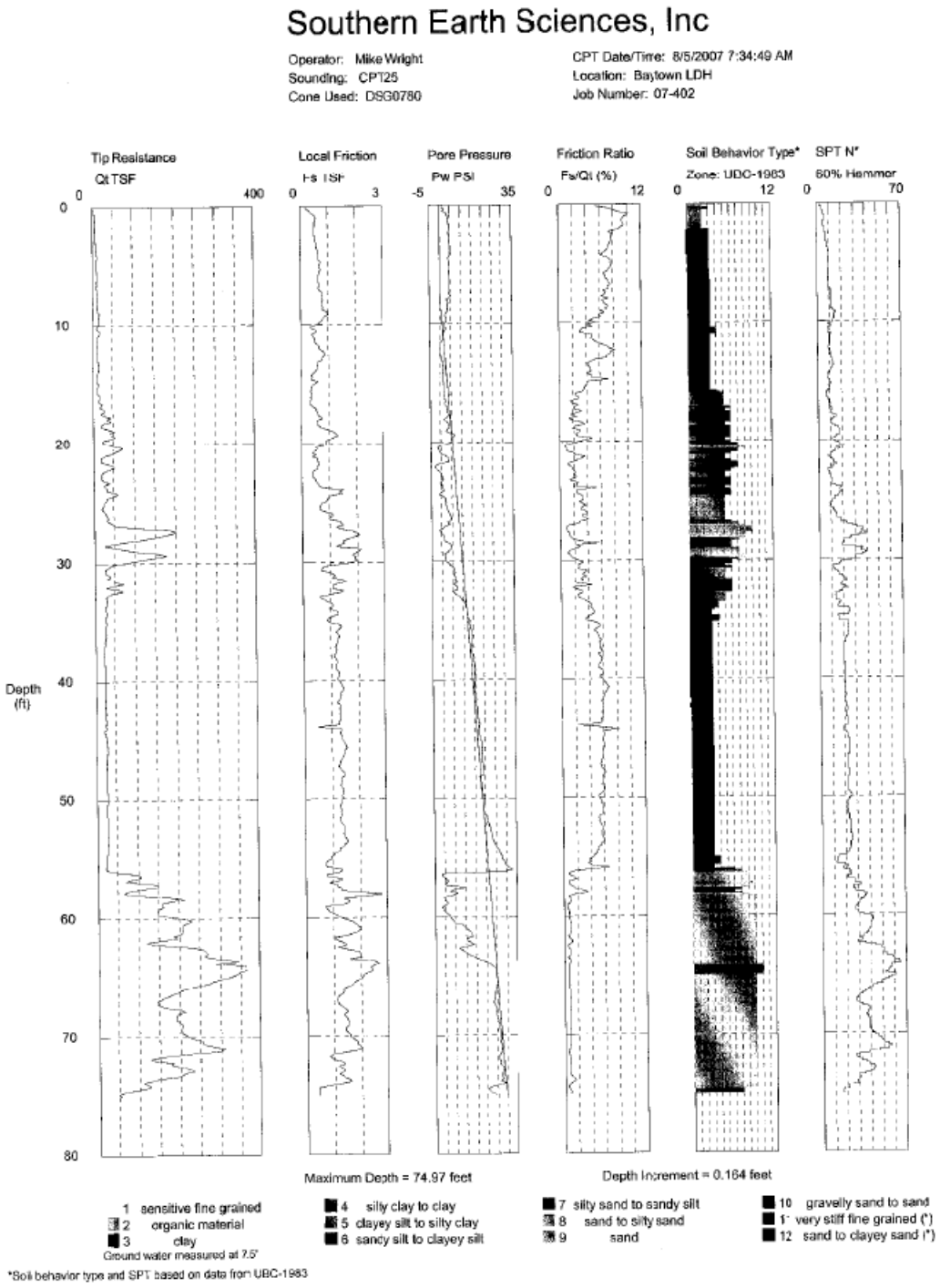

Figure C.10: Site 3 piezocone penetration sounding CPT25.

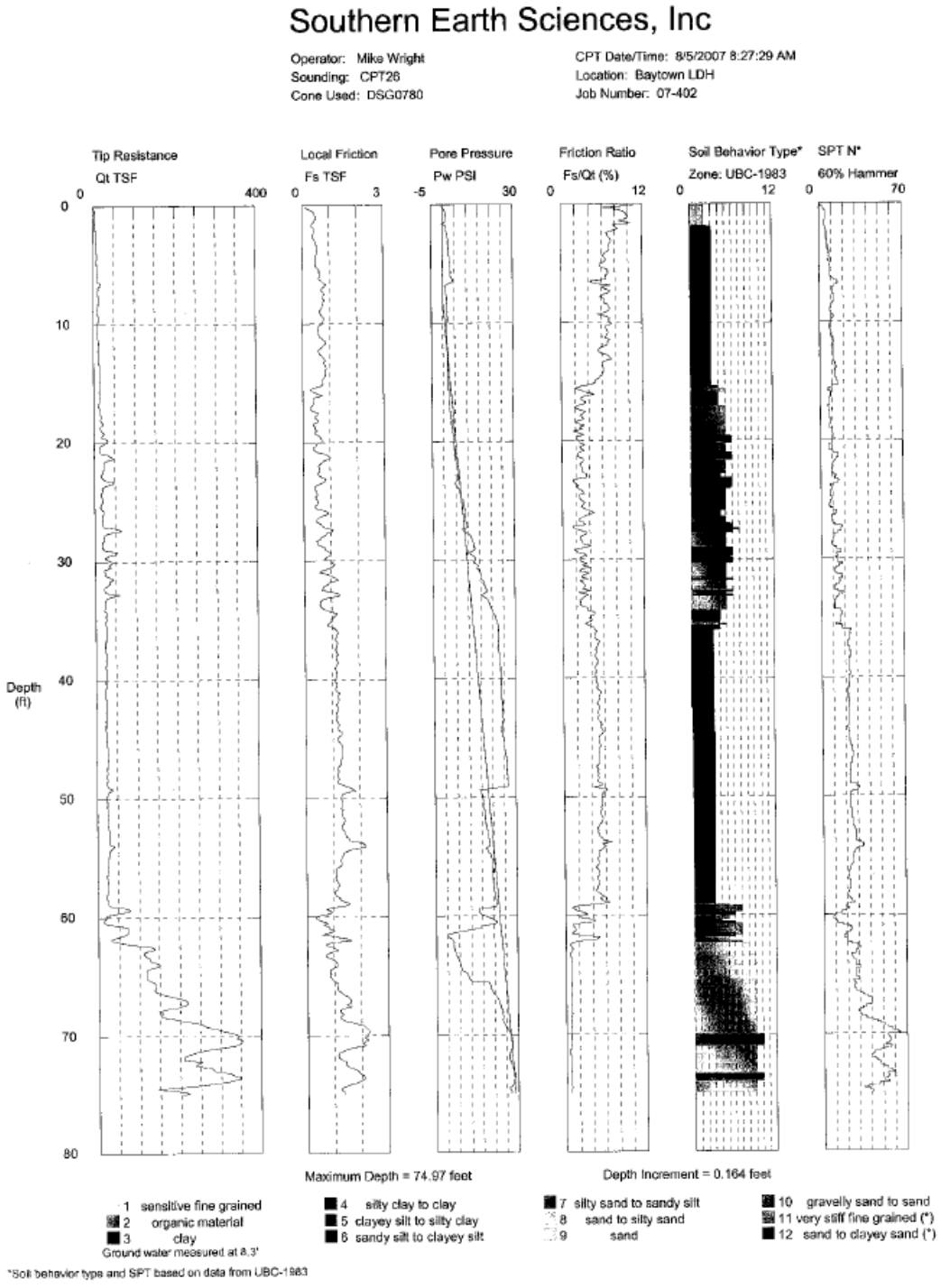

Figure C.11: Site 3 piezocone penetration sounding CPT26.

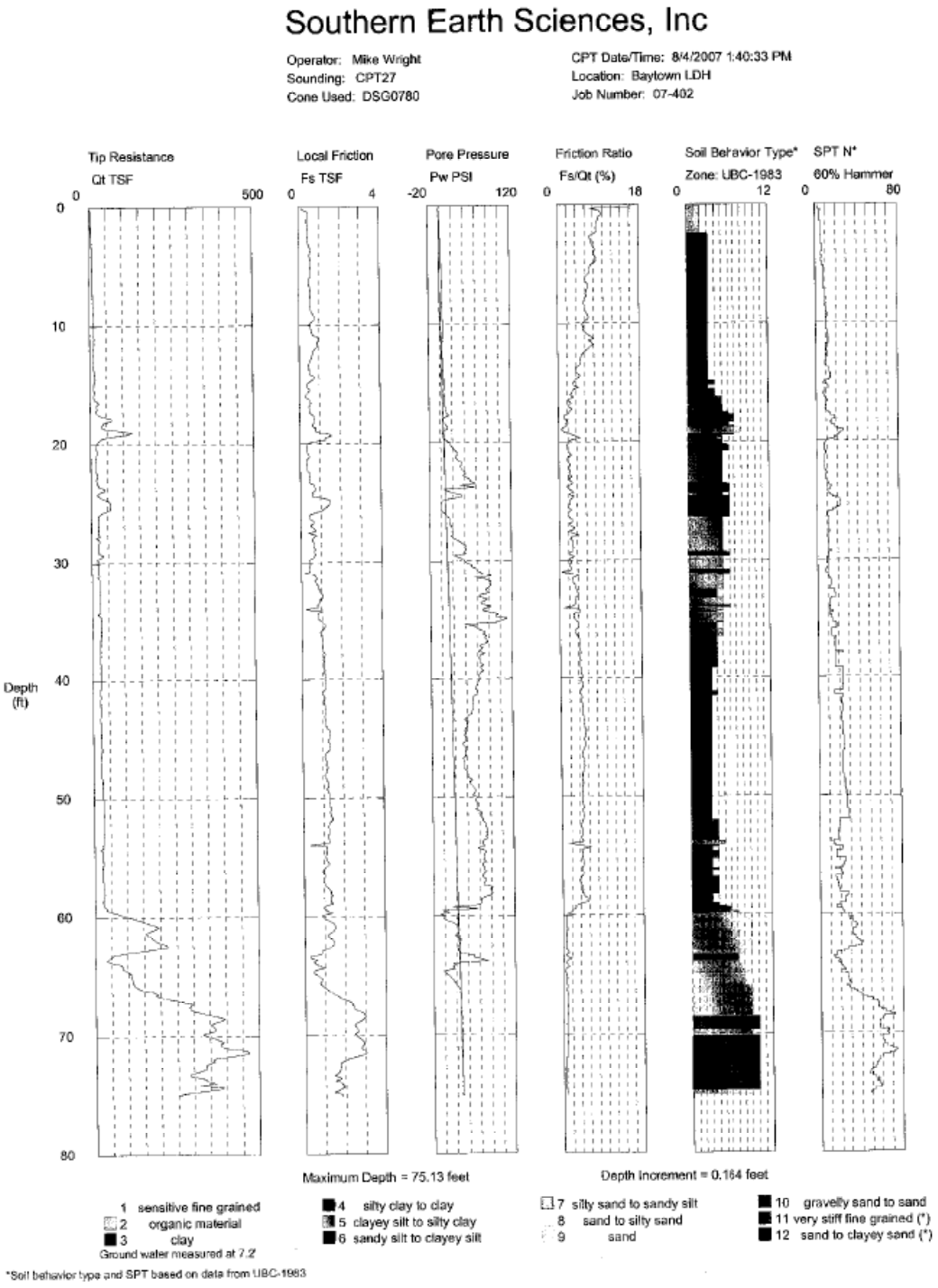

Figure C.12: Site 3 piezocone penetration sounding CPT27.

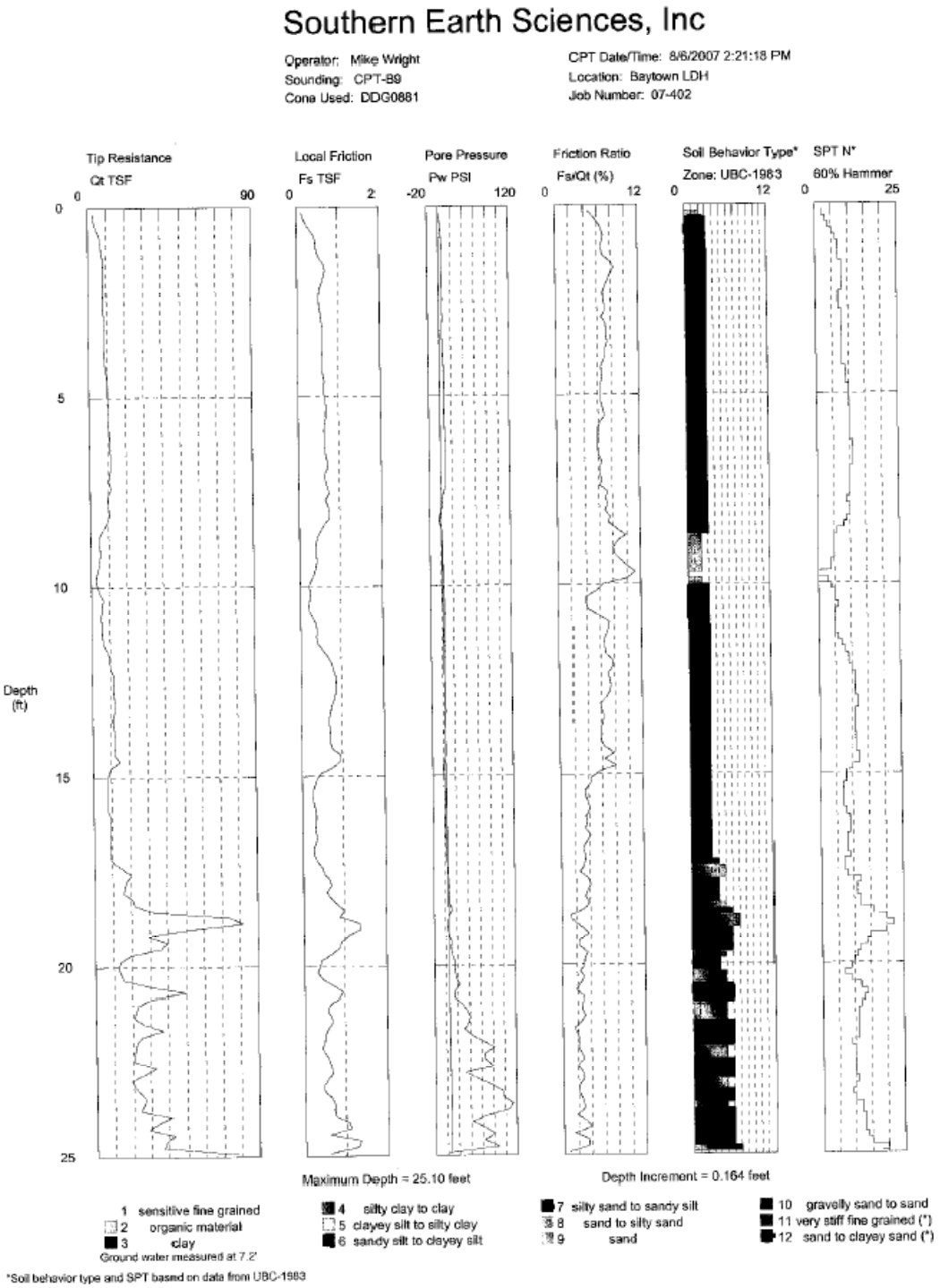

Figure C.13: Site 3 piezocone penetration sounding CPTB9.

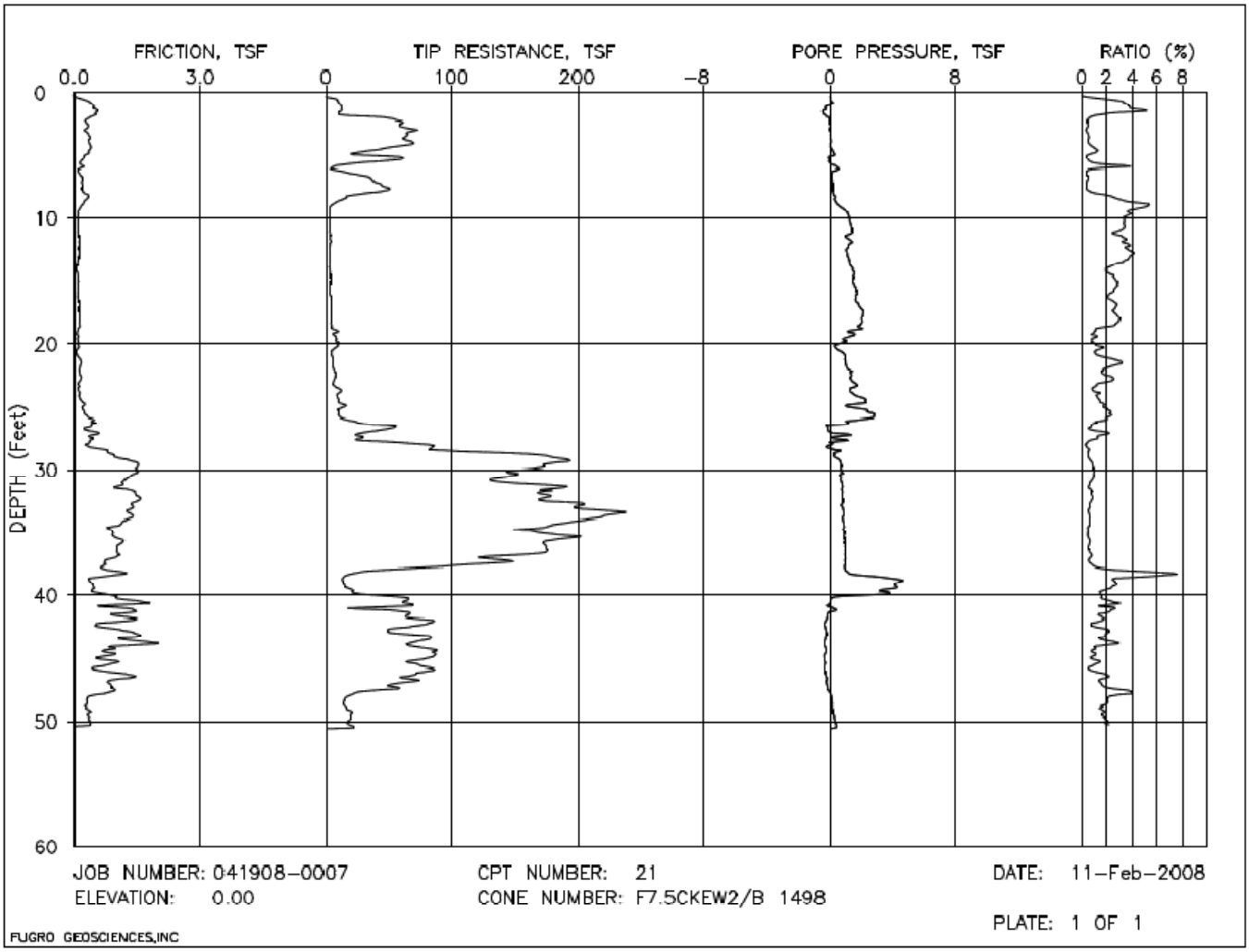

Figure C.14: Site 4 piezocone penetration sounding 21.

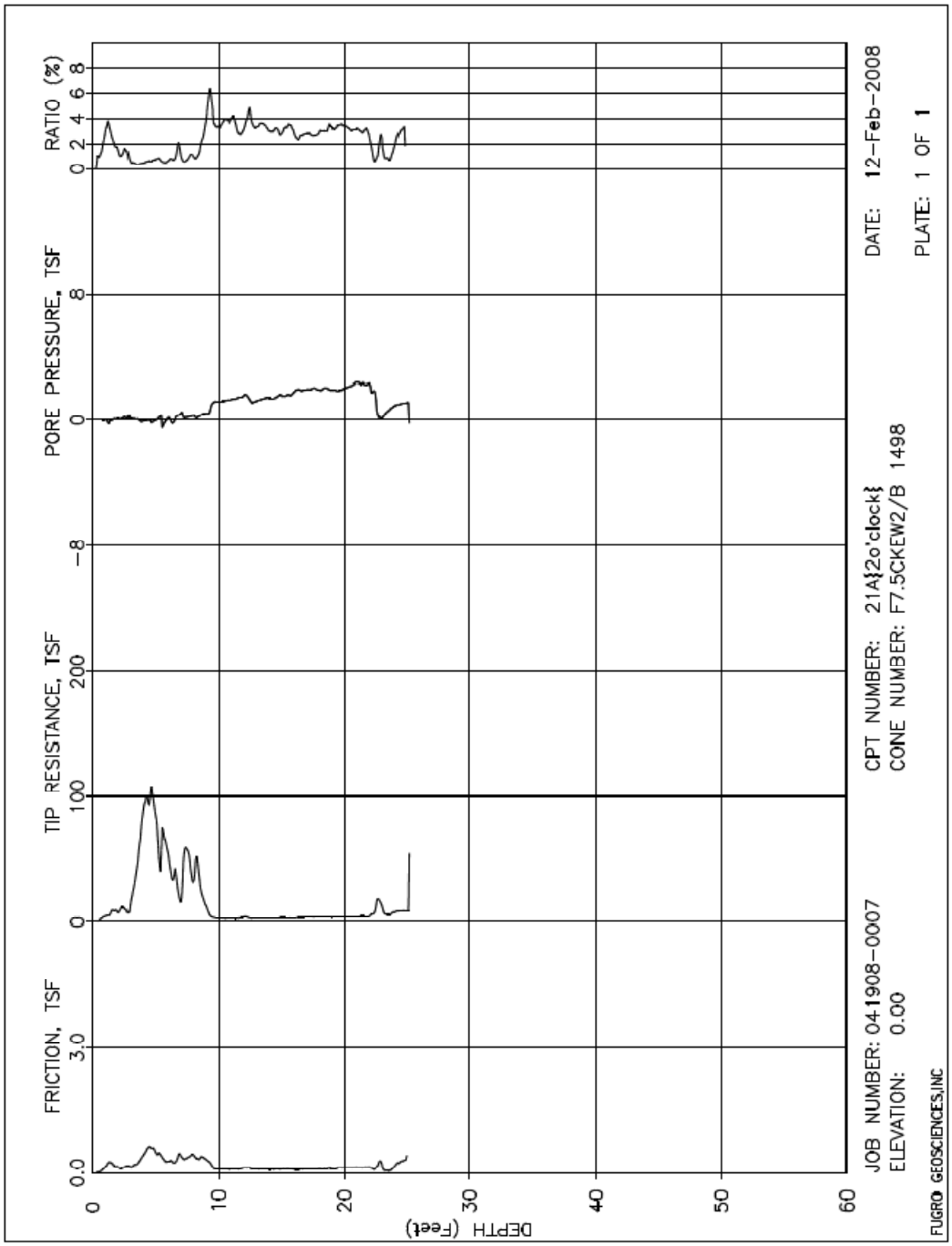

Figure C.15: Site 4 piezocone penetration sounding 21A.

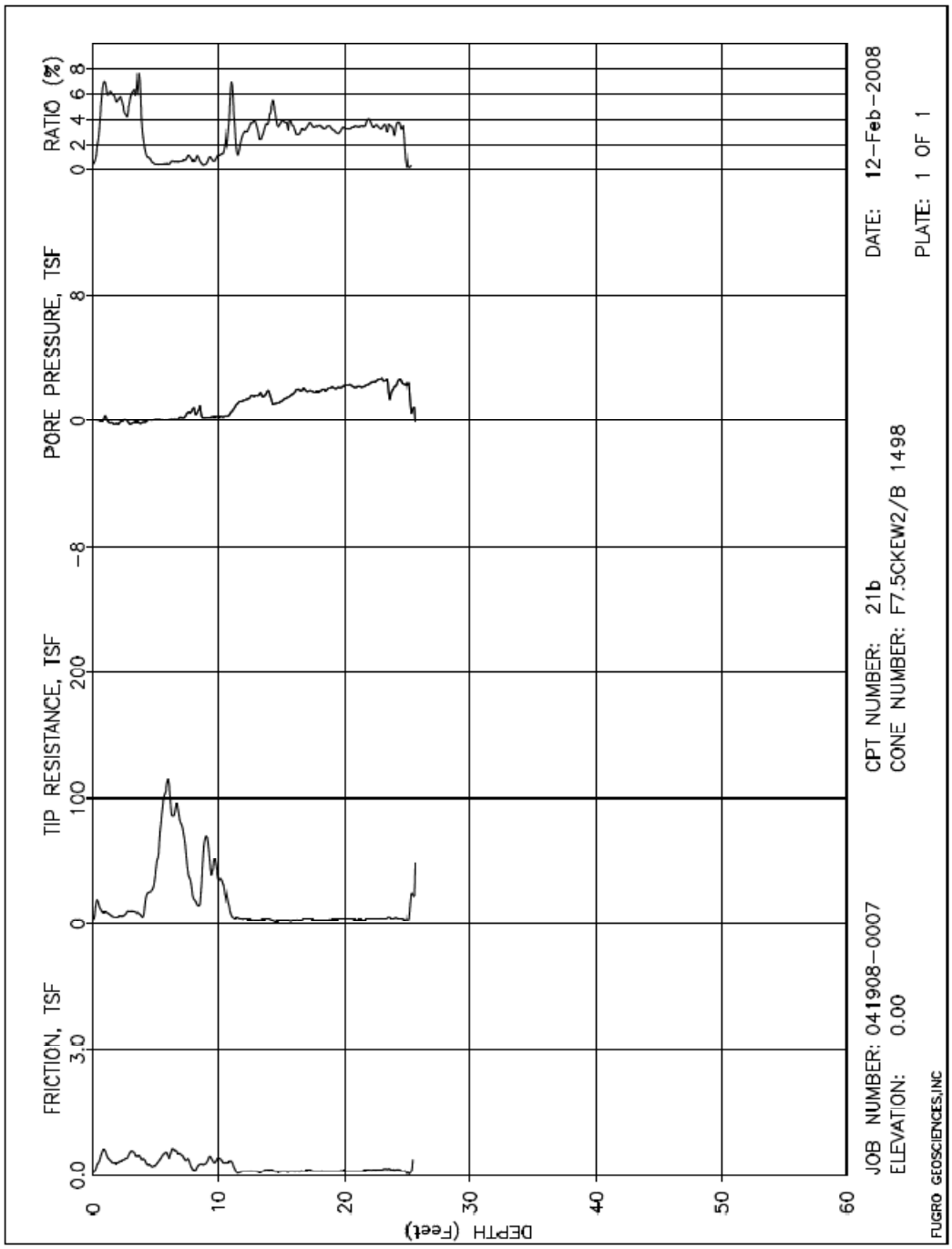

Figure C.16: Site 4 piezocone penetration sounding 21B.

References

American Society for Testing and Materials (2004). Standard Test Method for Consolidated-Undrained Triaxial Compression Test for Cohesive Soils, ASTM D 4767.

American Society for Testing and Materials (2007a). Standard Method for Field Vane Shear Test in Cohesive Soil, ASTM D 2573.

American Society for Testing and Materials (2007b). Standard Test Method for Unconsolidated-Undrained Triaxial Compression Test on Cohesive Soils, ASTM D 2850.

American Society for Testing and Materials (2007c). Standard Test Methods for Moisture, Ash, and Organic Matter of Peat and Other Organic Soils, ASTM D 2974.

Andersen, A., and Kolstad, P. (1979). "The NGI 54-mm sampler for undisturbed sampling of clays and representative sampling in coarser material," Proceedings of the International Conference on Soil Sampling, Singapore, 1-9.

Berre, T., and Bjerrum, L. (1973). "Shear strength of normally consolidated clays," Proceedings of the 8th International Conference on Soil Mechanics and Foundation Engineering, Moscow, 1, 39-49.

Bjerrum, L. (1972). "Embankments on soft ground," Proceedings of the ASCE Conference on Performance of Earth-Supported Structures, Purdue University, 2, 1-54.

Bjerrum, L. (1973). "Problems of soil mechanics and construction on soft clays," Proceedings of the 8th International Conference on Soil Mechanics and Foundation Engineering, Moscow, 3, 111-159.

Blight, G.E. (1963). "The effect of non-uniform pore pressures on laboratory measurements of the shear strength of soils," ASTM STP 361, American Society for Testing and Materials, Philadelphia, 184-191.

Blight, G.E. (1968). "A note on field vane testing of silty soils," Canadian Geotechnical Journal, 5(3), 142-149.

Campanella, R.G., and Robertson, P.K. (1988). "Current status of the piezocone test." Proceedings of the International Symposium on Penetration Testing, ISOPT-1, Orlando, 1, 93-116.

Chandler, R.J. (1988). "The in-situ measurement of the undrained shear strength of clays using the field vane," Vane Shear Strength Testing in Soils: Field and Laboratory Studies, ASTM STP 1014, American Society for Testing and Materials, Philadelphia, 13-44.

Chen, B.S.Y., and Mayne, P.W. (1996). "Statistical relationship between piezocone measurements and stress history of clays," Canadian Geotechnical Journal, 33, 488-498.

Demers, D. and Leroueil, S. (2002). “Evaluation of consolidation pressure and the overconsolidation ratio from piezocone tests of clay deposits in Quebec,” Canadian Geotechnical Journal, 39, 174-192.

Duderstadt, F.J., Coyle, H.M., and Bartoskewitz, R.E. (1977). Correlations of the Texas cone penetrometer test N-values with soil shear strength, Research Report 10-3F, Texas Transportation Institute.

Duncan, J.M. and Wright, S.G. (2005). Soil Strength and Slope Stability. John Wiley & Sons, New York.

Garfield, S.M. (2008). "Improved Correlation between Texas Cone Penetrometer Blow Count and Undrained Shear Strength of Soft, Shallow Clays," thesis submitted in partial satisfaction of the requirements for the degree of Master of Science in engineering, The University of Texas, Austin, TX.

Karlsrud, K., Lunne, T., and Brattlien, K. (1996). “Improved CPTU correlations based on block samples,” Proceedings of Nordic Geotechnical Conference, Reykjavik, 1, 195-201.

Karlsrud, K., Lunne, T., Kort, D.A., Strandvik, S. (2005). “CPTU correlations for clays,” Proceedings of the 16th International Conference on Soil Mechanics and Foundation Engineering, Osaka, 1, 1-8.

Karube, D., Shibuya, S., Baba, T., and Kotera, Y. (1988). “Analysis of a vane test based on effective stresses,” Vane Shear Strength Testing in Soils: Field and Laboratory Studies, ASTM STP 1014, American Society for Testing and Materials, Philadelphia, 131-149.

Kulhawy, F.H., and Mayne, P.W. (1990). Manual on Estimating Soil Properties for Foundation Design. Report EL-68000, Electric Power Research Institute, EPRI, August 1990. Palo Alto. 306.

Ladd, C.C, and DeGroot, D.J. (2003). “Recommended practice for soft ground site characterization: Arthur Casagrande lecture,” Proceedings of the 12th Panamerican Conference on Soil Mechanics and Geotechnical Engineering, Cambridge, MA.

Ladd, C.C., and Foot, R. (1974). “New design procedure for stability of soft clays,” Journal of the Geotechnical Engineering Division, 100(7), 763-786.

La Rochelle, P., Zebdi, P.M., Leroueil, S., Tavenas, F. and Virely, D. (1988). “Piezocone tests in sensitive clays of eastern Canada,” Proceedings of the International Symposium on Penetration Testing, ISOPT-1, Orlando, 2, 831-41.

Larsson, R., and Mulabdic, M. (1991). “Piezocone tests in clay,” Swedish Geotechnical Institute Report No. 42, Linköping, 240p.

Lunne, T. and Lacasse, S. (1985). “Use of in situ tests in North Sea soil investigations,” Proceedings of the Symposium: From Theory to Practice in Deep Foundations, Porto Allegre, Brazil, Oct. 1985, 169.

Lunne, T., Robertson, P.K., and Powell, J.J.M. (1997). Cone Penetration Testing in Geotechnical Practice, E & FN Spon, London.

Mayne, P.W. (2007). “Cone Penetration Testing.” NHCRP Synthesis 368, The Transportation Research Board.

Mayne, P.W., and Holtz, R.D. (1988). “Profiling stress history form piezocone soundings,” Soils and Foundations, 28(1), 16-28.

Mesri, G. (1975). Discussion of “New design procedure for stability of soft clays.” by C.C. Ladd and R. Foot, Journal of the Geotechnical Engineering Division, 101(4), 409-412.

Mesri, G. (1989). “A reevaluation of $s_{u(mob)} = 0.22\sigma'_p$ using laboratory shear tests.” Canadian Geotechnical Journal. 26, 162-164.

Peterson, R., Jaspar, J.L., Rivard, P.J., and Iverson, N.L. (1960). "Limitations of Laboratory Shear Strength in Evaluating Stability of Highly Plastic Clays," Proceedings of the ASCE Research Conference on the Shear Strength of Cohesive Soils, 765-791.

Powell, J.J.M., Quarterman, R.S.T., and Lunne, T. (1988). “Interpretation and use of the piezocone test in UK clays,” Proceedings of the Geotechnology Conference: Penetration Testing in the UK, Birmingham, 151-156.

Robertson, P.K., Campanella, R.G., Gillespie, D., and Greig, J. (1986). “Use of piezometer cone data,” Proceedings of the ASCE Specialty Conference In Situ ’86, Blacksburg, VA, 1263-1280.

Skempton, A.W. (1954). "The Pore Pressure Coefficients A and B," Geotechnique, 4(4), 143-147.

Skempton, A.W. (1957). Discussion of “The planning and design of the new Hong Kong airport,” Proceedings of the Institution of Civil Engineers, London, 7, 305-307.

Terzaghi, K., Peck, R.B., and Mesri, G. (1996). Soil Mechanics in Engineering Practice. 3rd edition, John Wiley & Sons, New York.

Texas Department of Transportation (2006). Geotechnical Manual, Texas Department of Transportation, Austin, TX.

U.S. Army Corps of Engineers (1986). Laboratory Soils Testing, Engineering Manual EM 1110-2-1906, Department of the Army, Washington, D.C.

Wissa, A.E.Z, Christian, J.T., Davis, E.H., and Heiberg, S. (1971). “Consolidation at constant rate of strain,” Journal of the Soil Mechanics and Foundation Division, 97(10), 1393-1413.